



Universidade do Minho
Escola de Engenharia

Helena Filipa Ribeiro da Silva Pereira

**Three dimensional cell-scaffold constructs
for application in bone tissue engineering**

Dissertação de Mestrado

Mestrado em Engenharia Biomédica

Trabalho efetuado sob a orientação de:

Professor Doutor Filipe Samuel Correia Pereira da Silva

Professor Doutor Joaquim Miguel Antunes Correia de Oliveira

Dezembro de 2017

DECLARAÇÃO

Nome: Helena Filipa Ribeiro da Silva Pereira

Endereço eletrónico: helenaf.rs.pereira@gmail.com Telefone: 912914161

Bilhete de Identidade/Cartão do Cidadão: 13986259

Título da dissertação: Three Dimensional cell–scaffold constructs for application in bone tissue engineering.

Orientadores:

Professor Doutor Filipe Samuel Correia Pereira da Silva

Professor Doutor Joaquim Miguel Antunes Correia de Oliveira

Ano de conclusão: 2017

Mestrado Integrado em Engenharia Biomédica

Ramo: Biomateriais, Reabilitação e Biomecânica

DE ACORDO COM A LEGISLAÇÃO EM VIGOR, NÃO É PERMITIDA A REPRODUÇÃO DE QUALQUER PARTE DESTA TESE/TRABALHO.

Universidade do Minho, ____/____/____

Assinatura:

To my parents.

“You may have to fight a battle more than once to win it.”
Margaret Thatcher

ACKNOWLEDGMENTS

I thank my supervisor, Prof. Dr. Filipe Silva, for all the support and encouragement he gave me throughout my master's thesis. I am grateful for the opportunities he gave me, the teachings, advice, for all motivational words and for being available. I would also like to extend my gratitude to my co-supervisor, Prof. Dr. Miguel Oliveira, for his assistance in developing this project and keeping me on track. Thank you for being always available to help me and to clarify my doubts.

I would like to thank to all my CMEMS colleagues, especially to Flávio Bartolomeu Mafalda Costa and Diana Faria for the teachings, help, support and friendship. I would like to thank all the members of the 3B's Group research for making me feel so welcome during my master's thesis. In particular, I would like to thank Raquel Maia who taught me everything I know about cells, culture cells and cellular assays. I will always be grateful to you for your support and for all afternoons you spent with me in lab. It was a great pleasure to work with you. This project would not have been possible without the help of Ibrahim Fatih Cengiz. I am truly grateful for all the teachings, help and support. Thank you for always be available to answer my doubts.

I am deeply grateful to my best friend, Décio Costa, for always being present and for supporting me in such important moment of my life. Thank you for believing in me, for always cheering me up, for your unconditional friendship and love.

Finally, I would not have made it through this busy and challenging year without the support of my family and friends. I thank my parents, Maria and Rui, for teaching me to be a hard working person, for giving me the best education, for all the encouragement and love. I thank my sister, Alexandra, for unconditional support and friendship. I thank my dearest friend, Adriana Temporão, for understand me and for the friendship.

RESUMO

O osso é um tecido dinâmico com uma incrível capacidade de auto reparação. No entanto, quando o defeito ósseo ultrapassa um tamanho crítico, o osso perde essa capacidade e a intervenção médica torna-se necessária. O osso é o segundo tecido mais transplantado do mundo e existe uma grande necessidade de enxertos e substitutos ósseos, o que por sua vez levam a uma diminuição da disponibilidade de osso nos Bancos de Tecidos. As matrizes tridimensionais porosas são de grande importância para a engenharia de tecidos e implantes ortopédicos uma vez que servem de meio biológico para que tecido ósseo envolvente cresça para o interior dos poros. Uma matriz deve ser porosa por forma a possibilitar a nutrição, proliferação, e migração celular e formação de um novo tecido ósseo vascularizado. As matrizes tridimensionais devem, ainda, possuir propriedades mecânicas próximas à do osso para evitar reabsorção óssea, a qual está associada à falha do implante.

Neste estudo, foram produzidas matrizes tridimensionais com resistência mecânica máxima capazes de serem usadas em aplicações ortopédicas e com o módulo de Elasticidade semelhante ao módulo de Elasticidade do osso. As matrizes tridimensionais porosas foram produzidas com três materiais diferentes: i) Ti_6Al_4V ; ii) ZrO_2 e iii) PEEK. Para a caracterização da microestrutura das matrizes tridimensionais com estrutura celular SEM e Micro CT foi realizado. Para a avaliação da fase e composição química da superfície as matrizes tridimensionais porosas foram analisados por XRD e XPS. Testes mecânicos de compressão foram realizados para avaliar o módulo Elasticidade e a força máxima de compressão. A eficácia das matrizes tridimensionais como material para aplicações de engenharia de tecidos foi avaliada *in vitro*, recorrendo a uma linha celular SaOS-2 que foi cultivada na superfície das diferentes matrizes porosas. A sua viabilidade, proliferação e diferenciação foi analisada até 14 dias de cultura. A viabilidade celular foi estudada recorrendo ao teste de *Alamar Blue* para o dia 1, dia 3, dia 7 e dia 14 de cultura celular. A proliferação e diferenciação celular foi avaliada através da quantificação do DNA e a atividade da ALP para os mesmos tempos de cultura. As matrizes tridimensionais porosas cultivadas com células SaOS-2 foram, ainda, coradas com *Fast Violet B* para a observação da fosfatase alcalina. Os resultados obtidos sugerem o potencial das matrizes tridimensionais para aplicações na engenharia de tecido do osso. Estas matrizes apresentam um módulo Elasticidade perto do osso que pode minimizar o fenómeno da reabsorção óssea. Os resultados *in vitro* revelaram a não toxicidade das matrizes assim como apresentarem uma superfície favoráveis à adesão e à proliferação das células.

Palavras-Chave: Ti_6Al_4V , ZrO_2 , PEEK, Propriedades mecânicas, Testes *in vitro*

ABSTRACT

Bone is a dynamic tissue with an amazing capacity of self-repair. However, when the defect reaches a critical size bone loses this capacity and medical intervention is needed. Bone is the second most transplanted tissue in the world and there is a huge need for bone grafts and substitutes and therefore leading to a decrease in bone banks donors. Scaffolds are of great importance for tissue engineering and orthopedic implants since they provide biological anchorage for the surrounding bony tissue via the ingrowth of tissue into pores. The pores of scaffolds have direct implications on their biofunctionality. Thus, a porous structure is critical for cell nutrition, proliferation, cell migration, and formation of newly vascularized tissue. Scaffold's mechanical properties should also match that of bone in order to prevent stress shielding which is one of the main causes for implant's failure.

In this study, three-dimensional porous scaffolds with maximized mechanical strength capable for load-bearing applications and with elastic modulus near of the bone were produced. The porous scaffolds were made of: i) Ti_6Al_4V , ii) ZrO_2 and iii) PEEK. Their microstructures were characterized by mean of performing SEM and Micro CT analyses. To assess the chemical composition of the scaffolds, XPS analysis was performed. The crystallographic phase of ZrO_2 was investigated by XRD. Mechanical compressive tests were performed in order to evaluate the elastic modulus and compressive stress. Their efficacy as scaffold material for bone regeneration applications was evaluated *in vitro* by seeding SaOS-2 cells onto the scaffolds. The viability, proliferation and differentiation of SaOS-2 cells was analyzed. The cellular viability was assessed by Alamar blue test at day 1, day 3, day 7 and day 14. For the study of cell proliferation, DNA quantification was performed for the same time points. To assess the differentiation of SaOS-2 cells, alkaline phosphatase was qualitatively and quantitatively evaluated by performing the ALP quantification and staining with Fast violet B.

Mechanical results showed an elastic modulus near of the bone which can minimize the phenomenon of stress shielding. The *in vitro* results revealed cytocompatibility with no cell alterations or death of SaOS-2 seeded on scaffolds surfaces.

The proposed scaffolds showed great potential *in vitro* to be used in bone tissue engineering scaffolding applications.

KEYWORDS: Ti_6Al_4V , ZrO_2 , PEEK, Mechanical properties, *in vitro* assays

INDEX

Acknowledgments.....	vii
Resumo.....	ix
Abstract.....	xi
List of Figures.....	xv
List of Tables.....	xix
List of abbreviations.....	xxi
1. Introduction	1
1.1 Motivation	1
1.2 Objectives	2
1.3 Structure of thesis	3
2. State of the art.....	5
2.1 Fundamental concepts	5
2.2 Geometry Characteristics.....	9
2.3 Methods for production of scaffolds	10
2.4 Validation of scaffolds.....	14
2.5 References.....	17
3. Non-degradable and degradable Biomaterials for Bone Tissue Engineering scaffolding	21
3.1 Bone structure	22
3.2 Current repair therapies	25
3.3 Bone tissue engineering products	28
3.4 Scaffolds for bone tissue engineering.....	30
3.4.1 Non degradable	30
3.4.2 Degradable.....	35
3.5 Biodegradable coatings	42
3.6 Other regenerative strategies	45
3.7 Conclusions and final remarks.....	47
3.8 References.....	48
4. Physicochemical properties and cytocompatibility assessment of non-degradable scaffolds for bone tissue engineering applications	63

4.1	Introduction.....	64
4.2	Materials and Methods	65
4.2.1	Scaffolds Preparation.....	65
4.2.2	Physicochemical characterization.....	66
4.2.3	Scaffolds <i>in vitro</i> characterization.....	68
4.2.4	Statistical analysis	70
4.3	Results.....	70
4.3.1	Physicochemical characterization.....	70
4.3.2	Biological characterization.....	78
4.4	Discussion	83
4.5	Conclusion	86
4.6	References.....	86
5.	Final Remarks and Future Work	90

LIST OF FIGURES

Figure 2-1 Bone composition and bone cells. a) Bone is arranged in two architecture forms: trabecular bone and compact bone. These two forms differ from each other in porosity and in location. Trabecular bone is more porous and is located in the inner part of bone.....	6
Figure 2-2 Bone ingrowth into porous titanium. Micro CT images of porous titanium implanted in rabbit femur (the yellow color represent the new bone) (Chang et al. 2016).....	10
Figure 2-3 Representation of solvent casting and freeze drying pore morphology and their process. a) Typical pore morphology obtained with solvent casting technique; b) Typical pore morphology obtained with freeze drying; c) Schematic representation of solvent casting process; d) Schematic representation of freeze drying process.....	11
Figure 0-1 Process of selective laser melting.....	13
Figure 2-5 3D print. Schematic representation of the process and examples of scaffolds.....	13
Figure 2-6 Example of a CNC milling machine.....	13
Figure 2-7 Steps towards the validation of a new scaffold.	15
Figure 3-1 Current solutions for the treatment of bone defects. A- D) quantification of bone ingrowth and contact area in an Actifuse® sample. A) A 3-D reconstruction of the middle third of the rat tibia (yellow) with the region-of-interest (blue) determined by applying convex hull to the biomaterial. The volume and surface area of the bone (yellow) and biomaterial (green) inside the region-of-interest are calculated in (B). Scale bar in A and B is 1 mm. (C) A top-down view slice through the region-of-interest and bone, with the region-of-interest outlined in blue. (D) The contact area between the bone (grey) and biomaterial (white) as a red outline (Midha et al. 2013); E) autograft; F) injectable cements; G) Morcelized homologous bone graft obtained from a banked (Campana et al. 2014); lower panel images of x ray. (a–c) X-ray of a 36 year-old male patient few days following curettage of a low-grade chondrosarcoma of the left proximal tibia. (b and c) Follow-up radiographs 7 and 13 months following index surgery showing integration but no resorption of the artificial bone graft substitute (Friesenbichler et al. 2017).	30
Figure 3-2 Gross morphologic, radiologic and three dimensional (3D) CT-scan images of the injured healed radial bones of rats (Oryan et al. 2017a).	37
Figure 3-3 Performance of coated scaffolds in vivo. Upper panel: a – h) Implantation of the scaffolds in skull defects for 1 and 2 months. a, b) The treated and control scaffolds implanted in the skull for 1 month were examined using micro-CT. c, d) The treated and control scaffolds implanted in the skull for	

2 months were examined by micro-CT. The micro-CT image was captured at the middle level of the entire scaffold. Green represents normal tissue, while red represents the titanium scaffold. The treated group showed more tissue ingrowth than the control group. Hard-tissue sections after H&E staining (e–h). The large black area represents the titanium edge under the microscope. The small and irregular pieces of black chips observed in the pores reflect cut titanium. Under H&E staining, the bone tissue was only slightly white and showed slight nuclear staining (Zhu et al. 2017); lower left panel: a-d) Histological observations of the TI and HA-TI groups at low magnification (Van Gieson stain, 16 ×). The distribution of new bone (red) and fibrous tissue (dark blue) in the TI group at 2 months post-implantation (A), the HA-TI group at 2 months post-implantation (B), the TI group at 4 months post-operation (C), and the HA-TI group at 4 months post-operation (D) (Huang et al. 2015); lower right panel: Histological images of transverse sections through titanium implants upon which had been deposited a layer of calcium phosphate bearing a BMP-2 concentration of 500 µg/g of coating (A) 3 and (B) 6 weeks after their insertion into the proximal tibial bone. (A) At the 3-week juncture, the resorption of bone outweighed its formation in both the mesh and the peri-implant spaces, as evidenced by the lack of staining for osseous tissue. (B) By the end of the 6th week, the balance between bone resorption and bone formation had been tipped in favour of the latter process (Hunziker et al. 2016). 45

Figure 4-1 XRD plot of tetragonal phase of ZrO₂. 71

Figure 4-2 XPS plot of Ti6Al4V. a) Survey scan XPS spectra (b) high-resolution XPS spectra of Ti6Al4V showing the peak of Ti 2p. 72

Figure 4-3 XPS plot of ZrO₂. a) Survey scan XPS spectra showing O 1s, Zr 3p_{3/2}, Zr 3p_{1/2} and Zr 3d peaks (b) high-resolution XPS spectra of Y 3d; c) high-resolution XPS spectra of Zr 3d. 73

Figure 4-4 XPS plot of PEEK. a) Survey scan XPS spectra showing O 1s and C 1s peaks; (b) high-resolution XPS spectra of O 1s; c) high-resolution XPS spectra of C 1s. 74

Figure 4-5 Mechanical Properties of scaffolds. a and b) Elastic modulus for vertical and horizontal position; b e c) Maximum compressive stress for vertical and horizontal position. Data is presented as mean±stdev (n=3), (*) denotes statistical differences (p<0.05) 77

Figure 4-6 SEM analysis. SEM image of a) Ti6Al4V scaffold; b) ZrO₂ scaffold; c) PEEK scaffold; d) unseeded Ti6Al4V scaffold; e) unseeded ZrO₂ scaffold f) unseeded PEEK scaffold; g) and j) seeded Ti6Al4V scaffold; h) and k) seeded ZrO₂ scaffold i) and l) seeded PEEK scaffold; m) cells adhered and spreaded on Ti6Al4V scaffolds at higher magnification; n) cells adhered and spreaded on ZrO₂ scaffolds at higher magnification; o) cells adhered and spreaded on PEEK scaffolds at higher magnification. 79

Figure 4-7 SaOS-2 cells' metabolic activity normalized by DNA concentration, along 14 days of culture. Symbols denote statistically significant differences ($p < 0.05$) in comparison to: (*) ZrO₂ and PEEK scaffolds, (\$) scaffolds; (#) PEEK scaffolds; (£) day 7; and (§) day 1. Data is presented as mean±stdev (n=3)..... 80

Figure 4-8 SaOS-2 cells' proliferation rates by DNA concentration, along 14 days of culture. Symbols denote statistically significant differences ($p < 0.05$) in comparison to: (\$) scaffolds; (#) PEEK scaffolds; (§) day 1; and (£) ZrO₂ scaffolds. Data is presented as mean±stdev (n=3). 811

Figure 4-9 SaOS-2 cells' ALP activity along 14 days of culture. Symbols denote statistically significant differences ($p < 0.05$) in comparison to: (£) ZrO₂ scaffolds; (\$) scaffolds; (§) day 3 (#) PEEK scaffolds; and (*) day 7. Data is presented as mean±stdev (n=3). 82

Figure 4.10 ALP stained SaOS-2 cells on scaffolds and respective controls (scaffolds without cells) after 14 days of culture. Insets shows ALP stained cells on scaffolds at higher magnification. 83

LIST OF TABLES

Table 2-1 Bone cells and respective functions and properties (Boskey 2007; Kalfas 2001; Salgado et al. 2004).....	6
Table 2-2 Examples of bone diseases and its consequences (Boskey 2007; Rodan and Martin 2000). .	8
Table 3-1 Mechanical properties of human bone and bulk materials, values from literature (Yang et al. 2001; Wang et al. 2016; Santos et al. 2016; Schwitalla et al. 2015; Najeeb et al. 2016; Osman and Swain 2015).....	23
Table 3-2 Advantages and disadvantages of the most commonly bone scaffolds.	26
Table 3-3 Requirements for the design of scaffolds in bone tissue engineering (Wang et al. 2016; Zakhary and Thakker 2017; Pina et al. 2016; Rahaman et al. 2011).....	31
Table 3-4 List of some bone tissue engineering products commercially available.....	38
Table 3-5 Scaffolding biomaterials used in the recent <i>in vivo</i> experiment for bone tissue engineering studies, and the outcomes.....	39
Table 4-1 3D reconstructions of Ti6Al4V, ZrO2 and PEEK samples, mean porosity, pore size and trabeculae thickness, calculated from the micro-CT data, presented as mean \pm standard deviation.. .	75
Table 4-2 Mean \pm standard deviation values of Ra for machined and polished samples.....	76
Table 4-3 Contact angle measurement values of machined and polished samples	76
Table 4-4 Surface energy measurement values of machined and polished samples	75

LIST OF ABBREVIATIONS

3D – Three – dimensional
BMP – Bone Morphogenetic protein
BTE – Bone Tissue Engineering
C - Carbon
CAD – Computer-aided design
CNC – Computer Numerical Control (CNC)
ECM – Extracellular Matrix
EDS – Energy – disperse X- ray spectroscopy analysis
EMA – European Medicines Agency
FDA – Food and Drug Administration
GDF – Growth differentiation factor
HA – Hydroxyapatite
ISO – International Organization for Standard
Micro CT – Micro Computed Tomography
O - Oxygen
PEEK – Polyetheretherketone
RM – Rapid manufacturing
RP – Rapid Prototyping
RT – Rapid Tooling
Y – TZP – Yttria-stabilised tetragonal zirconia
SEM – Scanning electron microscopy
TE – Tissue Engineering
Ti - Titanium
TGF – Transforming growth factor
VEGF – Vascular endothelial growth factor
XRD – X-ray diffraction
Zr - Zirconium

1. INTRODUCTION

1.1 Motivation

Bone loss has a tremendous effect on the patient's life. Additionally, with the increase of the life expectancy bone diseases that lead to trauma are more frequent. Different techniques have been used over the years for bone healing. These therapies have been using bone graft material removed from a different site in the patient (autograft), from another human donor (allograft), or from other living or nonliving species (heterografts or xenografts) and are limited by the material availability (Agarwal and García 2015). Furthermore, these therapies have complicated multistage surgery with the disadvantage of the harvest site and the risk of disease transmission. Adding to all these factors a great need for synthetic substitutes especially designed and manufactured to satisfy the requirements of functionality and biocompatibility criteria of tissue engineering is desirable (Sepulveda et al. 2002). The concept of tissue engineering (TE) embodies the development of a scaffold structure that has the appropriate physical, chemical, and mechanical properties aiming to allow cell penetration and tissue formation in three dimensions (Karp et al. 2003). As it was defined by Langer and Vacanti (Langer and Vacanti 1993), TE is "an interdisciplinary field of research that applies the principles of engineering and life sciences towards the development of biological substitutes that restore, maintain, or improve tissue function". The selection of the biomaterial to produce a bone scaffold is an important step during the construction of a scaffold (Salgado et al. 2004). These materials should possess excellent biocompatibility, superior corrosion resistance in body environment, excellent combination of high strength and low modulus, high fatigue and wear resistance, high ductility and be without cytotoxicity (Geetha et al. 2009). Up to now materials such as metals, polymers and ceramics, either both natural or synthetic origins have been proposed (Salgado et al. 2004). Metallic biomaterials, such as titanium alloys, have been widely used in orthopedic implants as they can provide favorable mechanical strength, excellent friction resistance and non-toxic properties as well as cytocompatibility. One of the most used titanium alloy is Ti_6Al_4V , this alloy is stabilized by Aluminium (Al) and Vanadium (V) creating a two-phase alloy that displays a high corrosion resistance, high biocompatibility and high strength (Ma and Tang 2014; Zhao et al. 2013). However, some disadvantages have hindered their more commonly medical applications. Their high strength and the mismatch of elastic modulus between the metal and the bone can cause stress shielding effect which

is characterized by the adsorption of adjacent bone tissues and can lead to the implant loosening. Also, there are concerns regarding potential metal ion release (Ma and Tang 2014; Zhao et al. 2013). Ceramics are commonly defined as “inorganic, non-metallic materials” (Chevalier and Gremillard 2009). The family of ceramic materials includes bioinert non-resorbable metal oxides such as alumina (Al_2O_3) or zirconia (ZrO_2) (Scarano et al. 2003). Zirconia ceramics have several advantages over other ceramic materials, due to the transformation toughening mechanisms operating in their microstructure which gives to components made out of them very interesting mechanical properties (Piconi and Maccauro 1999). Yttria-stabilized zirconia (Y-TZP) was the ceramic gold standard in terms of strength and toughness, but its lack of long term stability is a major issue for medical use (Chevalier and Gremillard 2009). One promising alternative is polyetheretherketone (PEEK) which is a linear, aromatic, semi-crystalline polymer with good chemical resistance, radiolucency, and mechanical properties similar to those of human bones (Edwards and Werkmeister 2012; Zhao et al. 2013). Besides, it is best known for its excellent thermal, chemical and mechanical resistance. It can be repeatedly sterilized and shaped by machining to fit the shape of bones. In spite of these excellent attributes, the chemical and biological inertness of PEEK tends to limit bone fixation (Edwards and Werkmeister 2012; Zhao et al. 2013).

1.2 Objectives

The main goal of this thesis focused on the characterization, mechanical and biological evaluation of three dimensional porous scaffolds made from different materials: $\text{Ti}_6\text{Al}_4\text{V}$, ZrO_2 and PEEK for bone tissue applications.

The detailed objectives of this thesis are:

1. Surface and mechanical characterization of $\text{Ti}_6\text{Al}_4\text{V}$, ZrO_2 and PEEK through the assessment of compressive test, contact angle, roughness and surface energy;
2. Surface and microstructure characterization by Micro CT, SEM, XPS and XRD. To assess the architecture of scaffolds Micro CT was performed, it also give us information about porosity and pore size. SEM was performed to study surface topography. XPS gives information about chemical composition of scaffold's surfaces, and XRD was used to study phase transformation.
3. *In vitro* evaluation of SaOS-2 cells seeded $\text{Ti}_6\text{Al}_4\text{V}$, ZrO_2 and PEEK scaffolds. Cell viability, proliferation and differentiation was studied by performing metabolic quantification, DNA quantification and ALP quantification.

1.3 Structure of thesis

This thesis is divided into 5 chapters. Chapter 1 presents the motivation, the objectives and the structure of the thesis.

The chapter 2 describes in detail the most fundamental concepts of bone anatomy and scaffold's production methods.

The chapter 3 consists in a review article, *Bone Regeneration: Non-degradable and degradable Biomaterials*, prepared during this project to elucidate about the current solutions in clinic, the gaps of scaffolds being tested and the requirements for the “gold standard” scaffold for bone tissue engineering.

The studies developed in this dissertation work resulted in one scientific paper, *Physicochemical properties and cytocompatibility assessment of non-degradable scaffolds for bone tissue engineering applications*, which corresponds to the Chapter 4 of the dissertation.

The last chapter, chapter 5, presents final remarks of this work and suggestions made for future work.

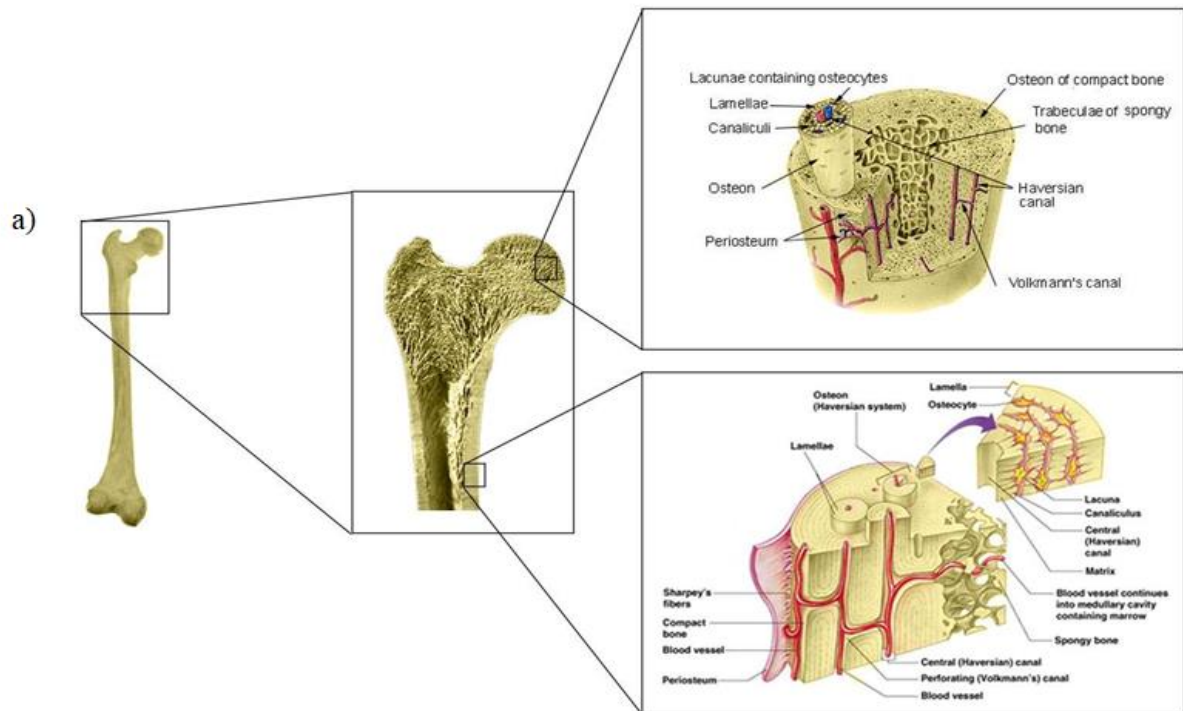
2.STATE OF THE ART

2.1 Fundamental concepts

Bone loss has, in general, significant effect on patient's quality of life. Moreover, as the world population continues to grow, the number of elderly population continues to increase which results in an escalation of bone degenerative diseases (Bhattacharjee et al. 2017; Roseti et al. 2017). Bone supports movement, provides skeleton to body, and provides protections to organs; while also regulating the storage of minerals and blood pH. Bone owns a unique hierarchical structure of self-assembled macromolecules within a bed of hydroxyapatite (HA) and carbonate. In figure 2-1 is represented the bone anatomy and images of the main bone cells.

Cellular components such as osteoblasts and osteoclasts harbor the intrinsic plasticity of bone in response to mechanical loading. Table 2.1 display their function and properties (Hadjidakis and Androulakis 2006). Osteoblasts are cuboidal cells that are located along the bone surface comprising 4–6% of the total bone cells. They are involved in the formation of new bone by expressing osteoclastogenic factors, production of bone matrix proteins and bone mineralization (Flores-Silva et al. 2015; Raggatt and Partridge 2010). Osteocytes which comprise 90-95% of the total bone cells possess long cell processes. Their function and morphology varies according to cell age. Therefore, a young osteocyte has structural characteristics of the osteoblast but presents a decreased cell volume and capacity of protein synthesis. On the other hand, an older osteocyte presents with a further decrease in cell volume and an accumulation of glycogen in the cytoplasm (Hadjidakis and Androulakis 2006). Osteoclasts are terminally differentiated multinucleated cells which originate from mononuclear cells of the hematopoietic stem cell lineage, under the influence of several factors. During bone remodeling osteoclasts divide; then, four types of osteoclast membrane domains can be observed: the sealing zone and ruffled border that are in contact with the bone matrix, as well as the basolateral and functional secretory domains, which are not in contact with the bone matrix (Flores-Silva et al. 2015; Raggatt and Partridge 2010). Bone lining cells cover the bone surface where neither bone resorption nor can bone formation occur. These cells exhibit a thin and flat nuclear profile. Their secretory activity depends on the bone physiological status (Flores-Silva et al. 2015). Long bone possesses a vascular system that provides nutrients, oxygen, and osteoprogenitor cells. After the arteries enter a bone through these blood vessels penetrate through

Volkman's and Haversian canals and branch throughout the cortical bone. This vascularization plays an important part in adult bone repair (Marrella et al. 2017).



Bone cells

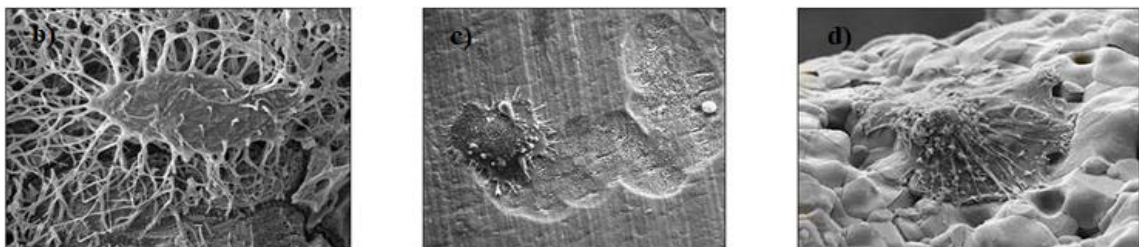


Figure 2-1 Bone composition and bone cells. a) Bone is arranged in two architecture forms: trabecular bone and compact bone. These two forms differ from each other in porosity and in location. Trabecular bone is more porous and is located in the inner part of bone. b) osteocyte; c) osteoclast; d) osteoblast. Adapted from Pearson Education Inc. publishing as Benjamin Cummings.

Table 2-1 Bone cells and respective functions and properties (Boskey 2007; Kalfas 2001; Salgado et al. 2004).

Cell Type	Function and Properties
Osteoblast	Round or flat bone-forming cell; Synthesis and regulation of bone ECM deposition and mineralization; Respond to mechanical stimuli.
Osteocytes	Osteoblasts surrounded by mineral;

	Linked to other similar cells by thin processes; Calcification of osteoid matrix; Blood-calcium homeostasis; Mechanosensor cells of bone.
Osteoclasts	Multinucleated large-bone reabsorbing cell; Binds to bone surface and releases acid enzymes that respectively remove mineral and matrix in response to signals.
Bone Lining Cells	Flat shape osteoblast; Secretory activity; Participate in osteoclast differentiation; Production of osteoprotegerin.

Two processes, remodeling and modeling, support the development and maintenance of the skeletal. Bone modeling is responsible for growth and mechanically induced adaption of bone and requires that the processes of bone formation and bone removal (resorption), although globally coordinated, occur independently at distinct anatomical locations (Raggatt and Partridge 2010). Bone remodeling, defined by Frost in 1990, is responsible for removal and repair of damaged bone to maintain integrity of the adult skeleton and mineral homeostasis (Raggatt and Partridge 2010; Frost 1990). The equilibrium between bone resorption and formation is necessary and depends on the action of several local factors like hormones, and biomechanical stimulation. There are a number of bone diseases that result from the imbalance between bone resorption and formation (table 2.2). For example, an excessive resorption without the corresponding amount of new formed bone can result in an appropriated bone loss and thus **osteoporosis**, whereas the opposite can result in **osteopetrosis** (Florencio-Silva et al. 2015). The reduction of bone mass and its deterioration after age 40 is one of the main characteristic of osteoporosis which results in an increase in the fragility of bone and its susceptibility to fractures (Rodan and Martin 2000). By definition **osteomalacia** means that osteoblasts have laid down a collagen matrix, but there is a defect in its ability to be mineralized (Holick 2014). **Osteogenesis imperfecta** is a share similar skeletal abnormalities causing bone fragility and deformity (Forlino and Marini 2016). **Osteonecrosis**, also known as avascular necrosis, ischemic necrosis and aseptic necrosis, it is a condition in which an area of bone becomes necrotic as a result of the loss of its blood supply. The most

common cause is trauma, a displaced fracture or dislocation which results in a mechanical injury to the local vessels (Steinberg and Steinberg 2014). **Paget's disease** is characterized by an increase in osteoclast numbers and activity. This leads to the increase bone resorption (Rodan and Martin 2000). Another common disease is **periodontal disease** which results from an accumulation of the bacteria that cause dental plaque leading to the destruction of cellular and structural components of the periodontium (Rodan and Martin 2000). All these diseases lead to bone fractures and for the most fractures bone tissue heals itself. However for fractures above critical size (> 6 mm) bone is not capable of healing by itself (Agarwal and García 2015).

Table 2-2 Examples of bone diseases and its consequences (Boskey 2007; Rodan and Martin 2000).

Type of Disease	Description
Osteoporosis	Increased porosity with tendency to fracture
Osteomalacia	Poorly mineralized bone with tendency to fracture
Osteogenesis imperfecta	Brittle bone disease due to abnormal collagen synthesis
Osteopetrosis	Rock-like bone with increased tendency to fracture
Osteonecrosis	Dead bone
Renal osteodystrophy	Kidney malfunction leading to osteoporotic bone
Paget's disease	Increase in osteoclast numbers and activity promoting the increase of bone resorption which leads to fracture.
Bone cancer	Increase in osteoclast formation and activity.

There are two main mechanisms of bone healing: i) direct bone growth and indirect bone growth after callous formation. Direct bone healing involves the growth of bone from the broken ends at fracture site without any intermediate fibrous tissue formation (Agarwal and García 2015). ii) Indirect bone healing involves inflammation leading to callous formation via intra-membranous ossification. This is followed by endochondral ossification and resorption of the callous (Agarwal and García 2015).

Engineered bone scaffolds have been gaining attention as a potential alternative to the conventional use of bone grafts, due to their limitless supply and no disease transmission. Bone tissue engineering aims to induce new functional bone regeneration via the synergistic combination of biomaterials, cells, and factor therapy (Amini et al. 2012). A scaffold can be used as acellular system or as vehicles for cells, growth factors or drugs.

2.2 Geometry Characteristics

In the design of tissue engineering scaffolds, design parameters including pore size, pore shape and mechanical properties should be optimized to maximize the bone ingrowth (Jones et al. 2009). Surface characteristics are crucial for the successful design and medical application of biomaterials as it is the earliest contact with the biological environment (Wu et al. 2014; Wennerberg and Albrektsson 2009). Surface properties, both chemical and topographical, can modulate and affect cellular adhesion and proliferation (Salgado et al. 2004). The morphology of the scaffolds is involved in a series of biological events occurring after implantation, which range from protein adhesion to bone remodeling (Albertini et al. 2015). For a proper integration with the host tissue a surface with roughness is favorable as it enhances attachment, proliferation and differentiation of anchorage dependent bone forming cells (Albertini et al. 2015; Karageorgiou and Kaplan 2005; Wennerberg and Albrektsson 2009).

Pore size, as we can see in figure 2-2, is also a very important parameter because if the pores are too small, occlusion by the cells can happen and it is also an important factor for protein adsorption, cellular migration and osteoconduction (Salgado et al. 2004; Prananingrum et al. 2016). There is hardly consensus regarding the optimal pore size for effective bone ingrowth (Li et al. 2007). The optimal pore size for bone ingrowth has been reported to be in range of 150-600 μm to support sufficient vascularization and blood vessels invasion (Liu et al. 2013; Li et al. 2007). Pore sizes greater than 300 μm are recommended for bone ingrowth in comparison with smaller pore size (Bohner et al. 2011; Karageorgiou and Kaplan 2005; Murphy et al. 2010; Jones et al. 2004). This subject will be further developed in the review "*Bone Regeneration: non-degradable and degradable biomaterials*" (chapter 3).

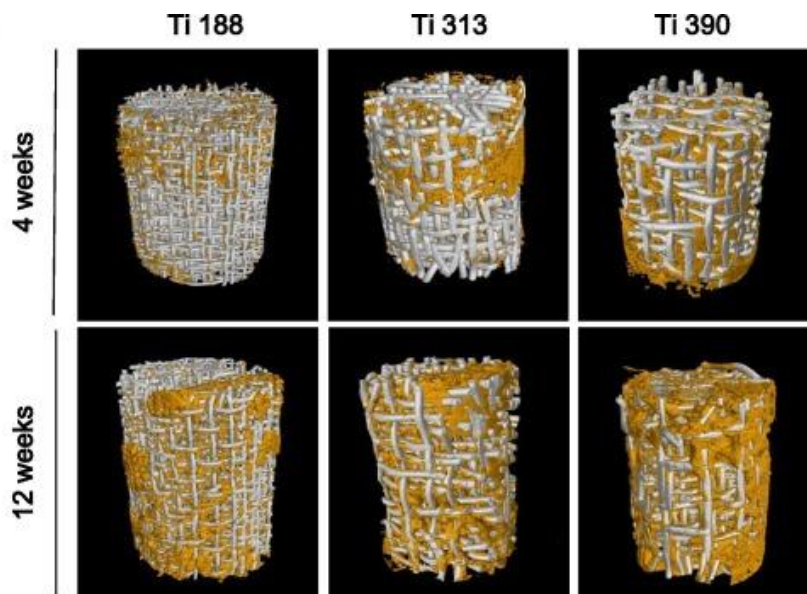


Figure 2-2 Bone ingrowth into porous titanium. Micro CT images of porous titanium implanted in rabbit femur (the yellow color represent the new bone) (Chang et al. 2016).

2.3 Methods for production of scaffolds

For a successful production of a 3D scaffolds or tissue substitutes for bone regeneration it should be considered the complex hierarchy and structural heterogeneity of the host tissue (Bose et al. 2013; Sun et al. 2004). Numerous methods have been developed to fabricate 3D porous scaffolds and each method results in a scaffold with different features such as internal architecture or pore size (Thavorniyutikarn et al. 2014). Chemical/gas foaming, solvent casting, and foam-gel are some of those that have been mostly used.

Solvent casting is a method in which a polymer solution is dissolved in a solvent with uniformly distributed salt particles of a specific size. The solvent evaporates, leaving the scaffold. This polymer matrix is then immersed in water to allow leaching of the salt particles, which results in the formation of a highly porous uniform 3D matrix (Bajaj et al. 2014; Thavorniyutikarn et al. 2014). **Freeze-drying**, also known as lyophilization, is a process in which a polymer (synthetic or natural) solution is poured into molds of specific dimensions and is cooled down below its freezing point, leading to the solidification of the solvent molecule (Thavorniyutikarn et al. 2014; Bajaj et al. 2014). In figure 2.3 is a comparison of the typical pores obtained by Solvent casting and freeze-casting as well as a description of both methods.

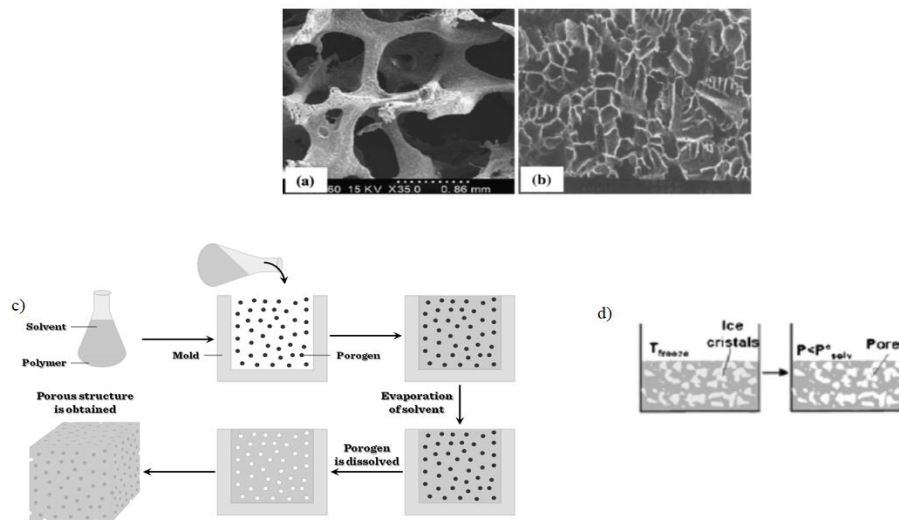


Figure 2-3 Representation of solvent casting and freeze drying pore morphology and their process. a) Typical pore morphology obtained with solvent casting technique; b) Typical pore morphology obtained with freeze drying; c) Schematic representation of solvent casting process; d) Schematic representation of freeze drying process.

Selective Laser Melting (SLM) is an additive manufacturing technique that allows the manufacture of 3D parts directly from CAD data. This process applies laser energy to powder beds in order to melt metals, ceramics or polymers and enables the production of nearly unlimited complex geometries. The selective laser melting process consist in first, the CAD model is broken down into layers and transferred to the Selective Laser Melting machine. Subsequently, the powder material is deposited as a defined thin layer on a substrate. The geometric information of the individual layers is transmitted by laser beam to the powder bed wherein the regions to contain solid material are scanned under an inert atmosphere, leaving a solid layer of the piece to be produced. After lowering the substrate by one layer thickness, the process steps are repeated until the part is finished (Bremen et al. 2012).

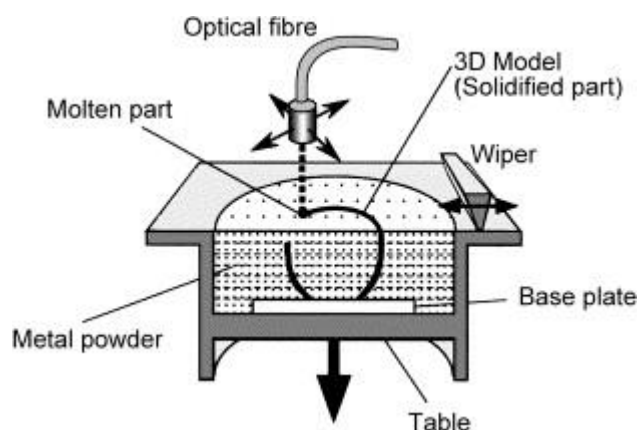


Figure 2-4 Process of selective laser melting (Abe et al. 2001).

Electrospinning is a versatile method that involves the use of an electrical charge to create non-woven scaffolds from a polymer solution, this process allows the fabrication of various fiber patterns with higher porosity (Thavornyutikarn et al. 2014). However, pore size, shape, and its interconnectivity cannot be fully controlled in these processes. Moreover scaffolds with tailored porosity for specific defects are difficult to manufacture with most of these approaches. Such scaffolds can be designed and fabricated using additive manufacturing (AM) approaches. Different manufacturing approaches including solid freeform fabrication, rapid prototyping (RP), allows complex shapes for scaffolds fabrication directly from computer aided design (CAD) file (Bose et al. 2013). **Rapid Prototyping** (RP) is a common name for a group of techniques such as 3D printing that can generate a physical model directly from computer-aided design data. This group of methods have tremendous potential to create 3D objects through repetitive deposition and processing material layers using computer-controlled equipment (Lam et al. 2002; Yeong et al. 2004). This process is defined as a set of manufacturing processes that are capable of producing complex-free form parts directly from computer-aided design (CAD) model of an object (Hutmacher 2000). The continuous improvement of RP systems accuracy and materials, expand gradually their applications to other areas of the industrial sector like rapid manufacturing (RM – the actual manufacturing of products in small batches) and rapid tooling (RT – fabrication of manufacturing tools and molds) (Giannatsis and Dedoussis 2009). The **3D printing technique**, invented in the Massachusetts Institute of Technology, is the only solid-phase RP technique that is compatible with hydrogels manufacturing. It is simple and versatile. A scheme of the process is represented in figure 2.4. The process starts with a binder jetting machine distributing a layer of powder onto a platform. Liquid droplets of a bonding agent are deposited onto the powder layer through inkjet print heads, bonding particles together. The platform is then lowered and a next layer of powder is laid out on top (Thavornyutikarn et al. 2014; Roseti et al. 2017).

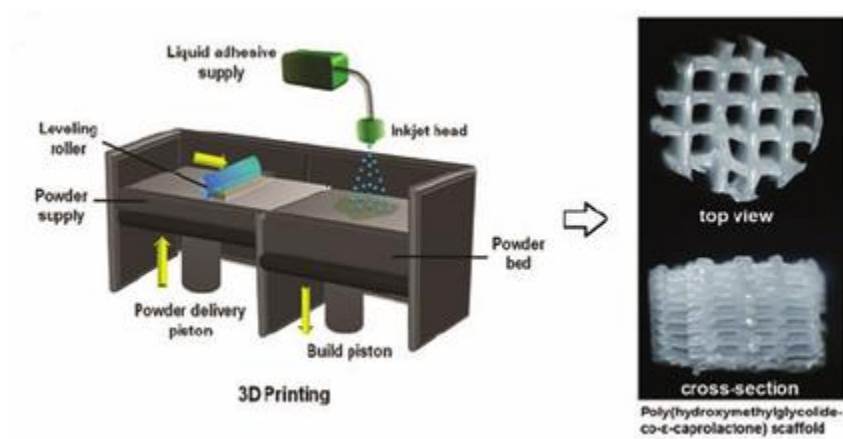


Figure 2-5 3D print. Schematic representation of the process and examples of scaffolds.

Although it is not commonly considered one of the many RP technologies, **computerized numerically controlled (CNC) milling** can successfully build some medical models (Winder and Bibb 2005). An example of a CNC machine is in figure 2.5. Machine tool automation was first introduced in the form of Computer Numerical Control (CNC) in the early 1970's, in which a dedicated computer replaced most of the digital hardware board of the Numerical Controlled (NC) machine. Process control is the automatic adjustment of programmed parameters such as speed. (Liang et al. 2002).



Figure 2-6 Example of a CNC milling machine.

2.4 Validation of scaffolds

After being produced, scaffolds must be characterized not only geometrically in terms of pore size, pore shape or surface topography but also in respect to the biological response to the environment of a living being. It is crucial to understand the factors and their influence in the biological response of the scaffold.

The development of a tissue engineering cell-scaffold requires the evaluation of its performance on pre-clinical *in vitro* and *in vivo* studies and clinical trial before their commercialization (Salgado et al. 2004; Böhner et al. 2011). National and international agencies are responsible for the authorization of every step in this process (Roseti et al. 2017). Figure 2.6 elucidate about the steps towards the validation of a new scaffold.

In vitro assays are important to provide information about material toxicity and immunogenicity, to evaluate the interaction between cells and biomaterials and to characterize cell activity while, *in vivo* research establishes a link between *in vitro* studies and clinical trials (Gomes and Fernandes 2011; Roseti et al. 2017).

Normally, to tests bone scaffolds *in vitro* cell lines are used, which is a homogenous population of cells with the ability to proliferate in culture without limit. Cell lines are obtained from bone tumors or from primary bone cells. The advantage of cell lines is their availability in enormous quantity without the need of isolation and the homogeneity of cell culture. However they do not express all tissue-specific characteristics (Bouët et al. 2014). Cell lines from human osteosarcoma, such as MG-63, SaOS-2 or U-2 OS, are extremely useful in studies to understand the interactions with osteoblasts and biomaterials. SaOS-2 cells have been characterized as exhibiting osteoblastic properties, including the ability to mineralize *in vitro* (Prideaux et al. 2014).

Animal models for bone regeneration fall into two categories: 1) ectopic models which are used in a first phase to distinguish between the proliferative and inductive capacity of the new biomaterial. Normally, for this phase, mice is the chosen animal and 2) orthotopic models are used to test the efficacy and safety of the new biomaterial, rabbits are commonly used for this phase but other animals such as goats, dogs and pigs are also used (Peric et al. 2015).

The next section is a literature review of the current state and recent developments of bone engineer.

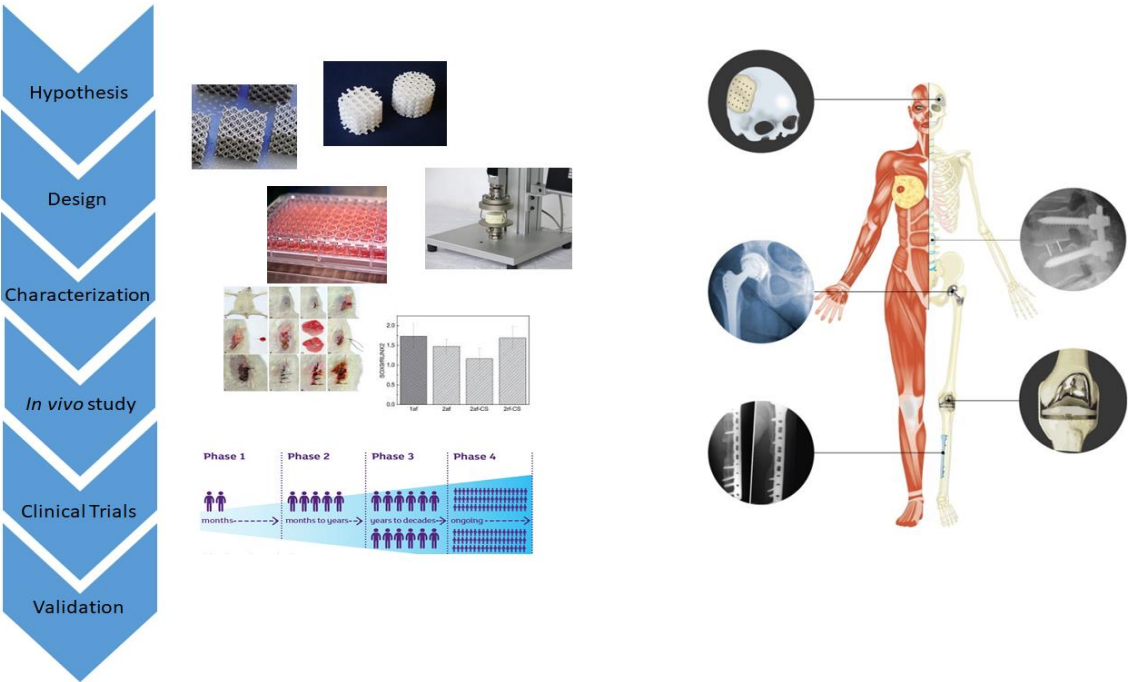


Figure 2-7 Steps towards the validation of a new scaffold.

2.5 References

- Abe F, Osakada K, Shiomi M, Uematsu K, Matsumoto M (2001) The manufacturing of hard tools from metallic powders by selective laser melting. *Journal of materials processing technology* 111 (1):210-213
- Agarwal R, García AJ (2015) Biomaterial strategies for engineering implants for enhanced osseointegration and bone repair. *Advanced drug delivery reviews* 94:53-62
- Albertini M, Fernandez-Yague M, Lázaro P, Herrero-Climent M, Rios-Santos J-V, Bullon P, Gil F-J (2015) Advances in surfaces and osseointegration in implantology. *Biomimetic surfaces. Medicina oral, patología oral y cirugía bucal* 20 (3):e316
- Amini AR, Laurencin CT, Nukavarapu SP (2012) Bone tissue engineering: recent advances and challenges. *Critical Reviews™ in Biomedical Engineering* 40 (5)
- Bajaj P, Schweller RM, Khademhosseini A, West JL, Bashir R (2014) 3D biofabrication strategies for tissue engineering and regenerative medicine. *Annual review of biomedical engineering* 16:247-276
- Bhattacharjee P, Kundu B, Naskar D, Kim H-W, Maiti TK, Bhattacharya D, Kundu SC (2017) Silk scaffolds in bone tissue engineering: an overview. *Acta Biomaterialia*
- Bohner M, Loosli Y, Baroud G, Lacroix D (2011) Commentary: deciphering the link between architecture and biological response of a bone graft substitute. *Acta biomaterialia* 7 (2):478-484
- Bose S, Vahabzadeh S, Bandyopadhyay A (2013) Bone tissue engineering using 3D printing. *Materials Today* 16 (12):496-504
- Bouët G, Marchat D, Cruel M, Malaval L, Vico L (2014) In vitro three-dimensional bone tissue models: from cells to controlled and dynamic environment. *Tissue Engineering Part B: Reviews* 21 (1):133-156
- Bremen S, Meiners W, Diatlov A (2012) Selective laser melting. *Laser Technik Journal* 9 (2):33-38
- Chang B, Song W, Han T, Yan J, Li F, Zhao L, Kou H, Zhang Y (2016) Influence of pore size of porous titanium fabricated by vacuum diffusion bonding of titanium meshes on cell penetration and bone ingrowth. *Acta biomaterialia* 33:311-321
- Chevalier J, Gremillard L (2009) Ceramics for medical applications: A picture for the next 20 years. *Journal of the European Ceramic Society* 29 (7):1245-1255
- Edwards S, Werkmeister J (2012) Mechanical evaluation and cell response of woven polyetheretherketone scaffolds. *Journal of Biomedical Materials Research Part A* 100 (12):3326-3331
- Florencio-Silva R, Sasso GRdS, Sasso-Cerri E, Simões MJ, Cerri PS (2015) Biology of bone tissue: structure, function, and factors that influence bone cells. *BioMed research international* 2015
- Forlino A, Marini JC (2016) Osteogenesis imperfecta. *The Lancet* 387 (10028):1657-1671
- Frost H (1990) Skeletal structural adaptations to mechanical usage (SATMU): 2. Redefining Wolff's law: the remodeling problem. *The Anatomical Record* 226 (4):414-422
- Geetha M, Singh A, Asokamani R, Gogia A (2009) Ti based biomaterials, the ultimate choice for orthopaedic implants—a review. *Progress in materials science* 54 (3):397-425
- Giannatsis J, Dedoussis V (2009) Additive fabrication technologies applied to medicine and health care: a review. *The International Journal of Advanced Manufacturing Technology* 40 (1):116-127
- Gomes P, Fernandes M (2011) Rodent models in bone-related research: the relevance of calvarial defects in the assessment of bone regeneration strategies. *Laboratory animals* 45 (1):14-24
- Hadjidakis DJ, Androulakis II (2006) Bone remodeling. *Annals of the New York Academy of Sciences* 1092 (1):385-396
- Holick MF (2014) *Osteomalacia and rickets*. Mosby Ltd Philadelphia, PA,

- Hutmacher DW (2000) Scaffolds in tissue engineering bone and cartilage. *Biomaterials* 21 (24):2529-2543
- Jones AC, Arns CH, Hutmacher DW, Milthorpe BK, Sheppard AP, Knackstedt MA (2009) The correlation of pore morphology, interconnectivity and physical properties of 3D ceramic scaffolds with bone ingrowth. *Biomaterials* 30 (7):1440-1451
- Jones AC, Milthorpe B, Averdunk H, Limaye A, Senden TJ, Sakellariou A, Sheppard AP, Sok RM, Knackstedt MA, Brandwood A (2004) Analysis of 3D bone ingrowth into polymer scaffolds via micro-computed tomography imaging. *Biomaterials* 25 (20):4947-4954
- Karageorgiou V, Kaplan D (2005) Porosity of 3D biomaterial scaffolds and osteogenesis. *Biomaterials* 26 (27):5474-5491
- Karp JM, Dalton PD, Shoichet MS (2003) Scaffolds for tissue engineering. *MRS bulletin* 28 (04):301-306
- Lam CXF, Mo X, Teoh S-H, Hutmacher D (2002) Scaffold development using 3D printing with a starch-based polymer. *Materials Science and Engineering: C* 20 (1):49-56
- Langer R, Vacanti J (1993) Tissue engineering. *Science* 260 (5110):920-926. doi:10.1126/science.8493529
- Li JP, Habibovic P, van den Doel M, Wilson CE, de Wijn JR, van Blitterswijk CA, de Groot K (2007) Bone ingrowth in porous titanium implants produced by 3D fiber deposition. *Biomaterials* 28 (18):2810-2820
- Liang SY, Hecker RL, Landers RG Machining process monitoring and control: the state-of-the-art. In: ASME 2002 International Mechanical Engineering Congress and Exposition, 2002. American Society of Mechanical Engineers, pp 599-610
- Liu Y, Lim J, Teoh S-H (2013) Review: development of clinically relevant scaffolds for vascularised bone tissue engineering. *Biotechnology advances* 31 (5):688-705
- Ma R, Tang T (2014) Current strategies to improve the bioactivity of PEEK. *International journal of molecular sciences* 15 (4):5426-5445
- Marrella A, Lee TY, Lee DH, Karuthedom S, Syla D, Chawla A, Khademhosseini A, Jang HL (2017) Engineering vascularized and innervated bone biomaterials for improved skeletal tissue regeneration. *Materials Today*
- Murphy CM, Haugh MG, O'Brien FJ (2010) The effect of mean pore size on cell attachment, proliferation and migration in collagen-glycosaminoglycan scaffolds for bone tissue engineering. *Biomaterials* 31 (3):461-466
- Peric M, Dumic-Cule I, Grcevic D, Matijasic M, Verbanac D, Paul R, Grgurevic L, Trkulja V, Bagi CM, Vukicevic S (2015) The rational use of animal models in the evaluation of novel bone regenerative therapies. *Bone* 70:73-86
- Piconi C, Maccauro G (1999) Zirconia as a ceramic biomaterial. *Biomaterials* 20 (1):1-25
- Prananingrum W, Naito Y, Galli S, Bae J, Sekine K, Hamada K, Tomotake Y, Wennerberg A, Jimbo R, Ichikawa T (2016) Bone ingrowth of various porous titanium scaffolds produced by a moldless and space holder technique: an in vivo study in rabbits. *Biomedical Materials* 11 (1):015012
- Prideaux M, Wijenayaka AR, Kumarasinghe DD, Ormsby RT, Evdokiou A, Findlay DM, Atkins GJ (2014) SaOS2 osteosarcoma cells as an in vitro model for studying the transition of human osteoblasts to osteocytes. *Calcified tissue international* 95 (2):183-193
- Raggatt LJ, Partridge NC (2010) Cellular and molecular mechanisms of bone remodeling. *Journal of Biological Chemistry* 285 (33):25103-25108
- Rodan GA, Martin TJ (2000) Therapeutic approaches to bone diseases. *Science* 289 (5484):1508-1514
- Roseti L, Parisi V, Petretta M, Cavallo C, Desando G, Bartolotti I, Grigolo B (2017) Scaffolds for Bone Tissue Engineering: State of the art and new perspectives. *Materials Science and Engineering: C*
- Salgado AJ, Coutinho OP, Reis RL (2004) Bone tissue engineering: state of the art and future trends. *Macromolecular bioscience* 4 (8):743-765

- Scarano A, Di Carlo F, Quaranta M, Piattelli A (2003) Bone response to zirconia ceramic implants: an experimental study in rabbits. *Journal of Oral Implantology* 29 (1):8-12
- Sepulveda P, Jones JR, Hench LL (2002) Bioactive sol-gel foams for tissue repair. *Journal of biomedical materials research* 59 (2):340-348
- Steinberg ME, Steinberg DR (2014) Osteonecrosis: historical perspective. In: *Osteonecrosis*. Springer, pp 3-15
- Sun W, Darling A, Starly B, Nam J (2004) Computer-aided tissue engineering: overview, scope and challenges. *Biotechnology and applied biochemistry* 39 (1):29-47
- Thavornnyutikarn B, Chantarapanich N, Sitthiseriratip K, Thouas GA, Chen Q (2014) Bone tissue engineering scaffolding: computer-aided scaffolding techniques. *Progress in biomaterials* 3 (2-4):61-102
- Wennerberg A, Albrektsson T (2009) Effects of titanium surface topography on bone integration: a systematic review. *Clinical oral implants research* 20 (s4):172-184
- Winder J, Bibb R (2005) Medical rapid prototyping technologies: state of the art and current limitations for application in oral and maxillofacial surgery. *Journal of oral and maxillofacial surgery* 63 (7):1006-1015
- Wu S, Liu X, Yeung KW, Liu C, Yang X (2014) Biomimetic porous scaffolds for bone tissue engineering. *Materials Science and Engineering: R: Reports* 80:1-36
- Yeong W-Y, Chua C-K, Leong K-F, Chandrasekaran M (2004) Rapid prototyping in tissue engineering: challenges and potential. *TRENDS in Biotechnology* 22 (12):643-652
- Zhao Y, Wong HM, Wang W, Li P, Xu Z, Chong EY, Yan CH, Yeung KW, Chu PK (2013) Cytocompatibility, osseointegration, and bioactivity of three-dimensional porous and nanostructured network on polyetheretherketone. *Biomaterials* 34 (37):9264-9277

3. NON-DEGRADABLE AND DEGRADABLE BIOMATERIALS FOR BONE TISSUE ENGINEERING SCAFFOLDING

Helena Filipa Pereira^{a,b,c}, Ibrahim Fatih Cengiz^{a,b}, Filipe Samuel Silva^c, Joaquim Miguel Oliveira^{a,b,d} and Rui Luís Reis^{a,b,d}

^a3B's Research Group - Biomaterials, Biodegradables and Biomimetics, University of Minho, Headquarters of the European Institute of Excellence on Tissue Engineering and Regenerative Medicine, Avepark - Parque de Ciência e Tecnologia, Zona Industrial da Gandra, 4805-017 Barco Guimarães Portugal;

^bICVS/3B's - PT Government Associated Laboratory, Portugal;

^cCenter for Micro-Electro Mechanical Systems - University of Minho, Azurém Campus, 4800-058 Guimarães – Portugal;

^dThe Discoveries Centre for Regenerative and Precision Medicine, Headquarters at University of Minho, Avepark, 4805-017 Barco, Guimarães, Portugal.

Abstract

The current “gold standard” treatment for large bone defects is the autograft, mostly due to its osteogenic, osteoinduction and osteoconduction properties. These allow new bone formation and vascularization, deliver growth factors and provide structural support. However, the use of autografts is painful, has a risk of infection and increases the demand for bone donors. The result of an appropriate scaffold for bone regeneration is a sum of several factors and the scaffolds that exist nowadays show limitations. One major drawback that tissue engineers have to solve is the lack of vascularization into bone scaffolds and several approaches are being proposed such as the introduction of pores. Other challenge is to meet a proper mechanical strength in a porous structure. In this review we focused on the biomaterials and methods used to improve scaffolds for bone regeneration. The clinical need for engineered alternatives, non-degradable biomaterials, degradable coatings and recent bone tissue engineering strategies are also reviewed herein. Despite of the great progress including the development of 3D structures, composites and hybrid scaffolds the gold standard scaffold for bone regeneration is not available and there still exists voids that need to be filled. It is extremely necessary to establish dosages for growth factors, protocols

for the usage of cells and procedures, and to conclude which biomaterials are more suitable for the treatment of bone critical defects.

Keywords: Biomaterials; Bone healing; Bone tissue engineering; *In vivo* studies; Scaffolds.

3.1 Bone structure

The regeneration to a functional bone is required due to tumor resection, extremity traumas or degenerative diseases and demands not only surgical advancement, but also the development of bone implants. In clinical the goal treatment is still autografting however its supply is limited. Thus new solutions for bone defects treatments are necessary (Wu et al. 2014; Sagomonyants et al. 2008). This first section of the review aims to provide a description of bone anatomy, bone healing and current repair therapies for the treatment of bone critical defects.

Bone is a complex heterogeneous tissue with high hierarchy consisting of a mineral phase, hydroxyapatite ($\text{Ca}_{10}(\text{PO}_4)_6(\text{OH})_2$) (analogous to geologic hydroxyapatite), an organic phase ($\approx 90\%$ type I collagen, $\approx 5\%$ non-collagenous proteins, $\approx 2\%$ lipids by weight) and contains between 10% and 20% of water (Boskey 2013). The cellular components of bone consist of osteogenic precursor cells, osteoblasts, osteoclast, osteocytes, and hematopoietic elements of bone marrow (Kalfas 2001). Osteoblasts are mature, metabolically active and use the correct bone forming cells which control the mineralization of the extracellular collagen (Boskey 2007; Kalfas 2001). When osteoblast become engulfed in mineral, they become a different type of cell, called osteocytes (Boskey 2007). Osteocytes are mature osteoblasts trapped within the bone matrix (Kalfas 2001). From each osteocyte a network of cytoplasmic processes extends through cylindrical canaliculi to blood vessels and other osteocytes allow their communication (Boskey 2007; Kalfas 2001). They are also involved in adaptive remodeling behavior via cell-to-cell interactions in response to local environment (Kalfas 2001). Finally, osteoclast cells are multinucleated which remove bone mineral and bone matrix and are controlled by hormonal and cellular mechanisms (Boskey 2007; Kalfas 2001).

The bones of the skeleton provide structural support and permit movement. They also provide protection to organs while also regulate mineral homeostasis and blood pH. The four general types of bone are: long bones, short bones, flat bones and irregular bones. The long bones are composed of diaphysis; metaphysis and epiphyses. The diaphysis is composed mostly by cortical bone, whereas the metaphysis and epiphysis are composed of trabecular meshwork bone surround by a thin layer of dense

cortical bone (Clarke 2008; Wu et al. 2014). There are three types of bone based on their anatomical shape and composition: woven bone, cortical bone and cancellous bone (Kalfas 2001). Woven bone is found during embryonic development, during fracture healing (callus formation), and in some pathologic states while cortical bone is dense and solid and surrounds the marrow space. Trabecular bone is composed of a honeycomb-like network of trabecular plates and rods interspersed in the bone marrow compartment (Kalfas 2001; Clarke 2008). At the macrostructure level, bone can be distinguished into: i) trabecular (corresponding to around 20% of the total skeleton), which forms a solid osseous shell around the bone and consists of dense and parallel, concentric, lamellar units – the osteons; ii) cortical bone (corresponding to around 80% of the total skeleton) which is remodeled from woven bone. The trabecular bone is supplied by diffusion from the surrounding bone marrow; there are no vessels within trabeculae and it is surrounded by cortical bone, but the thickness and strength of the cortical shell depends on location (Osterhoff et al. 2016; Kalfas 2001; Rho et al. 1998; Salgado et al. 2004). Although both types of bone are easily distinguished by their degree of porosity (trabecular bone is more porous) they have other differences such as trabecular bone being more metabolically active (Rho et al. 1998; Kalfas 2001).

Mechanical properties of bone depend on age, anatomical site and bone quality. The elastic modulus is the biomechanical property of bone that draws more interest because of its enormous importance for characterizing bone pathologies and guiding bone scaffolds design (Wang et al. 2016; Rho et al. 1998). In table 3-1 compressive strength and young modulus, the most important properties for the design of scaffolds are presented.

Table 3-1 Mechanical properties of human bone and bulk materials, values from literature (Yang et al. 2001; Wang et al. 2016; Santos et al. 2016; Schwitalla et al. 2015; Najeeb et al. 2016; Osman and Swain 2015).

Tissue/Biomaterial	Compressive strength	Young's modulus
	[MPa]	[GPa]
Cancellous Bone	4-12	0.02-2
Cortical Bone	130-180	3-30
Ti-6Al-4V	1080	113
ZrO2	5200	200
PEEK	130	3-4

The human skeleton has an exceptional healing capacity and is one of the most remarkable of all repair processes as it results not in a scar but in an actual reconstitution of the injured tissue (Fernandez-Yague et al. 2015; McKibbin 1978). Following bone trauma or disease the principal factors that influences the process of bone healing are: the availability of a blood supply; the mechanical stability; the size of defect; the incidence and severity of surrounding tissue injuries (Fernandez-Yague et al. 2015).

The process of fracture healing is a complex biological process and bone heals by either direct or indirect fracture healing. The most common process is indirect fracture healing and occurs in three distinct but overlapping stages: the early inflammatory stage; the repair stage; and the late remodeling stage (Kalfas 2001). In the inflammatory stage, a hematoma develops within the fracture site during the first few hours and days. Inflammatory cells (e.g. macrophages, monocytes, lymphocytes and polymorphonuclear cells) and fibroblasts infiltrate the bone under prostaglandin mediation. This results in the formation of a granulation tissue, ingrowth of vascular tissue and migration of mesenchymal cells. As vascular ingrowth progresses, a collagen matrix is laid down while osteoid is secreted and subsequently mineralized, which leads to the formation of a soft callus around the repair site. Eventually, the callus ossifies by the deposition of osteoblasts forming a bridge of woven bone between the fracture fragments (Kalfas 2001; Nyary and Scammell 2015; McKibbin 1978). Once the fracture has been satisfactorily bridged by callus, the newly formed bone is restored to its original shape, structure, and mechanical strength. Any excess callus is removed and the woven bone is remodeled into trabecular bone. The fracture healing is completed during this stage – remodeling stage. Remodeling of the bone continues long after the fracture has clinically healed (up to 7 years) (Kalfas 2001; Nyary and Scammell 2015). Direct healing is not a natural process. It requires an anatomical reduction of the fracture ends and a stable fixation, when these requirements are achieved the direct bone healing can occur (Marsell and Einhorn 2011). Bone healing is a major complex process that requires the recruitment of MSCs and once they are recruited, a molecular cascade starts involving collagen-I and collagen-II matrix production and the participation of several peptide signaling molecules. Growth factor-beta (TGF- β) superfamily members such as TGF- β 2, - β 3 and GDF-5 are also involved in the healing process. BMP-2, VEGF and the involvement of the metalloproteinase actions are key factors for the healing cascade (Marsell and Einhorn 2011). There are numerous biochemical and cellular factors related to the bone healing that associate with biomechanical and anatomical process completes an appropriate regeneration of bone defects. The translation of knowledge of bone healing process into clinics still isn't a reality as a strategy based of this healing steps could involve multiple surgical procedures or multiple injection.

3.2 Current repair therapies

Before addressing the solutions for bone regeneration it is important to define some concepts that are closely related. Osteogenesis, osteoinduction, osteoconduction and osteointegration are the four essential characteristics for the success of the scaffold. Osteogenesis is the capacity to produce new bone by the differentiation of osteoblasts. Osteoinduction has been defined as the process of recruitment, proliferation, and differentiation of host mesenchymal stem cells into chondroblasts and osteoblasts. Osteoconduction is the ability to provide an environment capable of hosting the indigenous mesenchymal stem cells, osteoblasts, and osteoclasts. The final bonding between host bone and the scaffold is called osteointegration (Ilan and Ladd 2002; Fillingham and Jacobs 2016).

Biomaterials

There are numerous approaches for promoting bone tissue regeneration. In figure 3-1 there are some examples of current products used in the treatment of bone defects. These products do not promote bone regeneration. They only fill the bone defect. One solution is a surgical procedure with autograft or allograft bone (Dimitriou et al. 2011; Murphy et al. 2013). Autograft bone graft consists in taking bone from another part of the patient's own body and is considered the clinical "gold standard". It is the most effective method for bone regeneration as it promotes bone formation over its surface by direct bone bonding and induces local stem cells to differentiate into bone cells without any associated immune response. It is commonly collected in the form of trabecular bone from the patient's iliac crest. Although it presents relatively good degree of success, the range of cases in which it can be used is restricted, mainly due to the limited amount of the autograft that can be obtained and due to donor site morbidity (García-Gareta et al. 2015; Salgado et al. 2004). Vascularized free fibular bone graft is a type of autogenous bone graft and it was first described in 1975 by Taylor (Taylor et al. 1975). It is used in large bone defects, more than 5-6 cm (Houdek et al. 2017). The advantage of these methods is the availability of bone stock, a faster union, less resorption of bone and fewer fatigue fractures. This process involves a long surgical procedure and can increase the morbidity on the donor site. In addition, there is a demand for further information about the factors that lead to failure. (Feuvrier et al. 2016; Houdek et al. 2017).

Allograft, bone taken from a donor, could be an alternative. However, when compared with autograft the rate of graft incorporation is lower. Allograft bone also introduces the possibilities of immune rejection and of pathogen transmission from donor to host, and although infrequent, infections could occur in the recipient's body after the transplantation (Salgado et al. 2004). To overcome the limitations described above, bone tissue engineering has been introduced (Ehrler and Vaccaro 2000). Presented

table 3-2 are the advantages and disadvantages of the most common bone scaffolds. In 1957 bovine bone was first introduced by Maatz and his colleagues (Maatz and Bauermeister 1957). Xenograft bone substitutes have their origin from a species other than human, it is similar to autologous bone grafts in that both are osteoconductive and relatively inexpensive (Campana et al. 2014).

Recently, the induced membrane technique (IMT) or Masquelet technique has been used to treat large bone defects. It is a two-step procedure: first, radical soft tissue and bone debridement is undertaken, then a cement spacer of polymethyl methacrylate (PMMA) is placed at the site of the bone defect and is stabilized with an external fixator (Giannoudis et al. 2011). The cement spacer prevents fibrous tissue invasion of the defect and induces the surrounding membrane that will revascularize the bone graft (Pelissier et al. 2004). Secondly, 6–8 weeks later the induced membrane is carefully incised. The spacer removed and cancellous bone from the iliac crest is implanted and the membrane closed with definitive fixation. Although these are interesting methods, there are complications, so studies for a better understanding of the procedures and complications are necessary (Morelli et al. 2016).

Table 3-2 Advantages and disadvantages of the most commonly used bone scaffolds.

Biomaterial	Advantages	Disadvantages	References
Autologous	Osteoinductive	Limited supply	(Oryan et al. 2014; Ehrler and Vaccaro 2000)
	Nonallogenic	Donor site morbidity	
	Osteogenic	Unpredictable resorption	
	Osteoinductive	Site pain Lack of vascularization	
Allograft	No donor site morbidity	Lack of vascularization	(Oryan et al. 2014; Ehrler and Vaccaro 2000)
	High availability	Lack of osteogenicity	
	Osteoconductive	Delayed incorporation	
	Osteoinductive	Availability of healthy grafts Rejection of the graft	

		Risk of disease transmission	
		Re-injury	
		Ethical concerns	
Xenograft	Cheaper	Lack of vascularization	(Oryan et al. 2014; Zakhary and Thakker 2017)
	No donor site morbidity	Lack of osteogenicity	
	High availability	Delayed incorporation	
	Osteoconductive	Availability of healthy grafts	
	Osteoinductive	Rejection of the graft more aggressively	
		Risk of zoonotic disease transmission	
		Re-injury	
		Ethical concerns	
Metals	Excellent mechanical properties	Corrosion	(Zakhary and Thakker 2017; Bhattacharya et al. 2016)
	Biocompatible	Risk of toxicity of metal ions	
	Osteointegration	Poor vascularization	
	Personalized manufacturing		
Ceramics	Biocompatible	Brittle	(Bhattacharya et al. 2016)
	High mechanical stiffness	Low elasticity	
	Good mechanical properties	Poor vascularization	
	Excellent resistance to corrosion	Bionert	

Polymers	Biocompatible	Poor vascularization	(Bhattacharya et al. 2016)
	Stable at high temperatures	Bionert	
	Good mechanical properties		
	Low young modulus		

3.3 Bone tissue engineering products

Tissue Engineering (TE) has evolved of the need to repair organs and tissues damaged and has been gaining importance in the last years (Karp et al. 2003; Salgado et al. 2004). A TE approach is based on the understanding of tissue formation and regeneration, and aims to induce new functional tissues, rather than just to implant new spare parts (Salgado et al. 2004). The main purpose of tissue regeneration is to support and facilitate the requisite physiological functions at the injury site (Shrivats et al. 2014). TE can be applied to all types of tissues that compose our body such as bone tissue (Shrivats et al. 2014; Roffi et al. 2017), osteochondral (Cengiz et al. 2014; Yousefi et al. 2015), cartilage (Devitt et al. 2017; Deng et al. 2016), neural tissue (Sensharma et al. 2017); skeletal tissue (Kwee and Mooney 2017); skin (Frueh et al. 2017); meniscus (Cengiz et al. 2017); or even blood vessels (Dimitrievska and Niklason 2017). A prospective randomized study was performed in 25 patients with benign bone tumors that were surgically treated with either bioactive glass S53P4 (BG) or autogenous bone (AB) as bone graft material. After 36 months that no significant difference between the AB and BG groups was observed, however, glass granules integrated in new bone were still visible (Lindfors et al. 2009). More recently developed calcium phosphate cements can be injected as a doughy substance that solidifies over several hours to yield a material with maximal compressive strength greater than that of normal cancellous bone (McAuliffe 2003).

The first injectable biologic cement was marketed in 1998 by FDA. Injectable mineral cements are widely used in bone tissue engineering due to their chemical composition being close to the mineral component of bone extracellular matrix. They have an advantage over blocks, granules, and pellets, that a custom fill of the defect is possible (Ilan and Ladd 2002). In a retrospective chart review a direct comparison of autografts, bone cement, and demineralized bone matrix in terms of function and outcomes was performed. A total of 28 patients underwent cranioplasty. Demineralized bone matrix was

the primary reconstructive material used in six patients. Seventeen patients had bone cement as the reconstructive material for cranioplasty; six patients had demineralized bone matrix; and five patients had bone autografts. It was concluded that residual defects and revision rates were significantly less when autograft or bone cement was used (Plum and Tatum 2015). An injectable BG/calcium sulfate composite cement with high content of BG was recently tested *in vivo* in a rabbit femoral condyle defect. The outcomes revealed that the cement had a better capacity than the PMMA and CSPC in terms of bone regeneration as well as the resorption rate observed in a critical-sized rabbit femoral condyle defect model which make this cement promising for the treatment of bone defects (Ren et al. 2017). A large number of bone-graft alternatives are currently commercially available for orthopedic use. They vary in composition, mechanism of action, characteristics and include mineral composites, ceramics, mineral cements, bioactive glasses and synthetic bone substitutes (Giannoudis et al. 2005; Ilan and Ladd 2002). The majority form of bone biomaterials used in clinics are presented in the form of putties or paste. An

important observation on what are being commercialize is that most of these products aim to fill the defect and not to promote bone regeneration. In figure 3-1 is represented some commercially solutions.

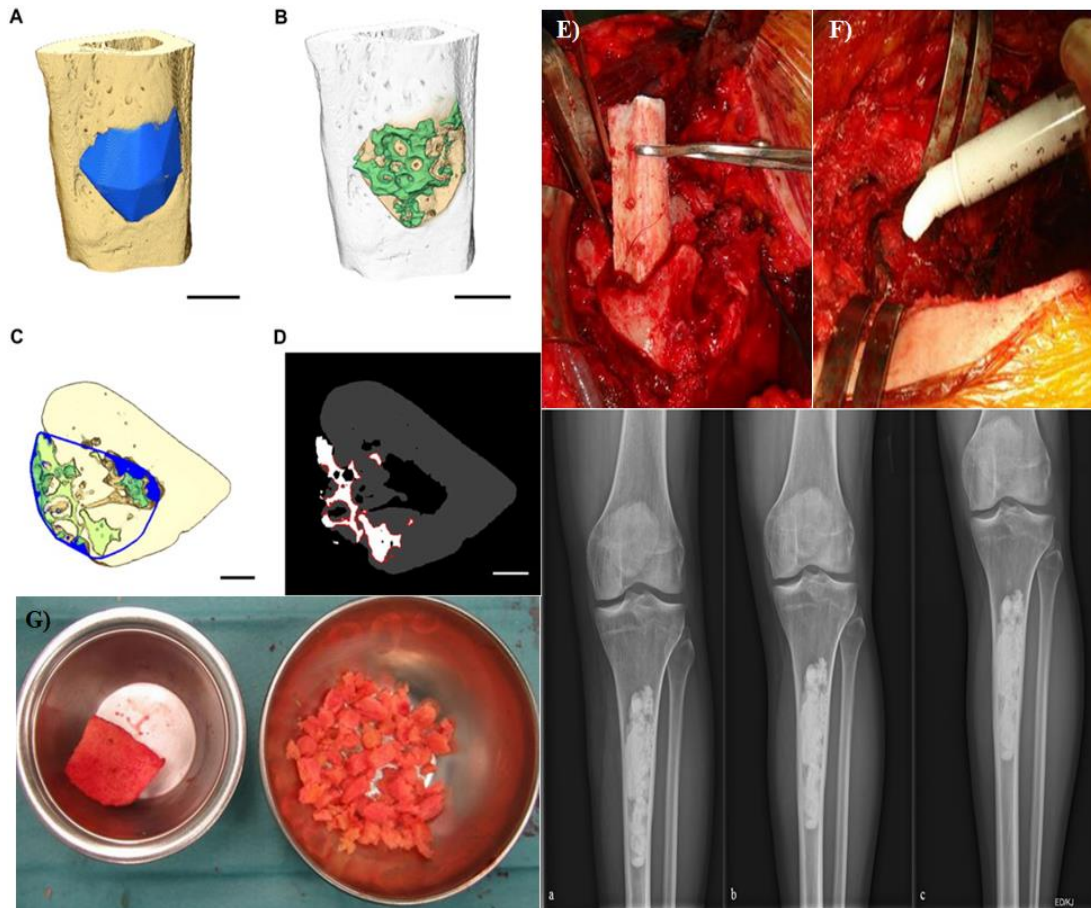


Figure 3-1 Current solutions for the treatment of bone defects. A- D) quantification of bone ingrowth and contact area in an Actifuse® sample. A) A 3-D reconstruction of the middle third of the rat tibia (yellow) with the region-of-interest (blue) determined by applying convex hull to the biomaterial. The volume and surface area of the bone (yellow) and biomaterial (green) inside the region-of-interest are calculated in (B). Scale bar in A and B is 1 mm. (C) A top-down view slice through the region-of-interest and bone, with the region-of-interest outlined in blue. (D) The contact area between the bone (grey) and biomaterial (white) as a red outline (Midha et al. 2013); E) autograft; F) injectable cements; G) Morcelized homologous bone graft obtained from a banked (Campana et al. 2014); lower panel images of x ray. (a–c) X-ray of a 36 year-old male patient few days following curettage of a low-grade chondrosarcoma of the left proximal tibia. (b and c) Follow-up radiographs 7 and 13 months following index surgery showing integration but no resorption of the artificial bone graft substitute (Friesenbichler et al. 2017).

3.4 Scaffolds for bone tissue engineering

3.4.1 Non degradable

A scaffold is a three-dimensional (3-D) construct that provides the necessary support for cells to proliferate and differentiate, they can appear in different shape like membranes or meshes (Hutmacher 2000; Kellomäki et al. 2000; Ribeiro et al. 2016). TE solutions for bone treatment can be divided into two groups: those that stimulates bone regeneration and those that provide a permanent solution, as a substitute of bone (Paxton 2017). For the treatment of bone defects the ideal scaffold should be developed to meet some requirements, in Table 3-3 is represented the most important.

Table 3-3 Requirements for the design of scaffolds in bone tissue engineering (Wang et al. 2016; Zakhary and Thakker 2017; Pina et al. 2016; Rahaman et al. 2011).

Criteria for scaffold design	Function
Biocompatibility	Capacity to be in a host tissue without initiate inflammatory response.
Suitable surface topography	Influence cellular behavior such as adhesion, proliferation and differentiation
3D structure	Host of the new formed tissue
Mechanical properties	Support the defect area
Porosity	Allow tissue ingrowth, nutrient and oxygen change and neovascularization
Osteoinductive	Able to recruit and differentiate mesenchymal cells

The biomaterial's biocompatibility can be evaluated by assessment methods which are provided by International Organizations Standards (ISO), Food and Drug Administration (FDA) and European Medicines Agency (EMA).

In the design of tissue engineering scaffolds, parameters including surface topography, chemistry, surface energy and wettability, pore size, shape, mechanical properties should be optimized to maximize the bone ingrowth (Jones et al. 2009; Tejero et al. 2014). Moreover, elasticity, compression or shear stress can influence cell behavior and even epigenetic status (Jean et al. 2004; Engler et al. 2006). Surface characteristics are critical for the successful design and medical application of

biomaterials as the surface is the earliest contact with the biological environment (Wu et al. 2014; Wennerberg and Albrektsson 2009). Surface properties, both chemical and topographical, can influence cellular adhesion and proliferation as it is involved in many of biological events occurring after implantation, which range from protein adhesion to bone remodeling (Albertini et al. 2015; Salgado et al. 2004). Topographies such as random nanofibers normally can influence cells into spreading and polygonal shapes which promotes the process of osteogenic differentiation (Liu et al. 2013). Many studies have shown a relation between cell attachment and surface roughness. Yavari and colleagues studied three variations of surface-modified porous titanium and concluded that the surface treatment improved cell response (Yavari et al. 2014). Cells can adapt their morphology according to the surface topography. It was observed by Qian et al. (Qian et al. 2013) that cells exhibit protruding filopodia in honeycomb-like scaffolds of PCL/nHA which indicates a proper cell spread. For a suitable scaffold integration, a surface with roughness is favorable as it enhances attachment, proliferation and differentiation of anchorage dependent bone forming cells (Albertini et al. 2015; Karageorgiou and Kaplan 2005; Wennerberg and Albrektsson 2009). Parameters such as wettability and surface free energy can influence cell growth more than surface roughness as Hallab et al. (Hallab et al. 2001) demonstrated. In their study, they concluded that surface free energy was a critical parameter for cellular adhesion and proliferation rather than roughness.

The importance of having a porous scaffold in bone regeneration was shown by Kuboki and his colleagues in 1998 when using a rat model to implant subcutaneously solid and porous scaffolds of hydroxyapatite for BMP-2 delivery (Kuboki et al. 1998). For proper bone regeneration in a scaffold, vascularization is necessary and cells from the surrounding must be able to penetrate. Pore size is a very important feature since if the pores are too small, pore occlusion by the cells will happen and which is also an important factor for protein adsorption, cellular migration and osteoconduction (Salgado et al. 2004; Prananingrum et al. 2016). Pore sizes greater than 300 μm are recommended for bone ingrowth in comparison with smaller pore size (Bohner et al. 2011; Karageorgiou and Kaplan 2005; Murphy et al. 2010; Jones et al. 2004). Fukuda et al. (Fukuda et al. 2011) compared the osteoinduction for different pore sizes, 500 μm , 600 μm , 900 μm , and 1200 μm , in identical environments. They concluded that the 500 μm pore size presented excellent osteoinduction. In another study with different pore sizes, Taniguchi et al. (Taniguchi et al. 2016) implanted porous titanium scaffolds with a pore size of 300 μm , 600 μm and 900 μm . They observed significantly higher fixation ability in 600 μm pore size than those with a pore size of 300 μm and 900 μm and the 300 μm implant exhibited inferior bone ingrowth in

cancellous bone. A experiment with scaffolds with pore sizes of 60 μm , 100 μm , 200 μm and 600 μm was performed by Prananingrum et al. (Prananingrum et al. 2016) three weeks after implanted into rabbit calvaria the scaffold with 600 μm pore size showed a greater bone ingrowth. Though, after 20 weeks the pore size of 100 μm presented greater bone ingrowth than the other pore sizes. In this study they suggested that bone regeneration into porous scaffolds is pore size-dependent whereas bone ingrowth was most prominent for the 100 μm -sized pores after 20 weeks *in vivo*. Porosity and pore size of a scaffold for bone tissue regeneration are key factors that will biologically improve allowing bone ingrowth and penetration of cells and nutrients. Nevertheless, these features become conflicting with others as the increase of pore size, the strength of the scaffold decreases which can lead to failure *in vivo*.

Metallic biomaterials

Metallic biomaterials are mainly used for the fabrication of scaffolds to replace hard tissue such as artificial hip joints, bone plates, and dental implants due to their mechanical properties and corrosion resistance (Nielsen 1987; Niinomi 2003, 2008). Stainless steel was the first metallic biomaterial used successfully as an implant and it is one of the main metallic materials used amongst with cobalt (Co) based alloys, titanium (Ti) and its alloys (Elias et al. 2008; Goriainov et al. 2014; Niinomi 2003). Stainless steel biomaterials are the most practical and are often used as acceptable cup (one half of an artificial hip joint) applications (Dewidar et al. 2007; Niinomi 2008). Stainless steel materials are resistant to a wide range of corrosive agents due to their high Cr (Chromium) content which allows the formation of the strongly adherent, self-healing and corrosion resistant coating oxide. Several types of stainless steel are available and the most widely used for implants manufacture is austenitic stainless steel (Navarro et al. 2008).

Co-Cr-based alloys are the representative Co alloys for biomedical applications (Niinomi 2002). They are advantageous for the fabrication of medical devices parts subjected to wear, such as the heads of artificial hip joints (Niinomi 2002, 2008). These materials have a high elastic modulus (240 GPa) similar to stainless steel (210 GPa) and an order of magnitude higher than that of cortical bone (3-30 GPa) as presented in Table 1. In contact with bone, the metallic devices will take most of the load due to their high modulus, producing stress shielding in the adjacent bone. The lack of mechanical stimuli on the bone may induce its resorption that will lead to the eventual failure and loosening of the implant (Navarro et al. 2008). Co alloys for biomedical devices are grouped into two categories: cast alloys and wrought alloys, the latter are used for applications where high strength is needed (Niinomi 2002, 2008).

Titanium and its alloys are getting much attention for biomedical applications because of their excellent mechanical, physical and biological performance, corrosion resistance and their outstanding biocompatibility (Rack and Qazi 2006; Niinomi 2003; Xiang and Spector 2006). Fujibayashi et al. in 2004 implanted porous titanium in the dorsal muscles of beagles and observed bone formation after twelve-months, this was the first report using only porous titanium (Fujibayashi et al. 2004). Titanium and its alloys, originally used in aeronautics, became materials of great interest in biomedical field, due to their excellent properties that include a good corrosion resistance and a low density (Navarro et al. 2008). Commercially pure Ti (CP Ti), typically with single phase alpha microstructure, is currently used in dental implants while titanium with 6% aluminum and 4% vanadium, Ti-6Al-4V, is mostly used in the orthopedic field. The Al and V alloy elements stabilize the alpha-beta microstructure, and improve the mechanical properties (Navarro et al. 2008). Ti-6Al-4V is used for its excellent corrosion resistance and their elastic modulus (113 GPa) that is approximately half that of stainless steel (210 GPa) and cobalt– chromium alloys (240 GPa) and consequently the stress shielding will be lower (Xiang and Spector 2006; Geetha et al. 2009; Wally et al. 2015).

Ceramic biomaterials

Ceramics are generally defined as inorganic, non-metallic materials (Chevalier and Gremillard 2009). Bioinert ceramics such as alumina, zirconia and several porous ceramics are the most used in orthopedic devices (Piconi et al. 2003; Navarro et al. 2008). Alumina have a great performance under compression, but is brittle under tension and has been used for nearly 20 years owing to its low friction and wear coefficients (Piconi et al. 2003; Navarro et al. 2008).

Zirconia is a polymorph that can be categorized into three crystallographic phases (El-Ghany and Sherief 2016; Piconi and Maccauro 1999). Pure zirconia is monoclinic (m) at room temperature and pressure in the form of a deformed prism with parallelepiped sides. As the temperature increases the material transforms to tetragonal (t) by approximately 1170 °C and it has the form of a straight prism with rectangular sides, and then to a cubic (c) fluorite structure starting about 2370 °C and melting by 2716 °C in the form of straight prism with square sides (El-Ghany and Sherief 2016; Kelly and Denry 2008; Piconi and Maccauro 1999). These transformations are characterized by: being diffusionless which means that only involves coordinated shifts in lattice positions versus transport of atoms); occurring athermally implying the need for a temperature change over a range rather than at a specific temperature

and involving a shape deformation (volumetric expansion) (Kelly and Denry 2008; Douillard et al. 2012). Alloying pure zirconia with stabilizing oxides such as CaO, MgO, Y_2O_3 or CeO₂ allows the retention of the tetragonal structure at room temperature (which is metastable) and therefore the control of the stress-induced due to the phase transformation, efficiently arresting crack propagation and leading to high toughness (Chevalier 2006; Denry and Kelly 2008). Zirconia is one of the ceramic materials with the highest strength suitable for implants and presents other advantages like being bioinert, having excellent resistance to corrosion and wear, high fracture toughness and is biocompatible (El-Ghany and Sherief 2016; Navarro et al. 2008; Scarano et al. 2003). These favorable mechanical properties are a consequence of phase transformation toughening, which increases its crack propagation resistance (Chevalier 2006; Chevalier and Gremillard 2009).

Biomedical grade zirconia containing 3mol% Yttria (Y_2O_3) as a stabilizer is a new ceramic material with unique properties: it has favorable mechanical properties comparatively to the highest values of oxide ceramics and has high fracture toughness because of the energy-absorption property during martensitic transformation of tetragonal particles to monoclinic ones, which results in a characteristic similar to steel (Ichikawa et al. 1992; Denry and Kelly 2008; Han et al. 2016).

Polymeric Biomaterials

PEEK is a semi-crystalline linear polycyclic aromatic thermoplastic and it represents the dominant member of the PAEK polymer family (Kurtz and Devine 2007; Ma and Tang 2014). PEEK is biocompatible, chemically and physically stable, with excellent mechanical properties and it can be processed using a variety of commercial techniques (Johansson et al. 2014; Kurtz and Devine 2007). Moreover, PEEK is stable at high temperatures with a high melting point of 334 °C, is insoluble in all conventional solvents at room temperature, with exception of 98% sulfuric acid and it remains stable in sterilization processes (Johansson et al. 2014; Kurtz and Devine 2007; Ma and Tang 2014). The major beneficial property for orthopedics application is its lower Young's (elastic) modulus (3-4 GPa) being close to human bone (17.7 GPa) in comparison with Ti alloy (113 GPa) and Co-Cr alloy (240 GPa) which reduces the stress shielding after implantation (Najeeb et al. 2016; Akkan et al. 2014; Ma and Tang 2014). Due to its strength PEEK is used in many orthopedic applications (Panayotov et al. 2016).

3.4.2 Degradable

Today, biomaterials that are used to prepare scaffolds can be natural or synthetic, degradable or non-degradable. For example natural polymers such as chitin and chitosan or collagen are being used for applications in tissue engineering (Deepthi et al. 2016; Kuttappan et al. 2016). Synthetic polymers such as Polycaprolactone (PCL) are biodegradable and can be produced with different features for applications in bone tissue engineering (Tian et al. 2012). Hydrogels which are hydrated polymer chains are gaining attention as a delivery system of cells and growth factors for bone tissue engineering applications (Bacelar et al. 2017; Rice et al. 2013). Biodegradable materials are materials that fragment over time after being implanted in the body. Many different terms have been used to describe them such as absorbable, resorbable and degradable. The concept of bioabsorbable was first introduced by Kulkarni et al. (Kulkarni et al. 1966).

Biodegradable Polymers

Biodegradable polymers can be classified into two types: natural polymers and synthetic polymers. Synthetic polymers have been widely studied especially polyglycolic acid (or polyglycolide (PGA)), polylactic acid (or polylactide (PLA)), polylactide-co-glycolide (PLGA), poly (D,L-lactic acid), polyethylene glycol (PEG), and poly(ϵ -caprolactone) (PCL) (Canadas et al. 2014). PGA is very similar to PLA however PLA exhibits different chemical, physical, and mechanical properties because of the presence of a pendant methyl group on the alpha carbon (Gentile et al. 2014). These polymers can be used as a drug delivery system (El Bialy et al. 2017). Although they present characteristics like having good processability and manageability they lack of rigidity and stability (Elgali et al. 2017).

In a recent study, Alenezi et al. (Alenezi et al. 2017) sustained release of clarithromycin from PLGA microspheres within β -TCP for bone regeneration was evaluated in rabbit a calvaria defect model. They showed that PLGA was capable of releasing clarithromycin increasing the bone regeneration.

Collagen is a natural polymer that provides strength and structural stability to tissues. Gelatin a derivative of collagen. Ren et al. (Ren et al. 2016) described a nanoparticulate mineralized collagen glycosaminoglycan scaffold that is capable of promote bone regeneration in rabbit cranial defects. These results are interesting as it was not added expanded stem cells or exogenous growth factors.

Chitosan is a polysaccharide that can be used in many applications. It exhibits antibacterial activity, along with antifungal, mucoadhesive, analgesic and haemostatic properties (Croisier and Jérôme 2013). Oryan et al. (Oryan et al. 2017b) studied the healing potential of a composite scaffold consisting of chitosan (CS), gelatin (Gel) and platelet gel (PG). They observed that their scaffold showed significantly

higher new bone formation, density of osseous and cartilaginous tissues, bone volume, and mechanical performance.

Biodegradable Ceramics

Calcium phosphate ceramics have been widely used as bone substitutes, coatings, cements, drug delivery systems and tissue engineering scaffolds (Lobo and Livingston Arinzeh 2010). Tricalcium phosphate (TCP) $\text{Ca}_3(\text{PO}_4)_2$ is a bioactive and biodegradable ceramic material. Tricalcium phosphate implants have been used for two decades as the synthetic bone void fillers in orthopedic and dental application, as it can be observed in table 3-4 the majority of commercially products are composed by calcium phosphates.

Bioactive glass and its related glass ceramic biomaterials are an interesting biodegradable biomaterial used in the production of scaffolds for bone regeneration (Fernandes et al. 2017). Gantar et al. (El-Rashidy et al. 2017) prepared a bioactive-glass-reinforced gellan-gum spongy-like hydrogel. In figure 3-2 there is a comparison of the performance *in vivo* of different materials.

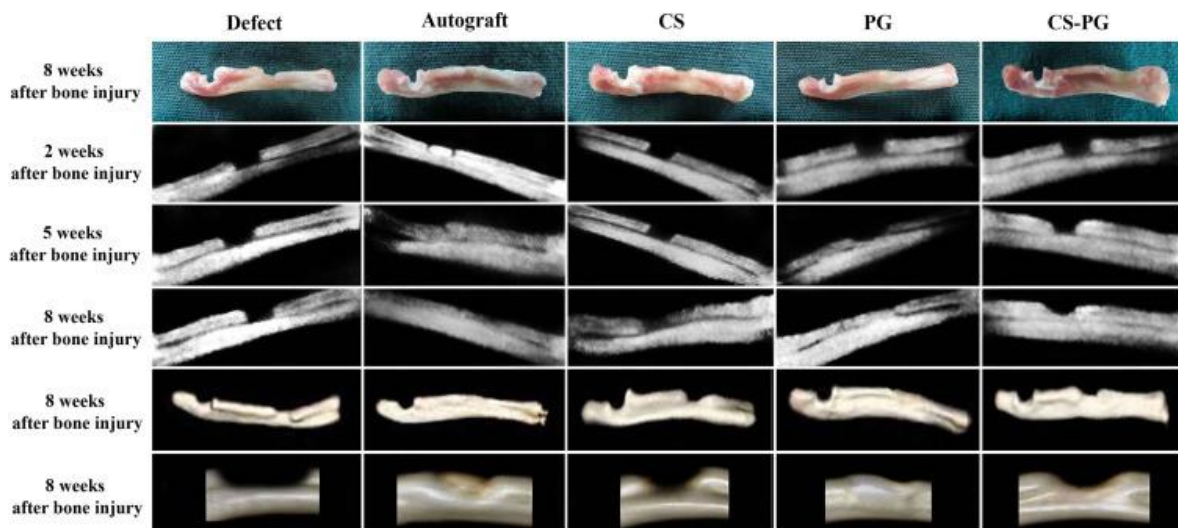


Figure 3-2 Gross morphologic, radiologic and three dimensional (3D) CT-scan images of the injured healed radial bones of rats (Oryan et al. 2017a).

Table 3-4 List of some bone tissue engineering products commercially available.

Company name	Product name	Composition	Reference
Synthes	Norian SRS	Calcium Phosphate	(Giannoudis et al. 2005).
Isotis Orthobiologics	OrthoBlast	19.5% demineralized bone and 12.5% cancellous allograft	(Kim et al. 2010).
Wright Medical Technology	PRO-STIM	50% calcium sulfate, 10% calcium phosphate, and 40% DBM	(Teufack et al. 2014)
Exactech	Optefil	DBM/gelatin	(Patel 2015)
Neo Dental Chemical Products	Vitapex	Mix of calcium hydroxide and iodoform	(Wu et al. 2016).
Medtronic	Infuse	Silicate substituted calcium phosphate	(Midha et al. 2013)
Zimmer	CopiOs	dibasic calcium phosphate and type 1 collagen	(Roberts et al. 2011).
Wright Medical Technology	Allomatrix	calcium sulphate and DBM	(D'Agostino and Barbier 2013).

Baxter International	ACTIFUSE	Porous silicon substituted HA granules	(Midha et al. 2013)
Pioneer Surgical Technology	nanOss Bioactive 3D	Porous hydroxyapatite granules + porous porcine gelatin-based foam matrix	(Walsh et al. 2013)
Orthovita	Vitoss	porous β -TCP combined with type I bovine collagen	(Walsh et al. 2017)

Regardless of notable progress in bone tissue engineering relatively few orthopedic designs have been used in clinical (Fernandez-Yague et al. 2015). The main limitation regarding to current solutions is insufficient vascularization and poor nutrient transport in the scaffold resulting in death of cells which leads to a reduced osteointegration. Another limitation and although there is a great demand in producing porous scaffolds, is the mechanical strength as it is heavily dependent on porosity and geometry of the scaffold. Therefore the big challenge in producing scaffolds for bone regeneration is in developing a solution that allows cell penetration, nutrient and oxygen exchange and still be able to support load (Sarkar and Lee 2015; Fernandez-Yague et al. 2015).

In vitro assays allow us to understand the fundamental biological mechanism, the biological activity, toxicity and also the evaluation of the cell response to the biomaterial. In this sense, animal models are crucial in providing complementary information on biological reactions such as inflammatory reactions between scaffolds and bone and even to evaluate the performance of the scaffold. A number of animal models, such as rat/mouse, rabbit, sheep, goat, and pig have been used to simulate human environment (Josset et al. 1999; Li et al. 2015a). Table 3-5 gives the current state of bone tissue engineering studies.

Table 3-5 Scaffold biomaterials used in the recent *in vivo* experiment for bone tissue engineering studies, and the outcomes.

Biomaterial	Cells	Growth factors	Animal model	Follow up	Reported outcome	Ref.
--------------------	--------------	-----------------------	---------------------	------------------	-------------------------	-------------

Three dimensional cell-scaffold constructs for application in bone tissue engineering

Ti-6Al-4V	-	-	Rabbit femoral bone	10 weeks	Osteointegration was observed.	(Cohen et al. 2017)
Ti-6Al-4V	-	-	Goats	12 months	At 12 months was observed new bone formation at both ends and in the middle of scaffold.	(Liu et al. 2016)
PEEK	-	-	Rat femoral segmental defect	12 weeks	Bone ingrowth into the pore network was observed.	(Evans et al. 2015)
PEEK	-	-	Rabbit femoral bone	12 weeks	Adjacent tissue integration and bone ingrowth was observed.	(Hildebrand et al. 2017)
Titanium + Gelatin	-	VEGF; TGF-β1; TGF-β2	Rabbit skull	8 weeks	Bone and vessels regeneration was observed.	(Zhang et al. 2017)
Ti6Al4V coated Hydroxyapatite	-	-	Rabbits	12 weeks	Osteointegration and osteogenesis observed.	(Liu et al.)

						2015b)
Titanium	-	-	Pigs skull	5 weeks	Osteointegration of the scaffold was observed.	(G uyer et al. 2016)
HA/Alumina	-	-	Dog Tibia	8 weeks	New bone formation in the defect.	(Ki m et al. 2015)
β- tricalcium Phosphate	BMSCs	-	Non-Human Primate femur	15 months	Five of seven cases showed bone union of the defect. In the group without BMSCs four of five failed the regeneration.	(M asaoka et al. 2016)
β- tricalcium Phosphate + platelet rich fibrin	-	-	Pig tibial defect	12 weeks	This study aimed to evaluate the effect of PRF alone and combined with β -TCP. They observed more new bone formation with the combination of PRF and β -TCP.	(Yil maz et al. 2014)

Poly(L – Lactic- acid) – poly (ε caprolactone	SSCs	-	Sheep Tibia	12 weeks	The analyses confirmed a trend towards increasing bone formation, however this study had a small number of animals studied (n=4).	(S mith et al. 2017)
Poly (glycerol sebacate)	Blood cells	-	Rabbits Ulna	8 weeks	The ulna critical defect was full regenerated in 8 weeks.	(Zaky et al. 2017)
β -tricalcium Phosphate coated with poly lactic-co-glycolic acid	MSCs and EPCs	VEGF	Dog mandibula	8 weeks	The bone formation was better in scaffolds containing MSC, either mixed with EPC or incorporating VEGF. In this study it can also be concluded that there is no benefit in adding both EPC and VEGF.	(Khoja steh et al. 2017)

3.5 Biodegradable coatings

Each biomaterial has its own advantages and disadvantages as bone scaffold material which could be overcome by combining different materials. To improve the properties of scaffolds for bone tissue applications, to take advantage of the good mechanical properties of some materials and the bioactivity

of other materials, researchers have been coating them with materials that mimic the natural bone surface (Shin et al. 2017; Galliano et al. 1998).

There are several different techniques to coat the scaffold surface such as: spin coating, which is one of the most popular technique to obtain uniformly thin coatings (Yuan et al. 2016); sol-gel process is being used to prepare bioactive glasses (Fathi and Doostmohammadi 2009); electrophoretic deposition (EPD) is gaining attention in biomedical field as it can achieve uniform coating in scaffolds with complex and porous shapes (Molino et al. 2017); auto-catalytic deposition (Oliveira et al. 2005); dip coating (Lee et al. 2017); spray deposition (Tang et al. 2006); ion beam assisted deposition (Bai et al. 2012) and other techniques.

Geesink et al. (Geesink et al. 1988), in 1988, used plasma-spray to coated titanium implants with apatite and evaluated *in vivo* in a canine model. They concluded that apatite-coated implants could bond as strong as cortical bone itself. Calcium phosphate-based materials such as hydroxyapatite (HA), β -tricalcium phosphate (β -TCP) and biphasic calcium phosphate have similar composition of natural bone which allows them to directly bond to living bone (Rahaman et al. 2011; Yazdimamaghani et al. 2017). HA ($\text{Ca}_5(\text{PO}_4)_3(\text{OH})$) is an important calcium phosphate, since its chemical composition and structure are very similar to the mineral component of bone. It has exceptional characteristics such as bioactivity, biocompatibility and can achieve very high mechanical strength. As a coating, it can provide to the scaffold osteoconductivity that enhance the cell attachments and proliferation (Zakaria et al. 2013; Campana et al. 2014; Søballe 1993). β -TCP is a well characterized osteoconductive biomaterial that can be used for bone regeneration applications.

In 1971, L. L. Hench and co-workers discovered that bioactive glass (BG), a silicate glass based, was able to bond with bone and soft tissues (Hench et al. 1971). 45S5 and 13-93 are two well-known bioactive glasses. This material has the amazing ability to form an interfacial bond with the host tissue; when implanted, they induce the formation of a dense surface layer of hydroxycarbonate apatite (HCA), which is very similar to the mineral component of bones and ensures a great adhesion. Bioactive glasses are a silicate based and by varying the proportions of sodium oxide, calcium oxide, and silicon dioxide, all range of forms can be produced from soluble to non-resorbable. They possess both osteointegrative and osteoconductive properties (Giannoudis et al. 2005; Rahaman et al. 2011). One limitation for the use of 45S5 glass and other bioactive glasses is that the local biological microenvironment is influenced by their degradation products (Rahaman et al. 2011). Borate bioactive glasses present properties that allow cell proliferation and differentiation *in vitro* (Liu et al. 2010). In a

study, Zhang et al. (Zhang et al. 2015) compared the ability to repair bone defects of both β -TCP and BG and concluded that BG had better performance, they also observe that the dissolution products of BG were capable of promoting osteogenic differentiation which lead to the regeneration of the defect. Although BG has good potential for regenerate bone the concentration of boron release is still a concern. Ye et al. (Ye et al. 2017) developed and tested a 3D porous structure of Ti-6Al-4V coated with BG. The in vitro results demonstrated cell attachment, proliferation and differentiation of human bone marrow stromal cells. The obtained coating presented stability and interfacial adhesion.

The surface properties are crucial for the good performance of a scaffold. The functionalization of the scaffolds surface with bioactive coats is a promising strategy. As can be observed in figure 3-3 surfaces with coatings promote a better bone growth and a better integration with the host tissue.

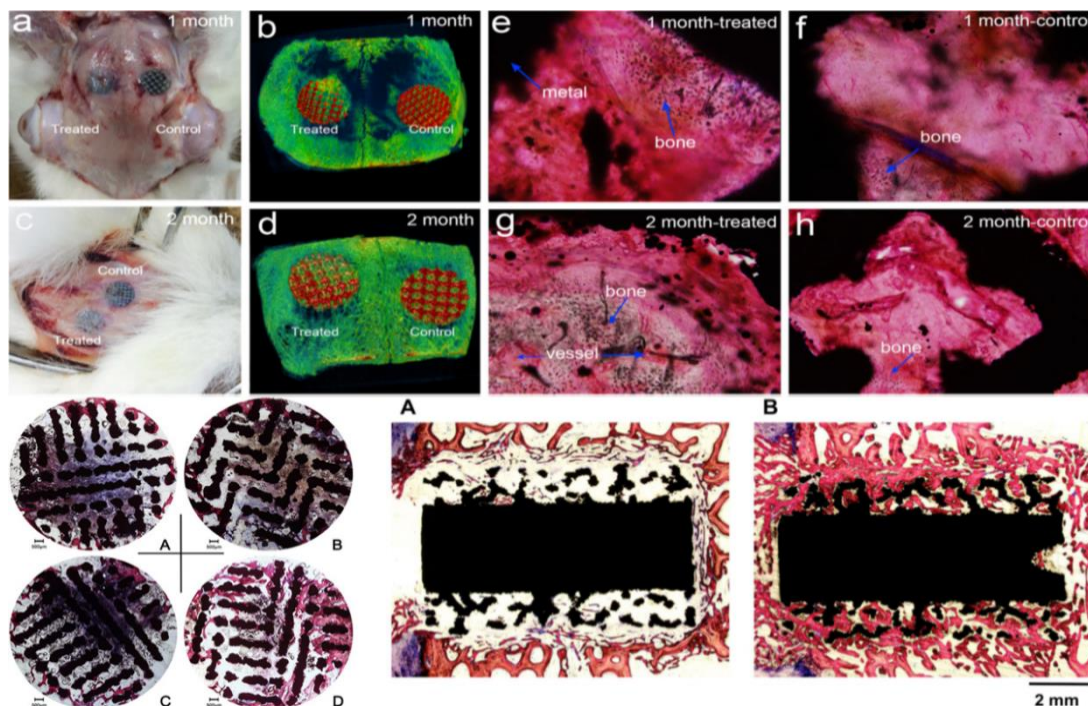


Figure 3-3 Performance of coated scaffolds *in vivo*. Upper panel: a – h) Implantation of the scaffolds in skull defects for 1 and 2 months. a, b) The treated and control scaffolds implanted in the skull for 1 month were examined using micro-CT. c, d) The treated and control scaffolds implanted in the skull for 2 months were examined by micro-CT. The micro-CT image was captured at the middle level of the entire scaffold. Green represents normal tissue, while red represents the titanium scaffold. The treated group showed more tissue ingrowth than the control group. Hard-tissue sections after H&E staining (e–h). The large black area represents the titanium edge under the microscope. The small and irregular pieces of black chips observed in the pores reflect cut titanium. Under H&E staining, the bone tissue was only slightly white and showed slight nuclear staining (Zhu et al. 2017); lower left panel: a-d) Histological observations of the TI and HA-TI groups at low magnification (Van Gieson stain, 16 ×). The distribution of new bone (red) and fibrous tissue (dark blue) in the TI group at 2 months post-implantation (A), the HA-TI group at 2 months post-implantation (B), the TI group at 4 months post-operation (C), and the HA-TI group at 4 months post-operation (D) (Huang et al. 2015); lower right panel: Histological images of transverse sections through titanium implants upon which had been deposited a layer of calcium phosphate bearing a BMP-2 concentration of 500 µg/g of coating (A) 3 and (B) 6 weeks after their insertion into the proximal tibial bone. (A) At the 3-week juncture, the resorption of bone outweighed its formation in both the mesh and the peri-implant spaces, as evidenced by the lack of staining for osseous tissue. (B) By the end of the 6th week, the balance between bone resorption and bone formation had been tipped in favour of the latter process (Hunziker et al. 2016).

3.6 Other regenerative strategies

To overcome the limitations of scaffolds researchers started to use different approaches such as introducing cells like bone marrow cells or incorporating growth factors into the scaffolds. There are five types of cell that are currently used in bone regeneration: embryonic stem cells (Kuhn et al. 2013); fetal stem cells (Todeschi et al. 2015); human umbilical vein endothelial cells (Kargozar et al. 2017); induced pluripotent stem cells (de Peppo et al. 2013) and adult stem cells (Grayson et al. 2015).

Mesenchymal stem cells (MSCs) are the main cells used for bone tissue approaches mostly due to their pluripotency and they were discovered in 1966 (Pittenger et al. 1999; Friedenstein et al. 1966). They can be isolated from mesenchymal tissues including bone marrow and are capable of differentiate into osteoblasts when submitted to a osteoinductive signal (Stanovici et al. 2016). Arne et al. (Berner et al. 2015) reported that a delayed injection of MSCs into a biodegradable composite scaffold 4 weeks after the defect occur led to an improvement of bone regeneration compared with pre seeded scaffolds. There are evidences of the paracrine effect of MSC on bone regeneration (Linero and Chaparro 2014). Moreover, recently evidence have shown that MSCs' ability to produce a large variety of trophic factors that stimulate adjacent parenchymal cells to start repairing damaged tissues can enhance a proper bone regeneration (Fu et al. 2017). Regardless to their potential, there are still concerns about sudden death of cells, sedimentation into other organs causing undesired differentiation, inflammation and secondary cancers (Bružauskaitė et al. 2016). Adipose tissue is abundant, accessible and a source of stem cells that as the potential to be an alternative to MSCs as they have the capacity to differentiate into osteoblast lineage (Gimble and Guilak 2003). The acquirement of adipose tissue is less expensive than bone marrow, with less invasive operation and available in more quantity (Zhu et al. 2008). Liao et al. (Liao et al. 2016) showed ADSCs high osteogenic differentiation rate in a study using porcine ADSCs in combination with polycaprolactone – β – TCP scaffolds coated with collagen.

More recent regeneration scaffolds are incorporating growth factors related with bone healing, osteoinduction and osteoconductivity such as platelet-derived growth factors (PDGFs), basic fibroblast growth factor (b FGF), transforming growth factor- β (TGF- β) and vascular endothelial growth factor (VEGF). BMP, known as bone morphogenetic protein are secreted signaling molecules that belongs to TGF- β superfamily and can induce new bone formation and it was discovered in 1965 (Urist 1965; Ducy and Karsenty 2000). BMP-2, BMP-4, BMP-6, and BMP-7 have long been recognized as osteoinductive, and BMP-2 is the most widely used BMP for conferring osteoinductivity to orthopedic implants (Wang et al. 2014; Bessa et al. 2008). However, only the use of recombinant human BMP2 and BMP7 has been approved for clinical application in treatment of open tibia shaft fractures and nonunion bone fractures, respectively. Moreover, suitable dosage, carcinogenesis and its long-term effects are still unknown (Barcak and Beebe 2017; DeVine et al. 2012). In a recent study Thoma et al. (Thoma et al. 2017) compared both recombinant human bone morphogenetic protein-2 (rhBMP-2) and recombinant platelet-derived growth factor (rhPDGF-BB) for bone regeneration. They concluded that rhBMP-2 shows a higher enhance of bone regeneration.

Vascular endothelial growth factor (VEGF) is a key regulator of physiological angiogenesis during embryogenesis, skeletal growth and reproductive functions. It promotes angiogenesis in tridimensional *in vitro* models and VEGF-releasing scaffolds demonstrated significant improvements in blood vessel density (Ferrara et al. 2003; Leach et al. 2006). Khojasteh and colleagues prepared a β -TCP scaffold coated with poly lactic co-glycolic acid (PLGA) containing VEGF as a carrier of MSC–endothelial progenitor cell and evaluated its performance in mandibular defect of dogs. They compared three types of scaffolds: scaffolds with VEGF; with VEGF and MSC; with VEGF and MSC/EPC. Khojasteh concluded that scaffolds with VEGF and MSC show better results as they present higher bone formation (Khojasteh et al. 2017).

3.7 Conclusions and final remarks

Bone loss persists to be an important challenge in surgery, and many alternatives are now available. There is a great demand in achieving the perfect combination of porous scaffolds with proper mechanical properties as it is crucial for bone regeneration support and pore size that allow cell and vessels penetration. The use of coatings with ions similar to the bone is an interesting solution for the lack of osteointegration. Hybrid materials incorporating cells and growth factors for tissue growth stimulation have been recognized as a key component in high-quality bone regeneration. Yet, due to the heterogeneity of the studies it is difficult to conclude which is the best solution for bone regeneration. The poor vascularization and poor diffusion of oxygen into the scaffolds remains the main limitation for bone tissue engineers. To achieve proper vascularization strategies such as: scaffold porosity, introduction of angiogenic factor delivery or pre-vascularization are being studied. Growth factors delivery treatments presented successful results in many studies but there have been increasing the issues about dangerous side effects caused by the use of certain growth factors, over dosage, long term results needing standard randomized clinical trials prior to be approved for routinely clinical use. It is important to optimize the scaffolds so they can match the mechanical characteristic of bone. The majority of the strategies were only tested in minor models and testing in superior models can add problems. It is crucial to establishing protocols such as the best dosage of growth factors, identify the more suitable biomaterial with the proper mechanical properties for bone defects and identify the best choice and dosage whether for the use of growth factors or cells. In brief, researchers are focused on the production of a single material to be able to promote bone regeneration and there is thoughtfulness to patient specific implant that would be designed to restore the specific defect.

Acknowledgements

This article is a result of the project FRONThERA (NORTE-01-0145-FEDER-000023), supported by Norte Portugal Regional Operational Programme (NORTE 2020), under the PORTUGAL 2020 Partnership Agreement, through the European Regional Development Fund (ERDF) and is supported by FCT in the scope of the projects UID/EEA/04436/2013 and NORTE-01-0145-FEDER-000018-HAMaBICo. I. F. Cengiz thanks the Portuguese Foundation for Science and Technology (FCT) for the Ph.D. scholarship (SFRH/BD/99555/2014). J. M. Oliveira also thanks the FCT for the funds provided under the program Investigador FCT 2012 and 2015 (IF/00423/2012 and IF/01285/2015).

3.8 References

- Akkan CK, Hammadeh ME, May A, Park H-W, Abdul-Khaliq H, Strunskus T, Aktas OC (2014) Surface topography and wetting modifications of PEEK for implant applications. *Lasers in medical science* 29 (5):1633-1639
- Albertini M, Fernandez-Yague M, Lázaro P, Herrero-Climent M, Rios-Santos J-V, Bullon P, Gil F-J (2015) Advances in surfaces and osseointegration in implantology. *Biomimetic surfaces. Medicina oral, patologia oral y cirugía bucal* 20 (3):e316
- Bacelar AH, Cengiz IF, Silva-Correia J, Sousa RA, Oliveira JM, Reisa RL (2017) “Smart” Hydrogels in Tissue Engineering and Regenerative Medicine Applications. *Handbook of intelligent scaffolds for tissue engineering and regenerative medicine* (2):327-361
- Bai X, Sandukas S, Appleford M, Ong JL, Rabiei A (2012) Antibacterial effect and cytotoxicity of Ag-doped functionally graded hydroxyapatite coatings. *Journal of Biomedical Materials Research Part B: Applied Biomaterials* 100 (2):553-561
- Barcak EA, Beebe MJ (2017) Bone Morphogenetic Protein. Is There Still a Role in Orthopedic Trauma in 2017? *Orthopedic Clinics of North America*
- Berner A, Henkel J, Woodruff MA, Steck R, Nerlich M, Schuetz MA, Hutmacher DW (2015) Delayed minimally invasive injection of allogenic bone marrow stromal cell sheets regenerates large bone defects in an ovine preclinical animal model. *Stem cells translational medicine* 4 (5):503-512
- Bessa PC, Casal M, Reis R (2008) Bone morphogenetic proteins in tissue engineering: the road from the laboratory to the clinic, part I (basic concepts). *Journal of tissue engineering and regenerative medicine* 2 (1):1-13

- Bhattacharya I, Ghayor C, Weber FE (2016) The use of adipose tissue-derived progenitors in bone tissue engineering—a review. *Transfusion Medicine and Hemotherapy* 43 (5):336-343
- Bohner M, Loosli Y, Baroud G, Lacroix D (2011) Commentary: deciphering the link between architecture and biological response of a bone graft substitute. *Acta biomaterialia* 7 (2):478-484
- Boskey AL (2007) Mineralization of bones and teeth. *Elements* 3 (6):385-391
- Boskey AL (2013) Bone composition: relationship to bone fragility and antiosteoporotic drug effects. *BoneKEy reports* 2
- Bružauskaitė, Bironaitė D, Bagdonas E, Bernotienė E (2016) Scaffolds and cells for tissue regeneration: different scaffold pore sizes—different cell effects. *Cytotechnology* 68 (3):355-369
- Campana V, Milano G, Pagano E, Barba M, Cicione C, Salonna G, Lattanzi W, Logroscino G (2014) Bone substitutes in orthopaedic surgery: from basic science to clinical practice. *Journal of Materials Science: Materials in Medicine* 25 (10):2445-2461
- Cengiz IF, Oliveira JM, Reis RL (2014) Tissue engineering and regenerative medicine strategies for the treatment of osteochondral lesions. In: *3D Multiscale Physiological Human*. Springer, pp 25-47
- Cengiz IF, Pereira H, Espregueira-Mendes J, Oliveira JM, Reis RL (2017) Treatments of Meniscus Lesions of the Knee: Current Concepts and Future Perspectives. *Regenerative Engineering and Translational Medicine*:1-19
- Chevalier J (2006) What future for zirconia as a biomaterial? *Biomaterials* 27 (4):535-543
- Chevalier J, Gremillard L (2009) Ceramics for medical applications: A picture for the next 20 years. *Journal of the European Ceramic Society* 29 (7):1245-1255
- Clarke B (2008) Normal bone anatomy and physiology. *Clinical journal of the American Society of Nephrology* 3 (Supplement 3):S131-S139
- Cohen DJ, Cheng A, Sahingur K, Clohessy RM, Hopkins LB, Boyan BD, Schwartz Z (2017) Performance of laser sintered Ti–6Al–4V implants with bone-inspired porosity and micro/nanoscale surface roughness in the rabbit femur. *Biomedical Materials* 12 (2):025021
- D'Agostino P, Barbier O (2013) An investigation of the effect of AlloMatrix bone graft in distal radial fracture. *Bone Joint J* 95 (11):1514-1520
- de Peppo GM, Marcos-Campos I, Kahler DJ, Alsalman D, Shang L, Vunjak-Novakovic G, Marolt D (2013) Engineering bone tissue substitutes from human induced pluripotent stem cells. *Proceedings of the National Academy of Sciences* 110 (21):8680-8685

- Deepthi S, Venkatesan J, Kim S-K, Bumgardner JD, Jayakumar R (2016) An overview of chitin or chitosan/nano ceramic composite scaffolds for bone tissue engineering. *International journal of biological macromolecules* 93:1338-1353
- Deng Z, Jin J, Zhao J, Xu H (2016) Cartilage defect treatments: with or without cells? Mesenchymal stem cells or chondrocytes? Traditional or matrix-assisted? A systematic review and meta-analyses. *Stem cells international* 2016
- Denry I, Kelly JR (2008) State of the art of zirconia for dental applications. *Dental materials* 24 (3):299-307
- DeVine JG, Dettori JR, France JC, Brodt E, McGuire RA (2012) The use of rhBMP in spine surgery: is there a cancer risk? *Evidence-based spine-care journal* 3 (02):035-041
- Devitt BM, Bell SW, Webster KE, Feller JA, Whitehead TS (2017) Surgical treatments of cartilage defects of the knee: Systematic review of randomised controlled trials. *The Knee*
- Dewidar MM, Khalil KA, Lim J (2007) Processing and mechanical properties of porous 316L stainless steel for biomedical applications. *Transactions of Nonferrous Metals Society of China* 17 (3):468-473
- Dimitrievska S, Niklason LE (2017) Historical Perspective and Future Direction of Blood Vessel Developments. *Cold Spring Harbor Perspectives in Medicine*:a025742
- Dimitriou R, Jones E, McGonagle D, Giannoudis PV (2011) Bone regeneration: current concepts and future directions. *BMC medicine* 9 (1):66
- Douillard T, Chevalier J, Descamps-Mandine A, Warner I, Galais Y, Whitaker P, Wu J, Wang Q (2012) Comparative ageing behaviour of commercial, unworn and worn 3Y-TZP and zirconia-toughened alumina hip joint heads. *Journal of the European Ceramic Society* 32 (8):1529-1540
- Ducy P, Karsenty G (2000) The family of bone morphogenetic proteins. *Kidney international* 57 (6):2207-2214
- Ehrler DM, Vaccaro AR (2000) The use of allograft bone in lumbar spine surgery. *Clinical orthopaedics and related research* 371:38-45
- El-Ghany OSA, Sherief AH (2016) Zirconia based ceramics, some clinical and biological aspects: Review. *Future Dental Journal* 2 (2):55-64
- Elias C, Lima JH, Valiev R, Meyers M (2008) Biomedical applications of titanium and its alloys. *JOM Journal of the Minerals, Metals and Materials Society* 60 (3):46-49
- Engler AJ, Sen S, Sweeney HL, Discher DE (2006) Matrix elasticity directs stem cell lineage specification. *Cell* 126 (4):677-689

- Evans NT, Torstrick FB, Lee CS, Dupont KM, Safranski DL, Chang WA, Macedo AE, Lin AS, Boothby JM, Whittingslow DC (2015) High-strength, surface-porous polyether-ether-ketone for load-bearing orthopedic implants. *Acta biomaterialia* 13:159-167
- Fathi M, Doostmohammadi A (2009) Bioactive glass nanopowder and bioglass coating for biocompatibility improvement of metallic implant. *Journal of materials processing technology* 209 (3):1385-1391
- Fernandez-Yague MA, Abbah SA, McNamara L, Zeugolis DI, Pandit A, Biggs MJ (2015) Biomimetic approaches in bone tissue engineering: integrating biological and physicochemical strategies. *Advanced drug delivery reviews* 84:1-29
- Ferrara N, Gerber H-P, LeCouter J (2003) The biology of VEGF and its receptors. *Nature medicine* 9 (6):669-676
- Feuvrier D, Sagawa Y, Béliard S, Pauchot J, Decavel P (2016) Long-term donor-site morbidity after vascularized free fibula flap harvesting: Clinical and gait analysis. *Journal of Plastic, Reconstructive & Aesthetic Surgery* 69 (2):262-269
- Fillingham Y, Jacobs J (2016) Bone grafts and their substitutes. *Bone Joint J* 98 (1 Supple A):6-9
- Friedenstein A, Piatetzky-Shapiro I, Petrakova K (1966) Osteogenesis in transplants of bone marrow cells. *Development* 16 (3):381-390
- Friesenbichler J, Maurer-Ertl W, Bergovec M, Holzer LA, Ogris K, Leitner L, Leithner A (2017) Clinical experience with the artificial bone graft substitute Calcibon used following curettage of benign and low-grade malignant bone tumors. *Scientific Reports* 7
- Frueh FS, Menger MD, Lindenblatt N, Giovanoli P, Laschke MW (2017) Current and emerging vascularization strategies in skin tissue engineering. *Critical reviews in biotechnology* 37 (5):613-625
- Fu Y, Karbaat L, Wu L, Leijten JC, Both S, Karperien M (2017) Trophic effects of mesenchymal stem cells in tissue regeneration. *Tissue Engineering (ja)*
- Fujibayashi S, Neo M, Kim H-M, Kokubo T, Nakamura T (2004) Osteoinduction of porous bioactive titanium metal. *Biomaterials* 25 (3):443-450
- Fukuda A, Takemoto M, Saito T, Fujibayashi S, Neo M, Pattanayak DK, Matsushita T, Sasaki K, Nishida N, Kokubo T (2011) Osteoinduction of porous Ti implants with a channel structure fabricated by selective laser melting. *Acta biomaterialia* 7 (5):2327-2336
- Galliano P, De Damborenea JJ, Pascual MJ, Duran A (1998) Sol-gel coatings on 316L steel for clinical applications. *Journal of sol-gel science and technology* 13 (1-3):723-727

- García-Gareta E, Coathup MJ, Blunn GW (2015) Osteoinduction of bone grafting materials for bone repair and regeneration. *Bone* 81:112-121
- Geesink R, de Groot K, Klein C (1988) Bonding of bone to apatite-coated implants. *Bone & Joint Journal* 70 (1):17-22
- Geetha M, Singh A, Asokamani R, Gogia A (2009) Ti based biomaterials, the ultimate choice for orthopaedic implants—a review. *Progress in materials science* 54 (3):397-425
- Giannoudis PV, Dinopoulos H, Tsiridis E (2005) Bone substitutes: an update. *Injury* 36 (3):S20-S27
- Giannoudis PV, Faour O, Goff T, Kanakaris N, Dimitriou R (2011) Masquelet technique for the treatment of bone defects: tips-tricks and future directions. *Injury* 42 (6):591-598
- Gimble J, Guilak F (2003) Adipose-derived adult stem cells: isolation, characterization, and differentiation potential. *Cytotherapy* 5 (5):362-369
- Goriainov V, Cook R, Latham JM, Dunlop DG, Oreffo RO (2014) Bone and metal: An orthopaedic perspective on osseointegration of metals. *Acta biomaterialia* 10 (10):4043-4057
- Grayson WL, Bunnell BA, Martin E, Frazier T, Hung BP, Gimble JM (2015) Stromal cells and stem cells in clinical bone regeneration. *Nature Reviews Endocrinology* 11 (3):140-150
- Guyer RD, Abitbol J-J, Ohnmeiss DD, Yao C (2016) Evaluating osseointegration into a deeply porous titanium scaffold: a biomechanical comparison with PEEK and allograft. *Spine* 41 (19):E1146-E1150
- Hallab NJ, Bundy KJ, O'Connor K, Moses RL, Jacobs JJ (2001) Evaluation of metallic and polymeric biomaterial surface energy and surface roughness characteristics for directed cell adhesion. *Tissue engineering* 7 (1):55-71
- Han J-m, Hong G, Lin H, Shimizu Y, Wu Y, Zheng G, Zhang H, Sasaki K (2016) Biomechanical and histological evaluation of the osseointegration capacity of two types of zirconia implant. *International Journal of Nanomedicine* 11:6507
- Hench LL, Splinter RJ, Allen W, Greenlee T (1971) Bonding mechanisms at the interface of ceramic prosthetic materials. *Journal of Biomedical Materials Research Part A* 5 (6):117-141
- HIEDA A, UEMURA N, HASHIMOTO Y, TODA I, BABA S (2017) In vivo bioactivity of porous polyetheretherketone with a foamed surface. *Dental Materials Journal* 36 (2):222-229
- Houdek M, Bayne C, Bishop A, Shin A (2017) The outcome and complications of vascularised fibular grafts. *Bone Joint J* 99 (1):134-138

- Huang H, Lan P-H, Zhang Y-Q, Li X-K, Zhang X, Yuan C-F, Zheng X-B, Guo Z (2015) Surface characterization and in vivo performance of plasma-sprayed hydroxyapatite-coated porous Ti6Al4V implants generated by electron beam melting. *Surface and Coatings Technology* 283:80-88
- Hunziker EB, Jovanovic J, Horner A, Keel M, Lippuner K, Shintani N (2016) Optimisation of BMP-2 dosage for the osseointegration of porous titanium implants in an ovine model. *European cells & materials eCM* 32:241-256
- Hutmacher DW (2000) Scaffolds in tissue engineering bone and cartilage. *Biomaterials* 21 (24):2529-2543
- Ichikawa Y, Akagawa Y, Nikai H, Tsuru H (1992) Tissue compatibility and stability of a new zirconia ceramic in vivo. *The Journal of prosthetic dentistry* 68 (2):322-326
- Ilan DI, Ladd AL (2002) Bone graft substitutes. *Operative Techniques in Plastic and Reconstructive Surgery* 9 (4):151-160
- Jean RP, Gray DS, Spector AA, Chen CS (2004) Characterization of the nuclear deformation caused by changes in endothelial cell shape. *Transactions of the ASME-K-Journal of Biomechanical Engineering* 126 (5):552-558
- Johansson P, Jimbo R, Kjellin P, Currie F, Ramos Chrcanovic B, Wennerberg A (2014) Biomechanical evaluation and surface characterization of a nano-modified surface on PEEK implants: a study in the rabbit tibia. *International journal of nanomedicine*
- Jones AC, Arns CH, Hutmacher DW, Milthorpe BK, Sheppard AP, Knackstedt MA (2009) The correlation of pore morphology, interconnectivity and physical properties of 3D ceramic scaffolds with bone ingrowth. *Biomaterials* 30 (7):1440-1451
- Jones AC, Milthorpe B, Averdunk H, Limaye A, Senden TJ, Sakellariou A, Sheppard AP, Sok RM, Knackstedt MA, Brandwood A (2004) Analysis of 3D bone ingrowth into polymer scaffolds via micro-computed tomography imaging. *Biomaterials* 25 (20):4947-4954
- Josset Y, Oum'Hamed Z, Zarrinpour A, Lorenzato M, Adnet J-J, Laurent-Maquin D (1999) In vitro reactions of human osteoblasts in culture with zirconia and alumina ceramics. *Journal of biomedical materials research* 47 (4):481-493
- Kalfas IH (2001) Principles of bone healing. *Neurosurgical focus* 10 (4):1-4
- Karageorgiou V, Kaplan D (2005) Porosity of 3D biomaterial scaffolds and osteogenesis. *Biomaterials* 26 (27):5474-5491

Kargozar S, Lotfibakhshaiesh N, Ai J, Mozafari M, Milan PB, Hamzehlou S, Barati M, Baino F, Hill RG, Joghataei MT (2017) Strontium-and cobalt-substituted bioactive glasses seeded with human umbilical cord perivascular cells to promote bone regeneration via enhanced osteogenic and angiogenic activities.

Acta Biomaterialia

Karp JM, Dalton PD, Shoichet MS (2003) Scaffolds for tissue engineering. MRS bulletin 28 (04):301-306

Kellomäki M, Niiranen H, Puumanen K, Ashammakhi N, Waris T, Törmälä P (2000) Bioabsorbable scaffolds for guided bone regeneration and generation. Biomaterials 21 (24):2495-2505

Kelly JR, Denry I (2008) Stabilized zirconia as a structural ceramic: an overview. Dental materials 24 (3):289-298

Khojasteh A, Fahimipour F, Jafarian M, Sharifi D, Jahangir S, Khayyatan F, Baghaban Eslaminejad M (2017) Bone engineering in dog mandible: coculturing mesenchymal stem cells with endothelial progenitor cells in a composite scaffold containing vascular endothelial growth factor. Journal of Biomedical Materials Research Part B: Applied Biomaterials 105 (7):1767-1777

Kim JM, Son JS, Kang SS, Kim G, Choi SH (2015) Bone regeneration of hydroxyapatite/alumina bilayered scaffold with 3 mm passage-like medullary canal in canine tibia model. BioMed research international 2015

Kim Y-K, Kim S-G, Lim S-C, Lee H-J, Yun P-Y (2010) A clinical study on bone formation using a demineralized bone matrix and resorbable membrane. Oral Surgery, Oral Medicine, Oral Pathology, Oral Radiology, and Endodontology 109 (6):e6-e11

Kuboki Y, Takita H, Kobayashi D, Tsuruga E, Inoue M, Murata M, Nagai N, Dohi Y, Ohgushi H (1998) BMP-induced osteogenesis on the surface of hydroxyapatite with geometrically feasible and nonfeasible structures: topology of osteogenesis. Journal of Biomedical Materials Research Part A 39 (2):190-199

Kuhn LT, Liu Y, Boyd NL, Dennis JE, Jiang X, Xin X, Charles LF, Wang L, Aguila HL, Rowe DW (2013) Developmental-like bone regeneration by human embryonic stem cell-derived mesenchymal cells. Tissue Engineering Part A 20 (1-2):365-377

Kurtz SM, Devine JN (2007) PEEK biomaterials in trauma, orthopedic, and spinal implants. Biomaterials 28 (32):4845-4869

Kuttappan S, Mathew D, Nair MB (2016) Biomimetic composite scaffolds containing bioceramics and collagen/gelatin for bone tissue engineering-A mini review. International journal of biological macromolecules 93:1390-1401

- Kwee BJ, Mooney DJ (2017) Biomaterials for skeletal muscle tissue engineering. *Current Opinion in Biotechnology* 47:16-22
- Leach JK, Kaigler D, Wang Z, Krebsbach PH, Mooney DJ (2006) Coating of VEGF-releasing scaffolds with bioactive glass for angiogenesis and bone regeneration. *Biomaterials* 27 (17):3249-3255
- Lee H, Liao J-D, Sivashanmugan K, Liu BH, Weng S-L, Juang Y-D, Yao C-K (2017) Dual properties of zirconia coated porous titanium for a stiffness enhanced bio-scaffold. *Materials & Design* 132:13-21
- Li G, Wang L, Pan W, Yang F, Jiang W, Wu X, Kong X, Dai K, Hao Y (2016) In vitro and in vivo study of additive manufactured porous Ti6Al4V scaffolds for repairing bone defects. *Scientific reports* 6:34072
- Li Y, Chen S-K, Li L, Qin L, Wang X-L, Lai Y-X (2015a) Bone defect animal models for testing efficacy of bone substitute biomaterials. *Journal of Orthopaedic Translation* 3 (3):95-104
- Li Y, Yang W, Li X, Zhang X, Wang C, Meng X, Pei Y, Fan X, Lan P, Wang C (2015b) Improving osteointegration and osteogenesis of three-dimensional porous Ti6Al4V scaffolds by polydopamine-assisted biomimetic hydroxyapatite coating. *ACS applied materials & interfaces* 7 (10):5715-5724
- Liao HT, Lee MY, Tsai WW, Wang HC, Lu WC (2016) Osteogenesis of adipose-derived stem cells on polycaprolactone- β -tricalcium phosphate scaffold fabricated via selective laser sintering and surface coating with collagen type I. *Journal of tissue engineering and regenerative medicine* 10 (10)
- Lindfors NC, Heikkilä JT, Koski I, Mattila K, Aho AJ (2009) Bioactive glass and autogenous bone as bone graft substitutes in benign bone tumors. *Journal of Biomedical Materials Research Part B: Applied Biomaterials* 90 (1):131-136
- Linero I, Chaparro O (2014) Paracrine effect of mesenchymal stem cells derived from human adipose tissue in bone regeneration. *PLoS One* 9 (9):e107001
- Liu W, Wei Y, Zhang X, Xu M, Yang X, Deng X (2013) Lower extent but similar rhythm of osteogenic behavior in hBMSCs cultured on nanofibrous scaffolds versus induced with osteogenic supplement. *ACS nano* 7 (8):6928-6938
- Liu X, Xie Z, Zhang C, Pan H, Rahaman MN, Zhang X, Fu Q, Huang W (2010) Bioactive borate glass scaffolds: in vitro and in vivo evaluation for use as a drug delivery system in the treatment of bone infection. *Journal of Materials Science: Materials in Medicine* 21 (2):575-582
- Ma R, Tang T (2014) Current strategies to improve the bioactivity of PEEK. *International journal of molecular sciences* 15 (4):5426-5445
- Maatz R, Bauermeister A (1957) A Method of Bone Maceration: Results in Animal Experiments. *JBJS* 39 (1):153-166

Marsell R, Einhorn TA (2011) The biology of fracture healing. *Injury* 42 (6):551-555

Masaoka T, Yoshii T, Yuasa M, Yamada T, Taniyama T, Torigoe I, Shinomiya K, Okawa A, Morita S, Sotome S (2016) Bone Defect Regeneration by a Combination of a β Tricalcium Phosphate Scaffold and Bone Marrow Stromal Cells in a Non-Human Primate Model. *The open biomedical engineering journal* 10:2

McAuliffe JA (2003) Bone graft substitutes. *Journal of Hand Therapy* 16 (2):180-187

McKibbin B The biology of fracture healing in long bones. In: *J Bone Joint Surg [Br]*, 1978. Citeseer, Midha S, Kim TB, van den Bergh W, Lee PD, Jones JR, Mitchell CA (2013) Preconditioned 70S30C bioactive glass foams promote osteogenesis in vivo. *Acta biomaterialia* 9 (11):9169-9182

Molino G, Bari A, Baino F, Fiorilli S, Vitale-Brovarone C (2017) Electrophoretic deposition of spray-dried Sr-containing mesoporous bioactive glass spheres on glass–ceramic scaffolds for bone tissue regeneration. *Journal of Materials Science*:1-12

Morelli I, Drago L, George DA, Gallazzi E, Scarponi S, Romanò CL (2016) Masquelet technique: myth or reality? A systematic review and meta-analysis. *Injury* 47:S68-S76

Murphy CM, Haugh MG, O'Brien FJ (2010) The effect of mean pore size on cell attachment, proliferation and migration in collagen–glycosaminoglycan scaffolds for bone tissue engineering. *Biomaterials* 31 (3):461-466

Murphy CM, O'Brien FJ, Little DG, Schindeler A (2013) Cell-scaffold interactions in the bone tissue engineering triad.

Najeeb S, Zafar MS, Khurshid Z, Siddiqui F (2016) Applications of polyetheretherketone (PEEK) in oral implantology and prosthodontics. *Journal of prosthodontic Research* 60 (1):12-19

Navarro M, Michiardi A, Castano O, Planell J (2008) Biomaterials in orthopaedics. *Journal of the Royal Society Interface* 5 (27):1137-1158

Nielsen K (1987) Corrosion of metallic implants. *British Corrosion Journal* 22 (4):272-278

Niinomi M (2002) Recent metallic materials for biomedical applications. *Metallurgical and materials transactions A* 33 (3):477

Niinomi M (2003) Recent research and development in titanium alloys for biomedical applications and healthcare goods. *Science and technology of advanced Materials* 4 (5):445

Niinomi M (2008) Metallic biomaterials. *Journal of Artificial Organs* 11 (3):105

Nyary T, Scammell BE (2015) Principles of bone and joint injuries and their healing. *Surgery (Oxford)* 33 (1):7-14

- Oliveira JM, Leonor IB, Reis RL Preparation of bioactive coatings on the surface of bioinert polymers through an innovative auto-catalytic electroless route. In: Key Engineering Materials, 2005. Trans Tech Publ, pp 203-206
- Oryan A, Alidadi S, Bigham-Sadegh A, Moshiri A (2017) Effectiveness of tissue engineered based platelet gel embedded chitosan scaffold on experimentally induced critical sized segmental bone defect model in rat. *Injury*
- Osman RB, Swain MV (2015) A critical review of dental implant materials with an emphasis on titanium versus zirconia. *Materials* 8 (3):932-958
- Osterhoff G, Morgan EF, Shefelbine SJ, Karim L, McNamara LM, Augat P (2016) Bone mechanical properties and changes with osteoporosis. *Injury* 47:S11-S20
- Panayotov IV, Orti V, Cuisinier F, Yachouh J (2016) Polyetheretherketone (PEEK) for medical applications. *Journal of Materials Science: Materials in Medicine* 27 (7):1-11
- Patel JJ (2015) Single and Dual Growth Factor Delivery from Poly-ε-caprolactone Scaffolds for Pre-Fabricated Bone Flap Engineering. University of Michigan,
- Paxton NC (2017) Designing patient-specific melt-electrospun scaffolds for bone regeneration. Queensland University of Technology,
- Pelissier P, Masquelet A, Bareille R, Pelissier SM, Amedee J (2004) Induced membranes secrete growth factors including vascular and osteoinductive factors and could stimulate bone regeneration. *Journal of orthopaedic research* 22 (1):73-79
- Piconi C, Maccauro G (1999) Zirconia as a ceramic biomaterial. *Biomaterials* 20 (1):1-25
- Piconi C, Maccauro G, Muratori F, Prever E (2003) Alumina and zirconia ceramics in joint replacements. *Journal of Applied Biomaterials & Biomechanics* 1 (1):19-32
- Pittenger MF, Mackay AM, Beck SC, Jaiswal RK, Douglas R, Mosca JD, Moorman MA, Simonetti DW, Craig S, Marshak DR (1999) Multilineage potential of adult human mesenchymal stem cells. *Science* 284 (5411):143-147
- Plum AW, Tatum SA (2015) A comparison between autograft alone, bone cement, and demineralized bone matrix in cranioplasty. *The Laryngoscope* 125 (6):1322-1327
- Prananingrum W, Naito Y, Galli S, Bae J, Sekine K, Hamada K, Tomotake Y, Wennerberg A, Jimbo R, Ichikawa T (2016) Bone ingrowth of various porous titanium scaffolds produced by a moldless and space holder technique: an in vivo study in rabbits. *Biomedical Materials* 11 (1):015012

- Qian J, Xu M, Suo A, Yang T, Yong X (2013) An innovative method to fabricate honeycomb-like poly (ϵ caprolactone)/nano-hydroxyapatite scaffolds. *Materials Letters* 93:72-76
- Rack H, Qazi J (2006) Titanium alloys for biomedical applications. *Materials Science and Engineering: C* 26 (8):1269-1277
- Rahaman MN, Day DE, Bal BS, Fu Q, Jung SB, Bonewald LF, Tomsia AP (2011) Bioactive glass in tissue engineering. *Acta biomaterialia* 7 (6):2355-2373
- Ren H, Li A, Liu B, Dong Y, Tian Y, Qiu D (2017) Novel bioactive glass based injectable bone cement with improved osteoinductivity and its in vivo evaluation. *Scientific Reports* 7 (1):3622
- Rho J-Y, Kuhn-Spearing L, Zioupos P (1998) Mechanical properties and the hierarchical structure of bone. *Medical engineering & physics* 20 (2):92-102
- Ribeiro VP, Almeida LR, Martins AR, Pashkuleva I, Marques AP, Ribeiro AS, Silva CJ, Bonifacio G, Sousa RA, Reis RL (2016) Influence of different surface modification treatments on silk biotextiles for tissue engineering applications. *Journal of Biomedical Materials Research Part B: Applied Biomaterials* 104 (3):496-507
- Rice JJ, Martino MM, De Laporte L, Tortelli F, Briquez PS, Hubbell JA (2013) Engineering the regenerative microenvironment with biomaterials. *Advanced healthcare materials* 2 (1):57-71
- Roberts SJ, Geris L, Kerckhofs G, Desmet E, Schrooten J, Luyten FP (2011) The combined bone forming capacity of human periosteal derived cells and calcium phosphates. *Biomaterials* 32 (19):4393-4405
- Roffi A, Krishnakumar GS, Gostynska N, Kon E, Candrian C, Filardo G (2017) The Role of Three-Dimensional Scaffolds in Treating Long Bone Defects: Evidence from Preclinical and Clinical Literature—A Systematic Review. *BioMed Research International* 2017
- Sagomonyants KB, Jarman-Smith ML, Devine JN, Aronow MS, Gronowicz GA (2008) The in vitro response of human osteoblasts to polyetheretherketone (PEEK) substrates compared to commercially pure titanium. *Biomaterials* 29 (11):1563-1572
- Salgado AJ, Coutinho OP, Reis RL (2004) Bone tissue engineering: state of the art and future trends. *Macromolecular bioscience* 4 (8):743-765
- Santos RL, Silva FS, Nascimento RM, Motta FV, Souza JC, Henriques B (2016) On the mechanical properties and microstructure of zirconia-reinforced feldspar-based porcelain. *Ceramics International* 42 (12):14214-14221
- Sarkar SK, Lee BT (2015) Hard tissue regeneration using bone substitutes: an update on innovations in materials. *The Korean journal of internal medicine* 30 (3):279

- Scarano A, Di Carlo F, Quaranta M, Piattelli A (2003) Bone response to zirconia ceramic implants: an experimental study in rabbits. *Journal of Oral Implantology* 29 (1):8-12
- Schwitalla A, Abou-Emara M, Spintig T, Lackmann J, Müller W (2015) Finite element analysis of the biomechanical effects of PEEK dental implants on the peri-implant bone. *Journal of biomechanics* 48 (1):1-7
- Sensharma P, Madhumathi G, Jayant RD, Jaiswal AK (2017) Biomaterials and cells for neural tissue engineering: Current choices. *Materials Science and Engineering: C*
- Shin K, Acri T, Geary S, Salem AK (2017) Biomimetic Mineralization of Biomaterials Using Simulated Body Fluids for Bone Tissue Engineering and Regenerative Medicine. *Tissue Engineering Part A*
- Shrivats AR, McDermott MC, Hollinger JO (2014) Bone tissue engineering: state of the union. *Drug discovery today* 19 (6):781-786
- Smith JO, Tayton ER, Khan F, Aarvold A, Cook RB, Goodship A, Bradley M, Oreffo RO (2017) Large animal in vivo evaluation of a binary blend polymer scaffold for skeletal tissue-engineering strategies; translational issues. *Journal of tissue engineering and regenerative medicine* 11 (4):1065-1076
- Søballe K (1993) Hydroxyapatite ceramic coating for bone implant fixation: mechanical and histological studies in dogs. *Acta Orthopaedica Scandinavica* 64 (sup255):1-58
- Stanovici J, Le Nail L-R, Brennan M, Vidal L, Trichet V, Rosset P, Layrolle P (2016) Bone regeneration strategies with bone marrow stromal cells in orthopaedic surgery. *Current research in translational medicine* 64 (2):83-90
- Tang C, Tsui C, Janackovic D, Uskokovic P (2006) Nanomechanical properties evaluation of bioactive glass coatings on titanium alloy substrate. *Journal of Optoelectronics and Advanced Materials* 8 (3):1194
- Taniguchi N, Fujibayashi S, Takemoto M, Sasaki K, Otsuki B, Nakamura T, Matsushita T, Kokubo T, Matsuda S (2016) Effect of pore size on bone ingrowth into porous titanium implants fabricated by additive manufacturing: an in vivo experiment. *Materials Science and Engineering: C* 59:690-701
- Taylor GI, Miller GD, Ham FJ (1975) The free vascularized bone graft: a clinical extension of microvascular techniques. *Plastic and reconstructive surgery* 55 (5):533-544
- Tejero R, Anitua E, Orive G (2014) Toward the biomimetic implant surface: Biopolymers on titanium-based implants for bone regeneration. *Progress in Polymer Science* 39 (7):1406-1447
- Teufack S, Harrop J, Prasad S (2014) Bone Graft Extenders. In: *Minimally Invasive Spinal Deformity Surgery*. Springer, pp 337-345

- Thoma DS, Lim HC, Sapata VM, Yoon SR, Jung RE, Jung UW (2017) Recombinant bone morphogenetic protein-2 and platelet-derived growth factor-BB for localized bone regeneration. Histologic and radiographic outcomes of a rabbit study. *Clinical Oral Implants Research*
- Tian H, Tang Z, Zhuang X, Chen X, Jing X (2012) Biodegradable synthetic polymers: preparation, functionalization and biomedical application. *Progress in Polymer Science* 37 (2):237-280
- Todeschi MR, El Backly R, Capelli C, Daga A, Patrone E, Introna M, Cancedda R, Mastrogiacomo M (2015) Transplanted umbilical cord mesenchymal stem cells modify the in vivo microenvironment enhancing angiogenesis and leading to bone regeneration. *Stem cells and development* 24 (13):1570-1581
- Urist MR (1965) Bone: formation by autoinduction. *Science* 150 (3698):893-899
- Wally ZJ, van Grunsven W, Claeysens F, Goodall R, Reilly GC (2015) Porous titanium for dental implant applications. *Metals* 5 (4):1902-1920
- Walsh W, Christou C, Low A, Yu Y, Oliver R, Bertollo N, Schlossberg B, Lloyd W, Ahn E (2013) Bone graft materials: a comparison of NanOss Bioactive 3d and VitOss BA in a challenging model. *Bone Joint J* 95 (SUPP 15):359-359
- Walsh WR, Oliver RA, Christou C, Lovric V, Walsh ER, Prado GR, Haider T (2017) Critical Size Bone Defect Healing Using Collagen–Calcium Phosphate Bone Graft Materials. *PloS one* 12 (1):e0168883
- Wang J, Guo J, Liu J, Wei L, Wu G (2014) BMP-functionalised coatings to promote osteogenesis for orthopaedic implants. *International journal of molecular sciences* 15 (6):10150-10168
- Wang X, Xu S, Zhou S, Xu W, Leary M, Choong P, Qian M, Brandt M, Xie YM (2016) Topological design and additive manufacturing of porous metals for bone scaffolds and orthopaedic implants: a review. *Biomaterials* 83:127-141
- Wennerberg A, Albrektsson T (2009) Effects of titanium surface topography on bone integration: a systematic review. *Clinical oral implants research* 20 (s4):172-184
- Wu M, Wu M, Wu M, Wu C (2016) A Novel Tracing Method in Differentiating between Ectopic Odontogenic Fistulous and Sinus Infections. *Oral health case Rep* 2 (121):2
- Wu S, Liu X, Yeung KW, Liu C, Yang X (2014) Biomimetic porous scaffolds for bone tissue engineering. *Materials Science and Engineering: R: Reports* 80:1-36
- Xiang Z, Spector M (2006) Biocompatibility of Materials. *Encyclopedia of Medical Devices and Instrumentation*

- Yang S, Leong K-F, Du Z, Chua C-K (2001) The design of scaffolds for use in tissue engineering. Part I. Traditional factors. *Tissue engineering* 7 (6):679-689
- Yavari SA, van der Stok J, Chai YC, Wauthle R, Birgani ZT, Habibovic P, Mulier M, Schrooten J, Weinans H, Zadpoor AA (2014) Bone regeneration performance of surface-treated porous titanium. *Biomaterials* 35 (24):6172-6181
- Yazdimamaghani M, Razavi M, Vashaei D, Moharamzadeh K, Boccaccini AR, Tayebi L (2017) Porous magnesium-based scaffolds for tissue engineering. *Materials Science and Engineering: C* 71:1253-1266
- Ye X, Leeflang S, Wu C, Chang J, Zhou J, Huan Z (2017) Mesoporous Bioactive Glass Functionalized 3D Ti-6Al-4V Scaffolds with Improved Surface Bioactivity. *Materials* 10 (11):1244
- Yilmaz D, Dogan N, Ozkan A, Sencimen M, Ora BE, Mutlu I (2014) Effect of platelet rich fibrin and beta tricalcium phosphate on bone healing. A histological study in pigs. *Acta chirurgica brasileira* 29 (1):59-65
- Yousefi AM, Hoque ME, Prasad RG, Uth N (2015) Current strategies in multiphasic scaffold design for osteochondral tissue engineering: a review. *Journal of biomedical materials research Part A* 103 (7):2460-2481
- Yuan Q, Wu J, Qin C, Xu A, Zhang Z, Lin S, Ren X, Zhang P (2016) Spin-coating synthesis and characterization of Zn-doped hydroxyapatite/poly(lactic acid) composite coatings. *Surface and Coatings Technology* 307:461-469
- Zakaria SM, Sharif Zein SH, Othman MR, Yang F, Jansen JA (2013) Nanophase hydroxyapatite as a biomaterial in advanced hard tissue engineering: a review. *Tissue Engineering Part B: Reviews* 19 (5):431-441
- Zakhary KE, Thakker JS (2017) Emerging Biomaterials in Trauma. *Oral and Maxillofacial Surgery Clinics of North America* 29 (1):51-62
- Zaky S, Lee K, Gao J, Jensen A, Verdelis K, Wang Y, Almarza A, Sfeir C (2017) Poly (glycerol sebacate) elastomer supports bone regeneration by its mechanical properties being closer to osteoid tissue rather than to mature bone. *Acta biomaterialia* 54:95-106
- Zhang J, Guan J, Zhang C, Wang H, Huang W, Guo S, Niu X, Xie Z, Wang Y (2015) Bioactive borate glass promotes the repair of radius segmental bone defects by enhancing the osteogenic differentiation of BMSCs. *Biomedical Materials* 10 (6):065011
- Zhu W, Zhao Y, Ma Q, Wang Y, Wu Z, Weng X (2017) 3D-printed porous titanium changed femoral head repair growth patterns: osteogenesis and vascularisation in porous titanium. *Journal of Materials Science: Materials in Medicine* 28 (4):62

Three dimensional cell-scaffold constructs for application in bone tissue engineering

Zhu Y, Liu T, Song K, Fan X, Ma X, Cui Z (2008) Adipose-derived stem cell: a better stem cell than BMSC.
Cell biochemistry and function 26 (6):664-675

4. PHYSICO-CHEMICAL PROPERTIES AND CYTOCOMPATIBILITY

ASSESSMENT OF NON-DEGRADABLE SCAFFOLDS FOR BONE TISSUE ENGINEERING APPLICATIONS

Pereira H. F.^{a,b,c}, Cengiz I. F.^{a,b}, Maia, F. R.^{a,b}, Silva F. S.^c, Oliveira J. M.^{a,b,d}, and Reis R. L.^{a,b,d}

^a3B's Research Group - Biomaterials, Biodegradables and Biomimetics, University of Minho, Headquarters of the European Institute of Excellence on Tissue Engineering and Regenerative Medicine, Avepark - Parque de Ciência e Tecnologia, Zona Industrial da Gandra, 4805-017 Barco Guimarães Portugal;

^bICVS/3B's - PT Government Associated Laboratory, Portugal;

^cCenter for Micro-Electro Mechanical Systems - University of Minho, Azurém Campus, 4800-058 Guimarães – Portugal;

^dThe Discoveries Centre for Regenerative and Precision Medicine, Headquarters at University of Minho, Avepark, 4805-017 Barco, Guimarães, Portugal.

Abstract

Bone is a dynamic tissue with an amazing capacity of self-healing. However, when the defect reach a critical size bone loses this capacity and medical intervention is needed. Bone is the second most transplanted tissue in the world and there is a huge need for bone grafts and substitutes which lead to a decrease in bone banks donors. In this study, we developed Ti_6Al_4V , ZrO_2 and PEEK three-dimensional cell scaffolds based on Ti_6Al_4V , ZrO_2 and PEEK for bone repair applications. Mechanical compressive tests were also performed to evaluate the elastic modulus and compressive stress. The scaffolds presented a maximized mechanical strength for load-bearing applications revealing an elastic modulus of 6.5 GPa, 9.04 GPa and 1.67 GPa minimizing the effect of stress shielding. The crystallographic phase of ZrO_2 was analysed by XRD revealing tetragonal phase of ZrO_2 . To assess the chemical composition of the scaffolds, XPS analyses were performed in Ti_6Al_4V , ZrO_2 and PEEK three-dimensional cell scaffolds. And results showed that the main elements, Titanium, Zirconium, Carbon and Oxygen, of the scaffolds were present. Overall, the scaffolds developed presented different hydrophilicity properties and an elastic modulus similar to bone which can minimized the phenomenon of stress shielding. Finally, their efficacy as scaffold material for bone tissue regeneration applications was evaluated *in vitro* by seeding SaOS-2 onto the

scaffolds. Then cells' viability, proliferation and differentiation were analyzed up to 14days of culturing. The *in vitro* results revealed that Ti_6Al_4V , ZrO_2 and PEEK scaffolds were cytocompatible allowing cell attachment, proliferation and differentiation along the osteogenic lineage. Our results suggest the potential applications in bone tissue engineering of these scaffolds.

Keywords: Ti_6Al_4V scaffolds; ZrO_2 scaffolds; PEEK scaffolds; SaOs-2 cells; Bone tissue engineering.

4.1 Introduction

Bone is a complex, hierarchic and dynamic tissue with an amazing capacity of self-healing, however when a defect exceeds a critical size it loses the capacity of repairing and external intervention is needed (Bose et al. 2013). Current strategies used for the treatment of bone defects such as Masquelet technique or the use of autografts requires invasive bone collection with donor site morbidity as well as painful surgical procedures. This leads bone to be considered one of the most common tissue transplantation procedure after blood and kidney (Bentley and Hanson 2014; Morelli et al. 2016). Bone tissue engineering (BTE) approaches are demanded to overcome the limitations of current solutions. A key component in BTE is the scaffold structure once it serves as a template for cell interactions and the formation of bone-extracellular matrix to provide structural support to the newly formed tissue.

When developing a successful bone engineered scaffold, it is important to understand bone structure and mechanics. Bone has a hierarchical structure and its mechanical properties vary with age, site and bone quality (Boskey 2013). There are various mechanical properties that can describe bone tissue but the most important in the conception of bone scaffolds is the elastic Modulus (Wang et al. 2016). The elastic Modulus of trabecular bone goes from 0.02-2 GPa and of compact bone can vary between 3 and 30 GPa (Yang et al. 2001; Wang et al. 2016). They must be sufficient and not collapse during the surgical procedure neither in patient's life. However, if the scaffold has higher elastic Modulus than bone the scaffold will take the load leading to bone resorption also known as stress shielding (Nair and Laurencin 2007; Leong et al. 2008).

Metallic biomaterials due to their mechanical properties and corrosion resistance are mainly used for the fabrication of scaffolds for the replacement of hard tissue, such as artificial hip joints, bone plates, and dental implants (Nielsen 1987; Niinomi 2003, 2008). Titanium alloy, Ti_6Al_4V , is used for their excellent corrosion resistance and their modulus of elasticity 113 GPa.

Ceramics are generally defined as inorganic, non-metallic materials. Ceramics such as alumina, and zirconia ceramics are the most used in orthopedic device. Zirconia combines high strength and fracture toughness with an attractive biocompatibility. Tetragonal zirconia, ZrO_2 , especially 3% Yttria stabilized has been used as a conventional material for medical restorations due to its mechanical properties with an elastic modulus of 200 GPa. (Denry and Kelly 2008; Yin et al. 2017).

Synthetic polymeric biomaterials are much more easily reproducible. Poly-ether-ether-ketone, PEEK, is a semicrystalline polymer with high chemical resistance and it also presents high fracture toughness. But the major beneficial property for orthopedics application its lower elastic modulus 3– 4 GPa (Rae et al. 2007).

The scaffold's architecture is critical and it should possess a pores that allows cells penetration, growth, proliferation and differentiation. It has been shown previous by Kuboki et al. the importance of porous scaffolds for the formation of new tissue (Kuboki et al. 1998; Wu et al. 2014). Additionally, other studies shown better results in pore size greater than 300 μm for bone ingrowth (Bohner et al. 2011; Karageorgiou and Kaplan 2005; Murphy et al. 2010; Jones et al. 2004). Although pore size of a scaffold for bone tissue regeneration is key factor however it becomes conflicting with others properties. In this sense the increase of pore size affects directly the strength of the scaffold

In this reasoning, the purposed of this study was to evaluate 3 different scaffolds made of Ti_6Al_4V , ZrO_2 and PEEK, produced by selective laser melting and CNC milling not only in terms of physicochemical properties but also in terms of its effect on cells' behavior as novel approaches for bone tissue engineering applications.

4.2 Materials and Methods

4.2.1 Scaffolds Preparation

In this study open-cellular structures were produced with an open pore size of 400 μm , these structures were designed having throughout holes.

The production of Ti_6Al_4V samples were performed under an Argon and Nitrogen atmosphere, using a platform at a constant temperature of 200 °C and using the processing parameters already described previous by Bartolomeu et al (Bartolomeu et al. 2016).

ZrO₂ and PEEK porous specimens with 5 mm of height and with an average pore diameter of 400 µm were produced by CNC milling (*Roland DWX-50*). ZrO₂ used to produce the scaffolds was *Zirconia comercial Dental Direkt Bio ZW iso* and for PEEK was *PEEK comercial Dental Direkt Peek MED*. The cutting tool used to produce the porous scaffolds of ZrO₂ was made of hard metal with a 0.5 mm diameter spherical top. During process the cutting tool penetrates 0.20 mm, rises and then penetrates a further 0.20 mm and so on until the hole is completed (feedrate), its rotation speed is 30000 rpm. The speed rate used was 5 mm sec⁻¹. After machined the samples are cleaned and sintered using a stage at 1500 ° for 2 hours with heating and cooling rates of 8°C min⁻¹. To machined PEEK samples a cutting tool used was made of hard metal with a 0.4 mm diameter spherical top and a speed rate of 30000 rpm. The speed rate used was 8 mm sec⁻¹ and the feedrate of the cutting tool was 0.10 mm. After the processing all samples were ultrasonically cleaned in isopropanol for 10 min in order to remove any loose debris or surface contamination.

4.2.2 Physicochemical characterization

X-ray diffraction

The qualitative analyses of crystalline phases presented on the samples were obtained by X-ray diffraction (XRD) using a conventional Bragg–Brentano diffractometer (*Bruker D8 Advance DaVinci, Germany*) equipped with CuKα radiation, produced at 40 kV and 40 mA. Data sets were collected in the 2θ range of 10–60° with a step size of 0.02° and 1s for each step.

X-ray photoelectron spectroscopy

Surface chemistry of each scaffold material was analyzed by X-ray photoelectron spectroscopy (XPS) using Axis Supra for the elemental composition of the scaffolds. The XPS analysis of a surface provides qualitative and quantitative information on all the elements present (except H and He) from the binding energies of the main lines and the peak area, respectively. Three regions were located in each scaffold and the analyzer was used at the constant Δ E mode with 20 eV pass energy.

X-ray micro-computed tomography

The quantitative and qualitative evaluation of the scaffolds' structure were performed using a high-resolution X-ray micro-computed tomography system Skyscan 1272 (*Skyscan, Kontich, Belgium*). The scanning of the scaffolds was conducted using a pixel size of 5 µm and an X-ray source fixed at 50 keV and 200 µA. The two-dimensional (2D) images in each data set were binarized automatically using the

manufacturer's software (*CT Analyzer v1.17, SkyScan, Kontich, Belgium*). Formerly, the images were used for morphometric analysis by quantification of mean porosity, mean pore size, mean wall thickness. The porosity, pore size and wall thickness were also determined on the 2D images. Three samples were used for the qualitative and quantitative microstructure evaluation.

Surface roughness

The polishing was performed using a MECAPOL P251 and different types of sand papers with different meshes. With this procedure, the purpose was to polish the surface of the samples in order to obtain smoother surfaces. The series of sand papers used for polishing all the samples were: Ti₆Al₄V specimens were polished with P4000 grit size, ZrO₂ with grit from P180 to P4000 size and PEEK samples were polished with P600 to P4000 grit size and then further polish was complete using a diamond suspension with particle size of 3 μm (*DiaPro Dur*). The roughness of both polished and processed surfaces were measure by means of profilometry (*Mitutoyo SJ 210*). Throughout the test the rugosimeter's needle dislocated horizontally with a 6 μs speed along the length of the sample with measurements being acquired in every 2.5 μm of dislocation. The presence of micro peaks and valleys, during the roughness measurement, created vertical movements in the touch probe that were, then, converted by the existing transducer into electrical signs and these were amplified vertically and horizontally being converted later into dimensional values.

Contact angle and surface energy

Wettability can be defined as the propensity of liquid to spread on a solid surface and normally consist on the measurement of contact angles as the primary data, which indicates the degree of wetting when a solid and liquid interact. Contact angles were obtained using the sessile drop method with an instrument (*GONIOMETER OCA15+*), this fully automated apparatus, with integrated pump, delivers accurate droplets and the built-in camera captures an image to measure the static contact angle. All specimens were ultrasonically cleaned with alcohol before the measurement to minimize physical and chemical contamination of the surfaces. Distilled water was used for contact angle measurements. The calculations were performed at room temperature and the drop was put directly on the scaffolds' surface. Diiodomethane (*Sigma-Aldrich Química, S.L., Portugal*) and distilled water were used for surface free energy calculations. Three drops were analyzed for each scaffold material. The final contact angle used for comparison of different samples was the average of left and right angles of each drop.

Scanning electronic microscope

To assess the microstructure of the different materials the scaffolds and the ability to cells adhere and spread along the porous scaffolds surface scanning electronic microscope was used (*JEOL JSM-6010LV*). For that, the scaffolds were collected after 14 days of culture and fixed with 10% formalin for 20 min. Then they were washed with ultra-pure water three times. The samples were then dehydrated in increased concentrations of ethanol from 30% to 100% and air dried overnight. Before observe in SEM the specimens were coated with gold.

Compression tests

The mechanical characterization of Ti_6Al_4V , ZrO_2 and PEEK was carried out in a compressive system (*Lloyd Instruments LR 50K plus*) which is equipped with a cell load of 50kN. The tests were performed at room temperature on dry samples and with a crosshead speed of $2 \times 10^{-3} \text{ mm} \cdot \text{min}^{-1}$ until mechanical failure of the scaffolds. Each sample was placed in the center of the compressive system's frame to ensure the compressive load was uniformly applied.

4.2.3 Scaffolds *in vitro* characterization

Cell culturing

In order to perform the seeding onto scaffolds osteosarcoma - derived cell line (SaOS-2) were expanded until 90% confluence using basic culture medium Dulbecco's modified Eagle's – DMEM - with 10% fetal bovine serum (*Life Technologies Europe BV, Netherland*) and 1% antibiotic/antimicotic (*Life Technologies, Scotland*) solution.

The scaffolds were transferred to non-adherent 48-well plates where the air inside the scaffolds was removed by flushing medium through the pores. Afterwards, the cells were detached with TripLETM Express with Fenol Red. A cell suspension was prepared ($33.19 \times 10^6 \text{ cells} \cdot \text{mL}^{-1}$) and seeded onto the scaffolds in a drop-wise manner, at a cellular density of 200 million cells per scaffold. After 3 hrs, 500 μL of culture medium was added to the well plates. A control was prepared by seeding 10×10^3 cells per well in adherent 12-well plates and maintained under the same conditions and for the same period of time. Medium was changed twice a week during the time of the experiment.

Cell viability

Samples were collected on days 1, 3, 7 and 14 after seeding for the assessment of cell viability by Alamar blue test (*Bio-Rad, UK*). For that, a solution with 10% of Alamar blue (*Bio-Rad, UK*) was prepared, added to each well and incubated for three hours at 37°C . Afterwards, 100 μL were transferred to a well of a

96-well black plate and the fluorescence was read at an excitation of 530/25 nm and an emission of 590/35 nm using a microplate reader (*Gen 5 2.01, Synergy HT*). The sample were analyzed in triplicates and the experience was performed once due to the limited number of scaffolds.

Cell proliferation

Cell proliferation was assessed by DNA quantification. For that, scaffolds used for Alamar blue assay were washed with PBS and transferred into 1.5 mL microtubes containing 1 mL ultra-pure water. The control with the 2D seeded cells was washed with PBS and then 1 mL of ultra-pure water was added. Then, both scaffolds and 2D control were incubated for 1 h at 37°C. Concerning 2D control, the volume of each well was transferred into a 1.5 mL microtubes. Then, all samples were stored in a -80°C freezer, promoting a thermal shock and thus potentiating the cell lyses. Additionally, before DNA quantification, cell lysates were defrosted at room temperature and then sonicated in an ultrasonic bath for 15 min. Finally, DNA concentration was quantified by using the kit Quant-IT PicoGreen dsDNA Assay kit 2000 assays (*Life Technologies, Scotland*), accordingly with manufacturer's instructions. Briefly, 28.7 μL of sample or standard, 71.3 μL of PicoGreen solution and 100 μL of Tris-HCl-EDTA buffer were mixed in each well of an opaque 96-well plate and were incubated in the dark for 10 min. Triplicates were made for samples and standards. After that, fluorescence was measured using an excitation wavelength of 485 nm and an emission wavelength of 530 nm. A DNA standard curve was prepared with concentrations varying between 0 and 2 $\mu\text{g}\cdot\text{mL}^{-1}$ and sample DNA values were read off from the standard graph.

Cell differentiation

For ALP activity assessment, molecular absorbance spectrophotometry measurement and Fast Violet B staining was performed. Concerning the first, for the quantification of ALP activity cell lysates produced for DNA quantification were used. Briefly, 20 μL of each sample and 60 μL of substrate solution (0.2% w/v p-nitrophenyl phosphate (pnPP) in 1 M Diethanolamine) were added to each well of a transparent 96-well plate and incubated in the dark for 45 min at 37 °C. Then, 80 μL of a solution to stop the reaction composed of 0.2 M NaOH and 0.2 mM EDTA was added to each well. Absorbance was read at 405 nm using a microplate reader (*Gen 5 2.01, Synergy HT*). A p-nitrophenol standard curve was prepared with concentrations varying between 0 and 0.2 $\text{nmol}\cdot\text{mL}^{-1}$ and sample values were read off from the standard graph.

In the case of ALP staining, after 14 days of culture, cells were fixed with 10% formalin for 20 minutes and stained with Fast violet B (*Sigma-Aldrich Química, S.L., Portugal*) with Naphthol (*Sigma-Aldrich Química, S.L., Portugal*). In this sense, as a result of phosphatase activity, Naphthol is liberated and immediately coupled with a diazonium salt, forming an insoluble, visible pigment at sites of phosphatase activity. For that, a mixture of both reagents was prepared and added to each sample. After 1 hour of incubation at 37°C, the solution was removed, washed with PBS and air dried. The images of the staining were taken in a Stereo Microscope (*Stemi 2000-C Zeiss*).

4.2.4 Statistical analysis

Statistical analyses were performed using GraphPad Prism 5.0 software version 5.0a. The non-parametric Mann–Whitney test was used to compare two groups, whereas comparison between more than two groups was performed using the Kruskal–Wallis test followed by Dunn’s comparison test. A value of $p < 0.05$ was considered statistically significant. Data are presented as mean \pm standard deviation. Data in each figure are from three independent experiments each one with $n=3$.

4.3 Results

4.3.1 Physicochemical characterization

X-ray diffraction

The X-ray Diffraction (XRD) was used to identify the crystalline phase of ZrO_2 scaffolds. As depicted in figure 4.1, the ZrO_2 scaffolds showed the typical intensity peaks corresponding to the tetragonal ZrO_2 phase (marked with *), with good consistency with their respective ICDD standard card 00-060-0502.

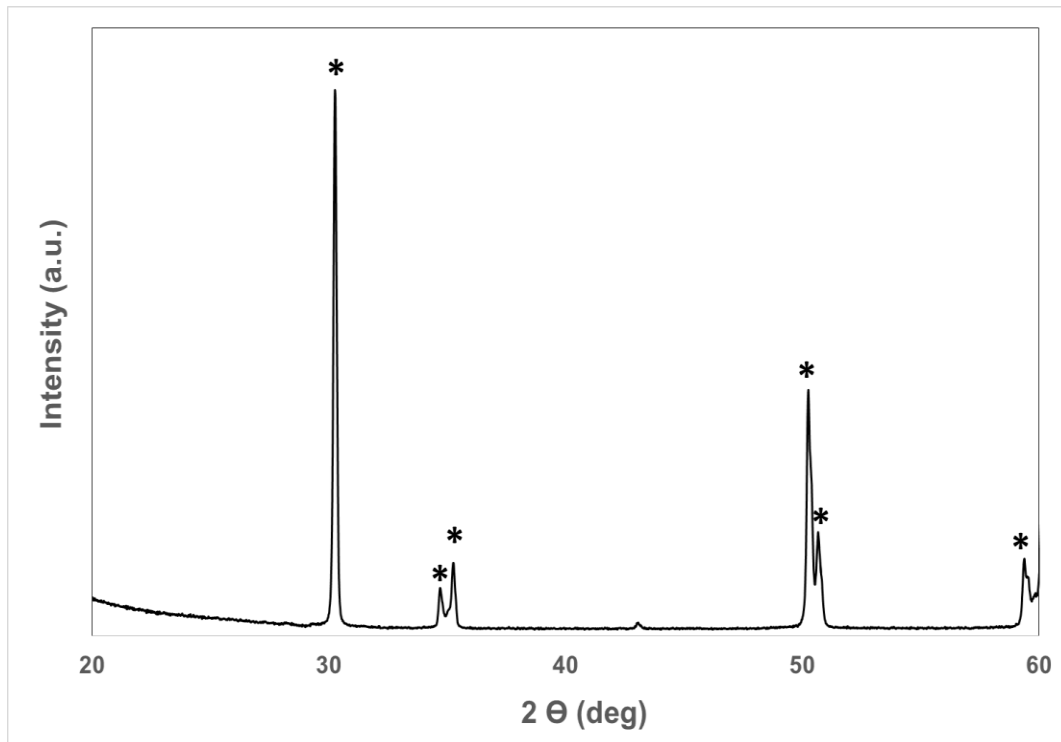


Figure 4-1 XRD plot of tetragonal phase of ZrO_2 .

X-ray photoelectron spectroscopy

In order to obtain information about the surface-near chemistry, all samples were analyzed by X-ray photoelectron spectroscopy (XPS) as depicted in figures 4.2, 4.3 and 4.4. Figure 4.2a shows the survey scan of Ti_6Al_4V scaffolds, showing the typical peaks of Oxygen (O) 1s, Titanium (Ti) 2p and Carbon (C) 1s, as expected. Additionally a high resolution XPS spectra of Ti_6Al_4V scaffolds was obtained (figure 4.2b), where it is possible to observe a peak with binding energy of 458.7 eV, corresponding to metallic titanium (Ti 2p).

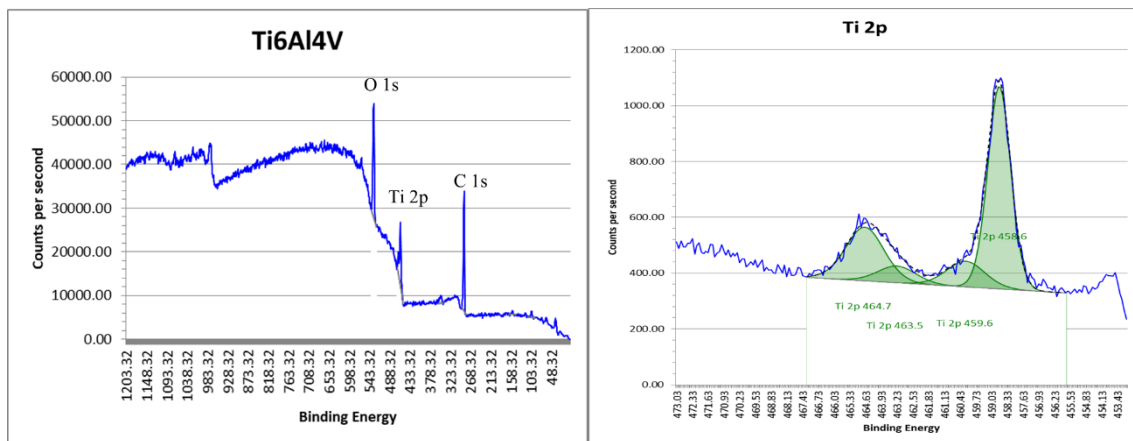


Figure 4-2 XPS plot of Ti₆Al₄V. a) Survey scan XPS spectra (b) high-resolution XPS spectra of Ti₆Al₄V showing the peak of Ti 2p.

In the case of ZrO₂ scaffolds, XPS analysis is shown in figure 4.3. The survey scan XPS spectrum of ZrO₂ scaffolds (figure 4.3a) showed a range of binding energies between 39.66 eV and 1205.66 eV with 4 different peaks that corresponds to O 1s, Zirconium (Zr) 3p_{3/2}, Zr 3p_{1/2} and Zr 3d. Moreover, in the high resolution XPS spectra of ZrO₂ scaffolds (figure 4.3 b) is possible to see the peak of Zr 3d that presented an energy binding of 182.0 eV. Furthermore, in the high resolution spectra was also possible to identify Yttria (Y) 3d with an energy binding of 157.0 eV (figure 4.3c), which was not visible in the survey scan due to its low quantity (3%).

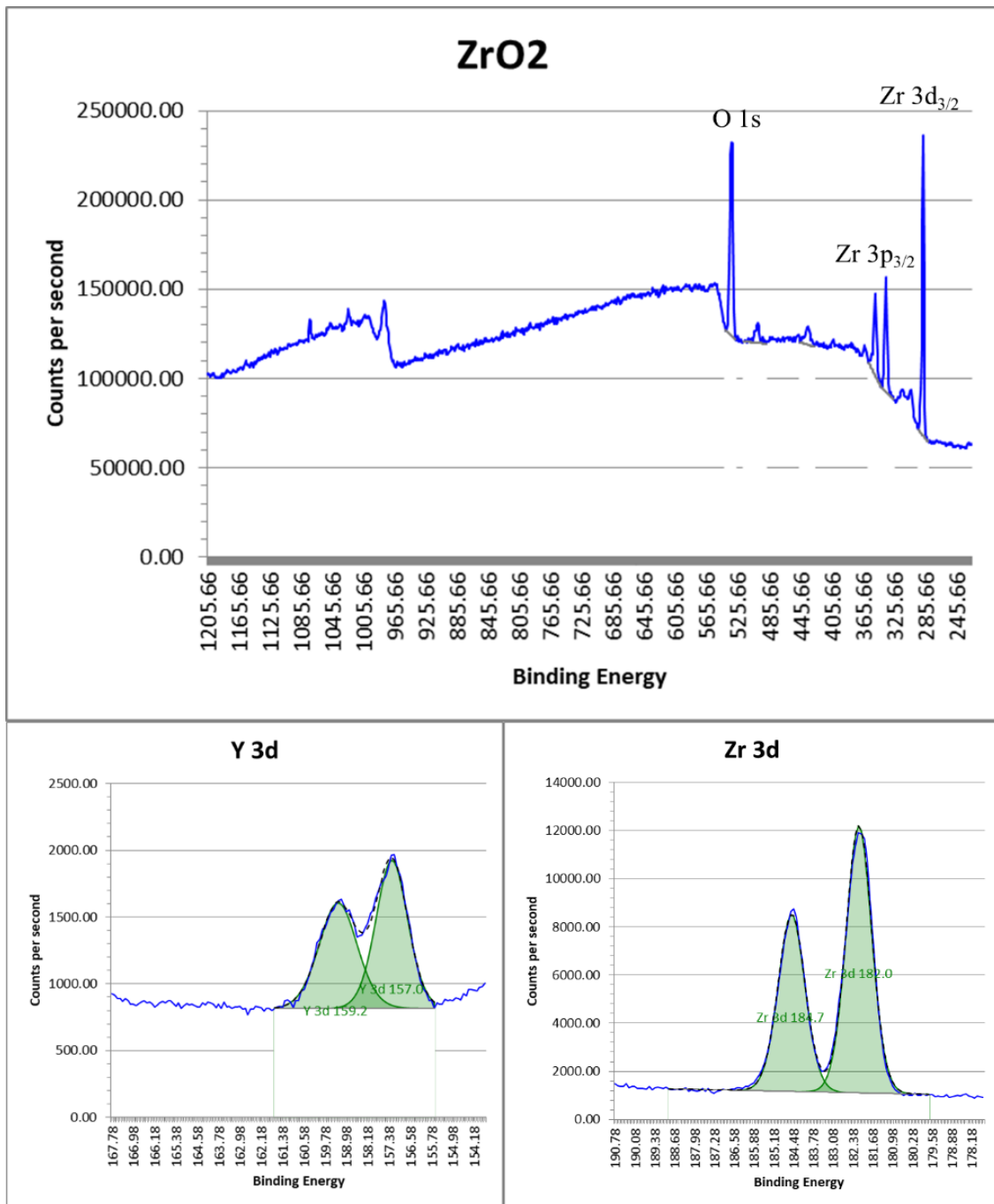


Figure 4-3 XPS plot of ZrO₂. a) Survey scan XPS spectra showing O 1s, Zr 3p_{3/2}, Zr 3d_{3/2} and Zr 3d peaks; (b) high-resolution XPS spectra of Y 3d; (c) high-resolution XPS spectra of Zr 3d.

The XPS spectra of PEEK is displayed in figure 4.4. As observed in figure 4.4 a, the peaks of O 1s and C 1s were detected in the survey scan of PEEK, as expected for polymers. These peaks had an energy binding of 533.6 eV, in the case of O 1s, and 285.0 eV, in the case of C 1s, as depicted in the high resolution XPS scan presented in figure 4.4 b and c respectively.

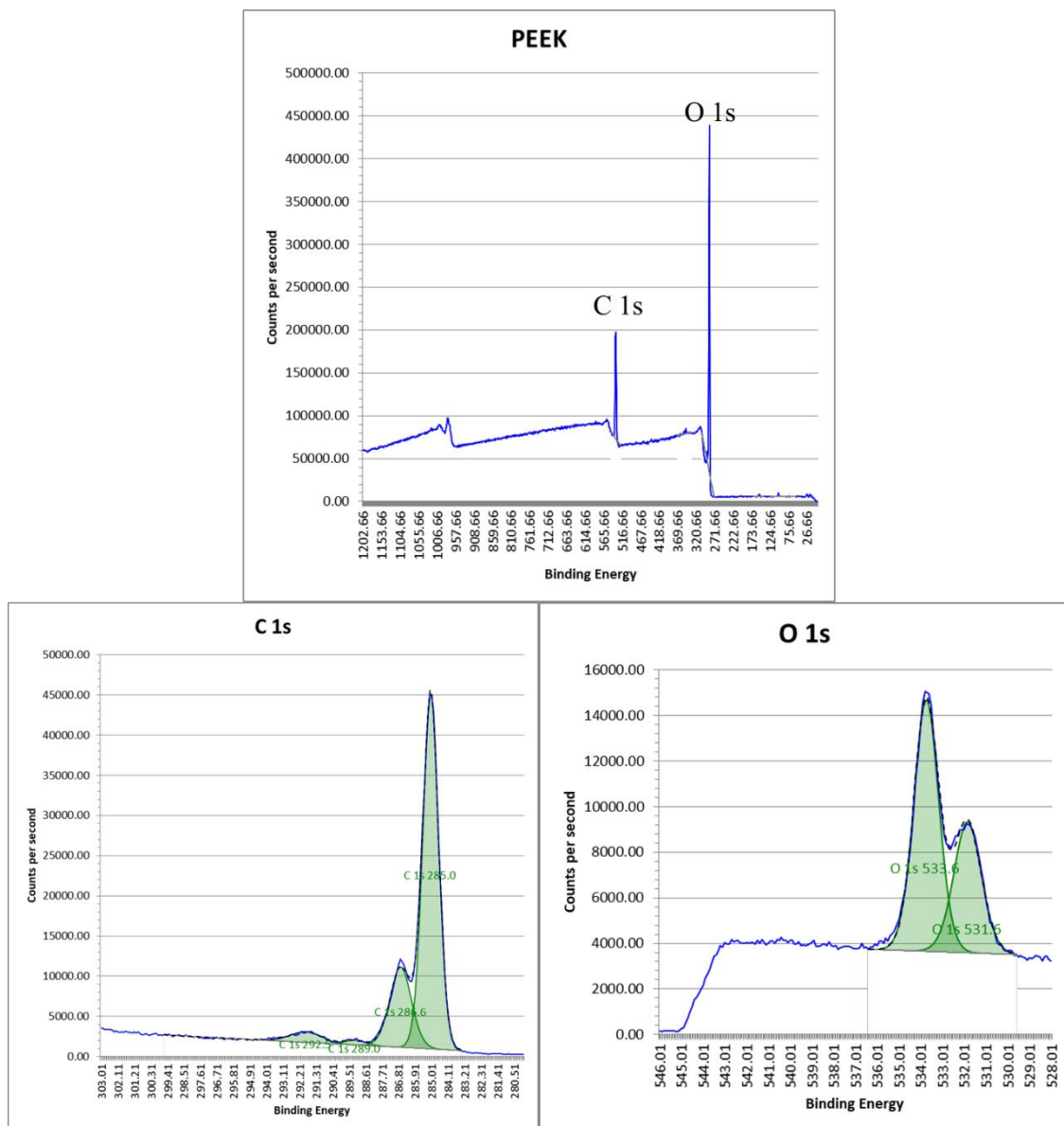
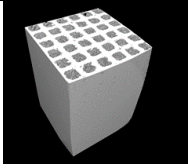
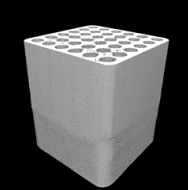
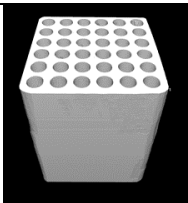


Figure 4-4 XPS plot of PEEK. a) Survey scan XPS spectra showing O 1s and C 1s peaks; (b) high-resolution XPS spectra of O 1s; c) high-resolution XPS spectra of C 1s.

X-ray micro-computed tomography

The qualitative and quantitative analysis of porosity, mean pore size and mean pore thickness of the scaffolds were assessed by micro-CT (Table 4-1). Micro-CT histomorphometric analysis did not show substantial differences in the mean porosity between the samples. As expected, significant differences were observed when comparing PEEK with Ti6Al4V samples in terms of mean wall thickness and mean pore size. In this sense, PEEK samples presented higher values of mean wall thickness and mean pore size.

Table 4-1 3D reconstructions of Ti₆Al₄V, ZrO₂ and PEEK samples, mean porosity, pore size and trabeculae thickness, calculated from the micro-CT data, presented as mean ± standard deviation.

Material	Scaffold image reconstruction	Mean porosity (%)	Mean wall thickness [µm]	Mean pore size [µm]
Ti ₆ Al ₄ V		38.0 ± 1.78	138.1 ± 4.62	172.8 ± 28.74
ZrO ₂		39.4 ± 0.77	224.3 ± 7.07	250.2 ± 3.36
PEEK		37.3 ± 0.74	250.1 ± 6.83	368.5 ± 10.09

Surface roughness

Another parameter analyzed was the surface roughness (Ra) as presented in table 4-2. The machined scaffolds analyzed by profilometry showed a surface roughness of Ra= 0.966 µm for Ti₆Al₄V, Ra= 2.03 µm for ZrO₂ and Ra= 1.051 µm for PEEK. After the polishing of the scaffolds, the average values of surface roughness significantly decreased (p = 0.0015), as expected. In this sense, the values obtained were Ra = 0.144 µm for Ti₆Al₄V; Ra = 0.013 µm for ZrO₂; and Ra = 0.192 µm for PEEK.

Table 4-2 Mean ± standard deviation values of Ra for machined and polished samples.

Type of scaffolds	Processed (µm)	Polished (µm)
Ti ₆ Al ₄ V	0.966 ± 0.13	0.144 ± 0.02
ZrO ₂	2.030 ± 0.35	0.039 ± 0.02
PEEK	1.501 ± 0.39	0.192 ± 0.07

Contact angle and surface energy

Contact angles were also assessed as shown in Table 4-3. The values were obtained by the sessile drop method on the different surfaces before (i.e. machined) and after (i.e. polished) the scaffolds had been processed. In both conditions, machined and polished, ZrO₂ samples demonstrated similar contact angles values, which were lower than 90°, indicating that these scaffolds presented a hydrophilic surface. Whereas, machined and polished Ti₆Al₄V and PEEK samples showed similar contact angles higher than 90°, which correspond to hydrophobic surfaces.

Table 4-3 Contact angle measurement values of machined and polished samples.

Machined Sample Contact angle (θ)		Sample Polished Contact angle (θ)	
Ti ₆ Al ₄ V	102.70 ± 10.72	Ti ₆ Al ₄ V	90.2 ± 12.29
ZrO ₂	78.75 ± 5.57	ZrO ₂	83.85 ± 8.24
PEEK	99.05 ± 9.65	PEEK	96.15 ± 3.24

Additionally, the surface energy of rough and polish surfaces was studied and the values obtained are presented in table 4-4. As shown, the values of surface energy increased for Ti₆Al₄V and PEEK samples after the polishment, while in the case of ZrO₂ samples, the surface energy decreased.

Table 4-4 Surface energy measurement values of machined and polished samples.

Machined Sample Surface Energy (mN.m ⁻¹)		Polished Sample Surface Energy (mN.m ⁻¹)	
Ti ₆ Al ₄ V	18.20	Ti ₆ Al ₄ V	25.16
ZrO ₂	31.68	ZrO ₂	29.8
PEEK	30.55	PEEK	34.36

Compression test

The elastic modulus was assessed since this parameter is important for the successful of new materials for bone tissue engineering approaches. In fact, this parameter measures the capability of a scaffold to resist to deformation once a stress is applied to it. For that, compression tests were performed in order to obtain the elastic modulus of each scaffolds. Moreover, the compressive maximum stress was also calculate. As depicted in figure 4.5a and b, ZrO₂ scaffolds presented the higher vertical elastic modulus values and horizontal elastic modulus values. Interestingly, as we can observe in figure 4.5a and b there was a significant decrease on the elastic modulus values comparing vertical and horizontal position of Ti₆Al₄V and ZrO₂. In this sense elastic modulus of Ti₆Al₄V decreased from 6.50 GPa to 4.36 GPa ($p = 0.0357$) and the elastic modulus of ZrO₂ decreased from 9.04 GPa to 6.14 GPa ($p = 0.0357$). This difference was caused by the position of pores. Considering the elastic modulus of PEEK, although the values decreased from 1.67 GPa to 0.59 GPa, the decrease was not significant, which can be explained by the composition of the scaffold. In what concerns maximum compressive stress, ZrO₂ also presented the higher values for vertical analysis but in the case of horizontal analysis no differences where observed.

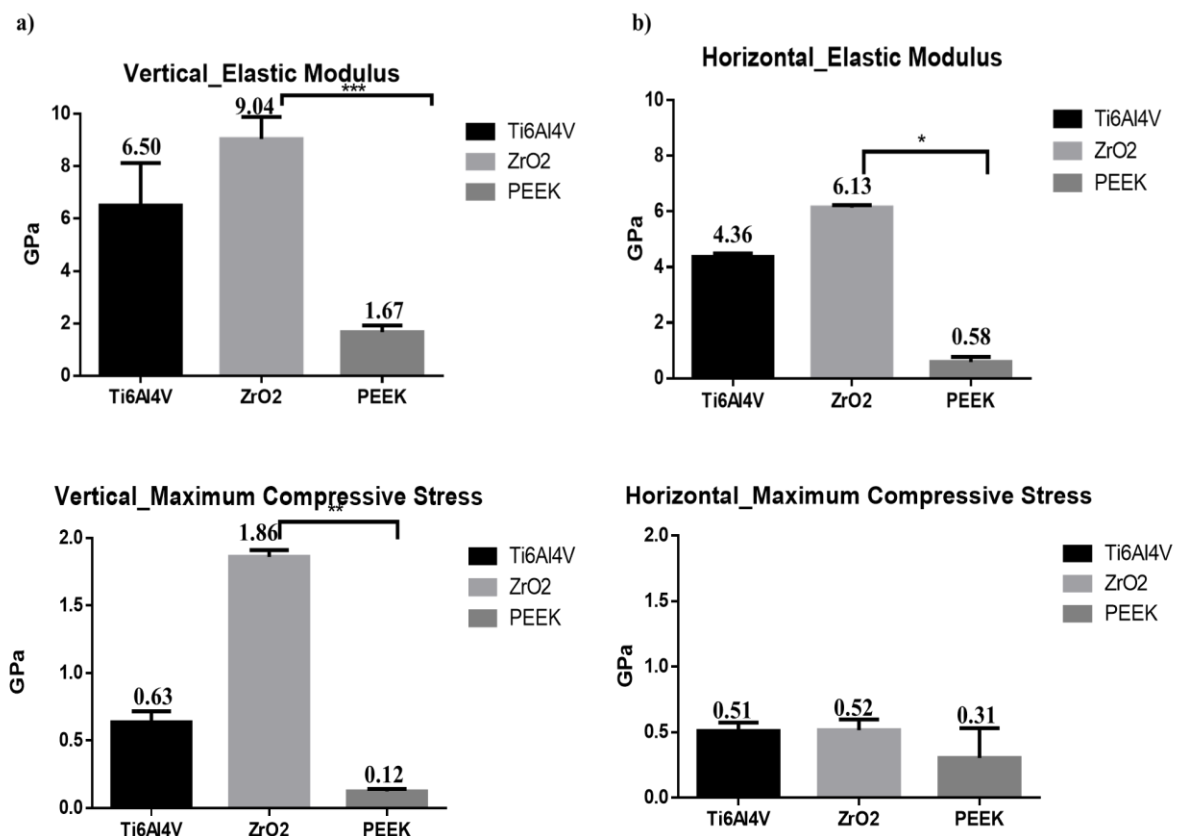


Figure 4-5 Mechanical Properties of scaffolds. a and b) Elastic modulus for vertical and horizontal position; b e c) Maximum compressive stress for vertical and horizontal position. Data is presented as mean±stdev (n=3), (*) denotes statistical differences ($p < 0.05$).

4.3.2 Biological characterization

Cell adhesion and spreading

Cell adhesion and spreading was visualized by Scanning electron microscopy (SEM) as depicted in figure 4.6. In figures 4.6 a, b and c, it is possible to observe the unseeded scaffolds, which presented an average height of 5mm. After the seeding of SaOS-2 it was possible to clearly observe that cells adhered to the surface (figure 4.6 g, h and i) when compared with unseeded scaffolds (figure 4.6 d, e and f). Looking more closely, it was visible that both, Ti_6Al_4V and ZrO_2 , presented more cells adhered and spreaded

throughout their surface, when compared with PEEK scaffold surface (Figures 4.6 j, k, l, m, n and o). As observed Ti6Al4V scaffolds present a quite high surface which should promote cell adhesion of SaOS-2.

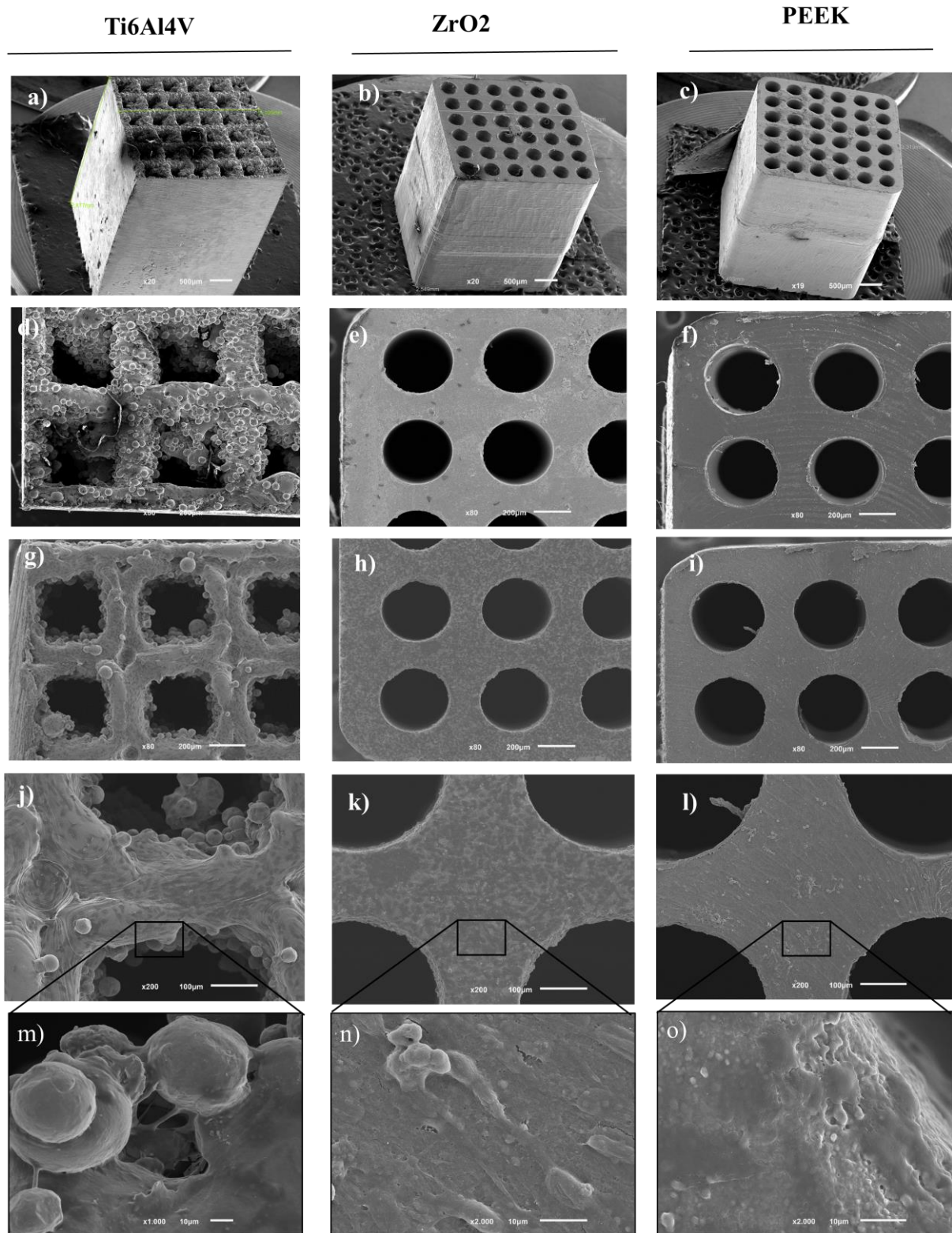


Figure 4-6 SEM analysis. SEM image of a) Ti₆Al₄V scaffold; b) ZrO₂ scaffold; c) PEEK scaffold; d) unseeded Ti₆Al₄V scaffold; e) unseeded ZrO₂ scaffold f) unseeded PEEK scaffold; g) and j) seeded Ti₆Al₄V scaffold; h) and k) seeded ZrO₂ scaffold i) and l) seeded PEEK scaffold; m) cells adhered and spread onto the surface Ti₆Al₄V scaffolds at higher magnification; n) cells adhered and spread onto the surface ZrO₂ scaffolds at higher magnification; o) cells adhered and spread onto the surface PEEK scaffolds at higher magnification.

Cell viability

The Alamar blue results elucidate about the cells' metabolic activity, which consequently can be transduced in cell viability. In this sense, cells are able to metabolize resazurin, the active ingredient of Alamar blue reagent, and reduce it into resorufin, a compound that is red in color and highly fluorescent. When viable cells convert resazurin to resorufin, the overall fluorescence of the media surrounding cells, increases. The results obtained along the 14 days of culture of SaOS-2 cells in 2D standard cultures (2D-Control) and on the scaffolds were normalized by DNA concentration and are presented in figure 4.7. As shown, after 1 day, cells cultured on Ti₆Al₄V scaffolds and 2D-Control were more metabolic active when compared with ZrO₂ and PEEK scaffolds. Nevertheless, the metabolic activity of these same cells decreased after 14 days of culture, while cells cultured on ZrO₂ and PEEK scaffolds presented similar values to day 1. Concerning ZrO₂ and PEEK scaffolds, although no differences between them were detected on day 1, cells cultured on ZrO₂ scaffolds showed to be more active than cells cultured on PEEK scaffolds on day 14. Noteworthy, the values presented by cells cultured in 2D-Control at day 14 were significantly lower than cells cultured on scaffolds. It is important also to point out that, in 2D-Control, cells were more metabolic active along the first 7 days of culture, decreasing on day 14, indicating that cells were differentiating along the osteoblastic lineage, as expected.

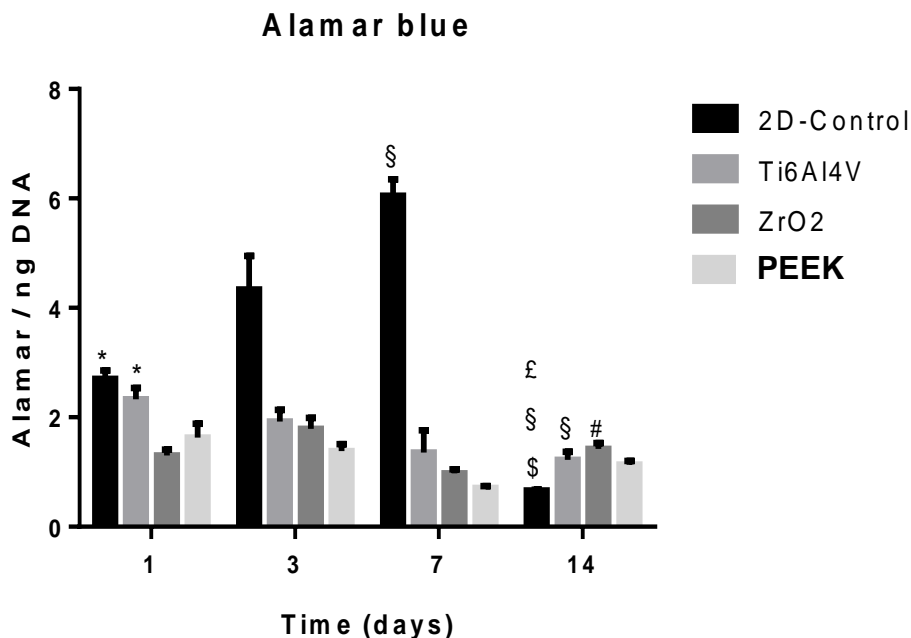


Figure 4-7 SaOS-2 cells' metabolic activity normalized by DNA concentration, along 14 days of culture. Symbols denote statistically significant differences ($p < 0.05$) in comparison to: (*) ZrO₂ and PEEK scaffolds, (\$) scaffolds; (#) PEEK scaffolds; (£) day 7; and (\$) day 1. Data is presented as mean \pm stdev ($n=3$).

Cell Proliferation

Cell proliferation was assessed by DNA quantification along the 14 days of culture of SaOS-2 cells on 2D standard cultures and scaffolds, as depicted in figure 4.8. At day 1 there is a clear difference between 2D control and scaffolds, which can be explained by the different cell concentration used for both conditions. Along the 14 days of culturing, although cells under all conditions proliferated, higher DNA content was observed in 2D control as compared with scaffolds. Interestingly, cells cultured on ZrO₂ scaffolds showed higher proliferation rates than cells cultured on PEEK scaffolds and slightly higher than Ti₆Al₄V scaffolds at day 1. But at day 14, cells showed an opposite proliferation rate, being significantly lower than Ti₆Al₄V and PEEK cell scaffolds.

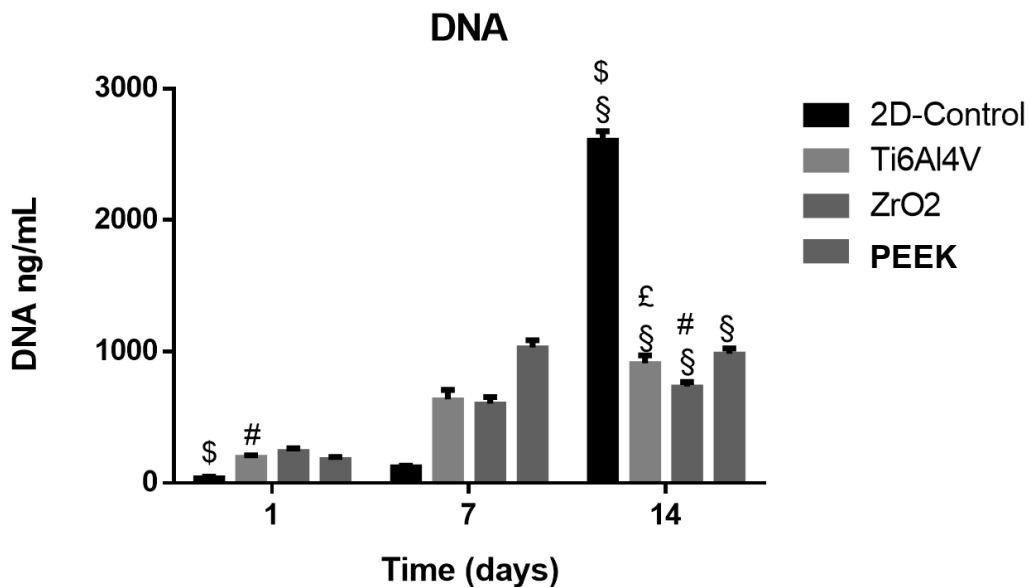


Figure 4-8 SaOS-2 cells' proliferation rates by DNA concentration, along 14 days of culture. Symbols denote statistically significant differences ($p < 0.05$) in comparison to: (\$) scaffolds; (#) PEEKI scaffolds; (\$) day 1; and (£) ZrO₂ scaffolds. Data is presented as mean \pm stdev ($n=3$).

Cell Differentiation

Alkaline phosphatase (ALP) activity is an early osteoblastic phenotypic marker and therefore an indicator of osteoblastic differentiation (Postiglione et al. 2003; Farley et al. 1991). For so, ALP activity was evaluated by molecular absorbance spectrophotometry measurement and by staining with Fast Violet B, figure 4.9 and 4.10 respectively. Considering ALP measurements at day 3, values were similar for all conditions. However, ZrO₂ scaffolds showed higher values when compared with 2D control. When looking to values of day 7, only cells on 2D control had higher activity than day 3, which decreased until day 14, showing the typical peak of expression. Moreover, the values of ALP activity of 2D control were higher

than scaffolds, while amongst the scaffolds, cell seeded Ti₆Al₄V and ZrO₂ showed higher values than cell seeded PEEK scaffolds. In the case of ALP activity at day 14, all conditions showed lower values than day 3 and day 7, however, ALP qualitative activity was still detected by Fast Violet B staining as depicted in figure 4.10. Interestingly, 2D control showed the lowest values at this time point. Once more, Ti₆Al₄V scaffolds showed higher values than PEEK and ZrO₂ scaffolds, which was corroborated by the ALP staining (figure 4.10).

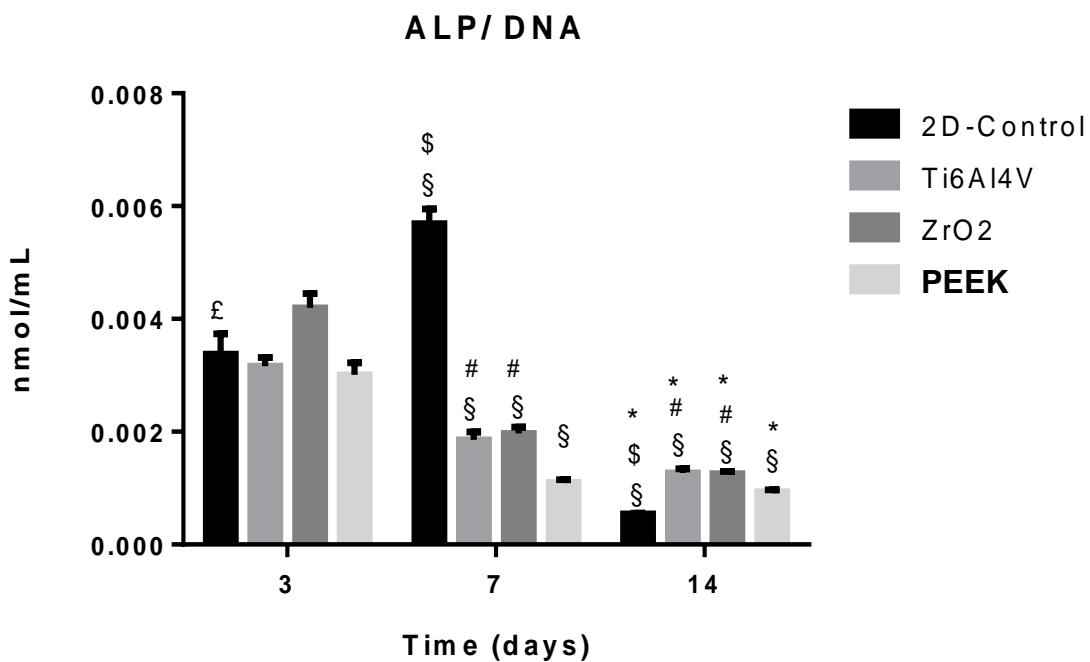


Figure 4-9 SaOS-2 cells' ALP activity along 14 days of culture. Symbols denote statistically significant differences ($p < 0.05$) in comparison to: (£) ZrO₂ scaffolds; (\$) Scaffolds; (\$) day 3 (#) PEEK scaffolds; and (*) day 7. Data is presented as mean±stdev (n=3).

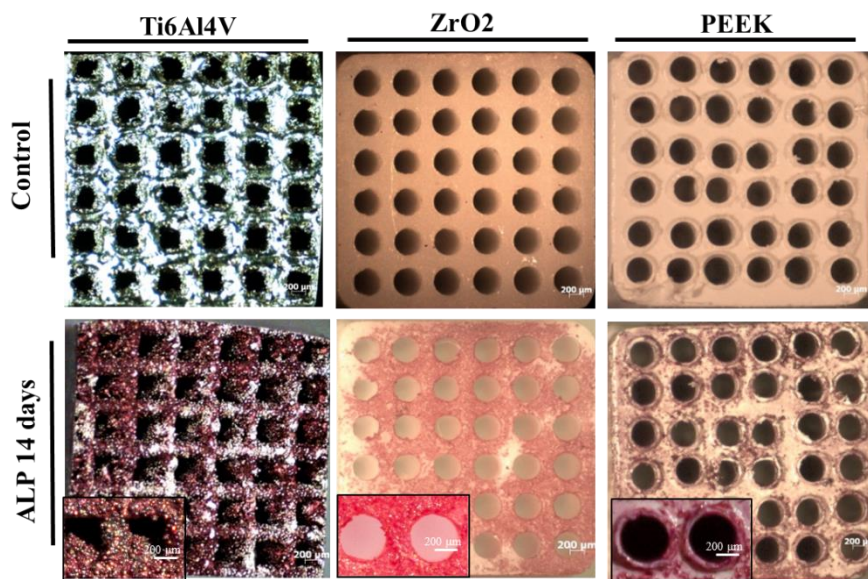


Figure 4-10 ALP stained SaOS-2 cells on scaffolds and respective controls (scaffolds without cells) after 14 days of culture. Insets shows ALP stained cells on scaffolds at higher magnification.

4.4 Discussion

Tissue engineering approaches have been essential for the development of some commercially available products for the use in bone defects treatments (Infuse; Vitoss). But none of those products is able to induce bone regeneration. In fact, for bone applications, it is crucial to have proper mechanical properties and have the capacity to host cells. A common problem with current available solutions is their mismatch with bone in terms of elastic modulus. It has been reported that when elastic modulus, between an implant and bone, presents a mismatch, stress transfer happens. This phenomenon calls stress shielding and leads to bone reabsorption (Navarro et al. 2008; Zhang et al. 2016). One approach to solve these problem is to reduce the elastic modulus of materials by introducing pores. Additionally, the introduction of pores presents another advantage for the scaffolds as it facilitates cell penetration, tissue ingrowth and vascularization.

In the presented study, three dimensional (3D)-scaffolds, with different material compositions, Ti6Al4V, ZrO₂ and PEEK, with a pore size of 400 µm chosen according to studies previous published were prepare (Yamane et al. 2007; Im et al. 2012). They were evaluated regarding their surface's characteristics, mechanical properties, and influence in cell. XRD was performed to assess the crystallographic phase of ZrO₂ scaffolds after processing. In fact, ZrO₂ can present three crystallographic

phases: monoclinic (m), tetragonal (t), and cubic (c), being the tetragonal the more stable phase for ZrO_2 (Denry and Kelly 2008). Each crystallographic phase can develop during heating or cooling processes. As we can observed in 4-1 the ZrO_2 XRD plot present a typical tetragonal phase plot, indicating that the ZrO_2 materials used during this study were stable and is in agreement with published data related to tetragonal phase of ZrO_2 (Tsunekawa et al. 2005; Watanabe and Yoshinari 2016). For the chemical composition XPS was performed and all the main compounds of scaffolds. The peaks of Ti, Zr, C and O were identify as expected (Ramires and Guastaldi 2002; Shard and Badyal 1992; Lu et al. 2015; Tsunekawa et al. 2005; Watanabe and Yoshinari 2016).

Furthermore, micro-CT analysis was used to assessed porosity, mean pore size and mean pore thickness of the scaffolds. As expected the porosity was similar in all scaffolds. But, interestingly, only in the case of PEEK scaffolds it was obtained pore size values similar to the theoretical size ($\approx 400 \mu\text{m}$).

There are several topographical parameters that influence cells' behavior. For example, it was previously shown that contact angle and surface energy can influence the cell adhesion (Hallab et al. 2001). Moreover, the measurement of contact angles is extremely useful as they characterize the average of wettability of material's surface (Yuan and Lee 2013). Since all the scaffolds were polished, the influence of roughness on the wetting properties was evaluated by contact angle measurement analysis of rough and polished Ti_6Al_4V , ZrO_2 and PEEK samples. As it was observed on table 4-3, rough ZrO_2 showed an angle lower than 90° , indicating that ZrO_2 exhibited a hydrophilic surface, whereas Ti_6Al_4V and PEEK, with an angle higher than 90° , exhibited a hydrophobic surface. Surface energy is also an important parameter in surface topography that influences biological response, once it is related with the wettability of the surface and thus its hydrophilicity. In fact, it is known that hydrophilic surfaces allow protein absorption to the implant surface and subsequent interaction with cells. In contrast, hydrophobic surfaces that are subjected to air bubbles entrapment hinder forbidding protein absorption and thus cell adhesion. In this context, many studies have concluded that a moderate hydrophilicity improves the biological response (Gittens et al. 2014).

Finally, the last property analyzed were the mechanical properties assessed by the elastic modulus analysis. In the literature is possible to find that the typical values of elastic modulus for bulk Ti_6Al_4V , ZrO_2 and PEEK materials are: 113 GPa; 200 GPa and 3-4 GPa, respectively (Osman and Swain 2015; Najeeb et al. 2016; Jung et al. 2014). During the compression test all scaffold presented a typical stress-strain curve. As expected, the elastic modulus obtained when tested the scaffolds was lower than in bulk structure as shown in figure 4-5 and were in agreement with previous data published (Weißmann

et al. 2016). This difference can be explained by the presence of pores. Moreover, the values obtained were in the range of elastic modulus of cortical bone, which is compromised between 3 GPa and 30 GPa. Another interesting finding was that the scaffolds presented high values of maximum compressive stress with improved capacity to withstand the applied loads, corroborating the suitability of the scaffolds to be used in bone tissue applications.

After physicochemical properties analysis, cells' behavior, namely, cell adhesion and spreading, cell viability, cell proliferation and cell differentiation was assessed. For that, an osteosarcoma - derived cell line (SaOS-2) was used since it was more physiologically relevant when considering the ultimate application. SaOS-2 cells, a good and well-characterized osteosarcoma human cell line, have been widely used as a model system for osteoblastic cells mostly due to their exhibition of the entire differentiation sequence of osteoblastic cells (Postiglione et al. 2003; Hausser and Brenner 2005).

By observing SEM images in figure 4-6 it was possible to observe that cells were able to adhere and spread at some extent in each material. Nevertheless, it was noticed a higher cell adhesion and spreading in Ti_6Al_4V and ZrO_2 scaffolds when compared to PEEK scaffolds. This could be explained by the higher roughness presented by Ti_6Al_4V and ZrO_2 scaffolds, which was described to improve not only cell adhesion but also cell spreading (Huang et al. 2004; Yang et al. 2016).

In the case of cell viability evaluation, metabolic activity was assessed. As shown in figure 4-7, the metabolic activity of SaOS-2 cultured on standard 2D cultures (2D control) followed a normal profile. In this sense, cells' metabolic activity increased until day 7 and decreased until day 14 indicating that at this time point cells were probably differentiating along the osteoblastic lineage. On the other hand, scaffolds showed always similar or lower values along the culture as compared to day 1. Even so, DNA quantification results showed that cells proliferated along the entire time of culture in all conditions.

Considering the application of these materials for bone tissue approaches, the differentiation of SaOS-2 along the osteogenic lineage was also motif of study. In fact, the information about osteogenic differentiation markers, as alkaline phosphatase, are important to evaluate the influence of the different materials on bone formation and implant osseointegration. Several studies suggest that differentiation toward an osteoblastic phenotype correlates with a decrease in cell proliferation and an increase in alkaline phosphatase activity (Postiglione et al. 2003). Indeed, the 2D – control, as shown in figure 4-9, showed a typical development in terms of ALP activity, i.e. SaOS-2 ALP activity peaked at day 7 and decreased, but cells were proliferating the entire time of culture. For so, one can conclude that cells were only in the beginning of the differentiation pathway. In the case of Ti_6Al_4V , ZrO_2 and PEEK scaffolds,

although cells expressed ALP the entire culture as observed by ALP activity quantification and detection by staining, it decreased along the 14 days. One explanation for the low levels of ALP activity observed is the deficient cell-cell contact as reported in previous studies (Cao et al. 2015; Tang et al. 2010) and supported by the continuous increase in the proliferation rate throughout the experiment time. Another explanation is that this study was not realized in osteogenic differentiation conditions, i.e. in the presence of ascorbic acid, dexamethasone and β -glycerophosphate, resulting in a slower differentiation profile.

All together the obtained results demonstrated the suitability of the proposed scaffolds for bone tissue engineering applications. As determined by their improved mechanical properties and their effect on cell's behavior, especially in the case of $\text{Ti}_6\text{Al}_4\text{V}$ and ZrO_2 scaffolds.

4.5 Conclusion

In this study, novel scaffolds were prepared by SLM and CNC machining. The scaffolds presented suitable porosity and mechanical properties for bone applications, with special attention for the superior mechanical properties of $\text{Ti}_6\text{Al}_4\text{V}$ and ZrO_2 . Their *in vitro* cytocompatibility and osteogenic ability were screened using SaOS-2 cells showing that samples were non cytotoxic for cells and were able to host cells for the time of culture and allowed them to differentiate along the osteoblastic lineage. Thus, this type of porous architecture and materials can be used for bone tissue engineering applications. Although complementary *in vivo* studies are necessary to evaluate the long-term biological performance and stability of the scaffolds in subcutaneous and orthotopic models, the obtained results indicated that the developed scaffolds are promising structures for bone regeneration applications.

Acknowledgements

The work was supported by Portuguese Foundation for Science and Technology (FCT) through the project UID/EEA/04436/2013 and NORTE-01-0145-FEDER-000018-HAMaBICo, B-FABULUS (PTDC/BBB-ECT/2690/2014) and 3BioMeD (FCT/4773/4/5/2017/S). FCT/MCTES is also acknowledged for the PhD scholarship attributed to F.I.C (SFRH/BD/99555/2014) and the financial support provided to J.M.O. (IF/01285/2015) under the program "Investigador FCT".

4.6 References

- Bartolomeu F, Faria S, Carvalho O, Pinto E, Alves N, Silva F, Miranda G (2016) Predictive models for physical and mechanical properties of Ti6Al4V produced by selective laser melting. *Materials Science and Engineering: A* 663:181-192
- Bentley TS, Hanson SG (2014) 2014 US organ and tissue transplant cost estimates and discussion. Milliman Research Report: Milliman
- Bohner M, Loosli Y, Baroud G, Lacroix D (2011) Commentary: deciphering the link between architecture and biological response of a bone graft substitute. *Acta biomaterialia* 7 (2):478-484
- Bose S, Vahabzadeh S, Bandyopadhyay A (2013) Bone tissue engineering using 3D printing. *Materials Today* 16 (12):496-504
- Boskey AL (2013) Bone composition: relationship to bone fragility and antiosteoporotic drug effects. *BoneKEY reports* 2
- Cao B, Li Z, Peng R, Ding J (2015) Effects of cell–cell contact and oxygen tension on chondrogenic differentiation of stem cells. *Biomaterials* 64:21-32
- Denry I, Kelly JR (2008) State of the art of zirconia for dental applications. *Dental materials* 24 (3):299-307
- Gittens RA, Scheideler L, Rupp F, Hyzy SL, Geis-Gerstorfer J, Schwartz Z, Boyan BD (2014) A review on the wettability of dental implant surfaces II: biological and clinical aspects. *Acta biomaterialia* 10 (7):2907-2918
- Hallab NJ, Bundy KJ, O'Connor K, Moses RL, Jacobs JJ (2001) Evaluation of metallic and polymeric biomaterial surface energy and surface roughness characteristics for directed cell adhesion. *Tissue engineering* 7 (1):55-71
- Hausser H-J, Brenner RE (2005) Phenotypic instability of Saos-2 cells in long-term culture. *Biochemical and biophysical research communications* 333 (1):216-222
- Huang H-H, Ho C-T, Lee T-H, Lee T-L, Liao K-K, Chen F-L (2004) Effect of surface roughness of ground titanium on initial cell adhesion. *Biomolecular engineering* 21 (3):93-97
- Im G-I, Ko J-Y, Lee JH (2012) Chondrogenesis of adipose stem cells in a porous polymer scaffold: influence of the pore size. *Cell transplantation* 21 (11):2397-2405
- Jones AC, Milthorpe B, Averdunk H, Limaye A, Senden TJ, Sakellariou A, Sheppard AP, Sok RM, Knackstedt MA, Brandwood A (2004) Analysis of 3D bone ingrowth into polymer scaffolds via micro-computed tomography imaging. *Biomaterials* 25 (20):4947-4954
- Jung H-D, Park HS, Kang M-H, Lee S-M, Kim H-E, Estrin Y, Koh Y-H (2014) Polyetheretherketone/magnesium composite selectively coated with hydroxyapatite for enhanced in vitro bio-corrosion resistance and biocompatibility. *Materials Letters* 116:20-22
- Karageorgiou V, Kaplan D (2005) Porosity of 3D biomaterial scaffolds and osteogenesis. *Biomaterials* 26 (27):5474-5491
- Kuboki Y, Takita H, Kobayashi D, Tsuruga E, Inoue M, Murata M, Nagai N, Dohi Y, Ohgushi H (1998) BMP-induced osteogenesis on the surface of hydroxyapatite with geometrically feasible and nonfeasible structures: topology of osteogenesis. *Journal of Biomedical Materials Research Part A* 39 (2):190-199
- Kurtz SM, Devine JN (2007) PEEK biomaterials in trauma, orthopedic, and spinal implants. *Biomaterials* 28 (32):4845-4869
- Leong K, Chua C, Sudarmadji N, Yeong W (2008) Engineering functionally graded tissue engineering scaffolds. *Journal of the mechanical behavior of biomedical materials* 1 (2):140-152
- Lu T, Wen J, Qian S, Cao H, Ning C, Pan X, Jiang X, Liu X, Chu PK (2015) Enhanced osteointegration on tantalum-implanted polyetheretherketone surface with bone-like elastic modulus. *Biomaterials* 51:173-183
- Morelli I, Drago L, George DA, Gallazzi E, Scarponi S, Romanò CL (2016) Masquelet technique: myth or reality? A systematic review and meta-analysis. *Injury* 47:S68-S76

- Murphy CM, Haugh MG, O'Brien FJ (2010) The effect of mean pore size on cell attachment, proliferation and migration in collagen–glycosaminoglycan scaffolds for bone tissue engineering. *Biomaterials* 31 (3):461-466
- Nair LS, Laurencin CT (2007) Biodegradable polymers as biomaterials. *Progress in polymer science* 32 (8):762-798
- Najeeb S, Zafar MS, Khurshid Z, Siddiqui F (2016) Applications of polyetheretherketone (PEEK) in oral implantology and prosthodontics. *Journal of prosthodontic Research* 60 (1):12-19
- Navarro M, Michiardi A, Castano O, Planell J (2008) Biomaterials in orthopaedics. *Journal of the Royal Society Interface* 5 (27):1137-1158
- Nielsen K (1987) Corrosion of metallic implants. *British Corrosion Journal* 22 (4):272-278
- Niinomi M (2003) Recent research and development in titanium alloys for biomedical applications and healthcare goods. *Science and technology of advanced Materials* 4 (5):445
- Niinomi M (2008) Metallic biomaterials. *Journal of Artificial Organs* 11 (3):105
- Osman RB, Swain MV (2015) A critical review of dental implant materials with an emphasis on titanium versus zirconia. *Materials* 8 (3):932-958
- Postiglione L, Di Domenico G, Ramaglia L, Montagnani S, Salzano S, Di Meglio F, Sbordone L, Vitale M, Rossi G (2003) Behavior of SaOS-2 cells cultured on different titanium surfaces. *Journal of dental research* 82 (9):692-696
- Rae P, Brown E, Orlor E (2007) The mechanical properties of poly (ether-ether-ketone)(PEEK) with emphasis on the large compressive strain response. *Polymer* 48 (2):598-615
- Ramires I, Guastaldi AC (2002) Estudo do biomaterial Ti-6Al-4V empregando-se técnicas eletroquímicas e XPS. *Química Nova*:10-14
- Shard A, Badyal J (1992) Surface oxidation of polyethylene, polystyrene, and PEEK: the synthon approach. *Macromolecules* 25 (7):2053-2054
- Sproesser O, Schmidlin PR, Uhrenbacher J, Eichberger M, Roos M, Stawarczyk B (2014) Work of adhesion between resin composite cements and PEEK as a function of etching duration with sulfuric acid and its correlation with bond strength values. *International Journal of Adhesion and Adhesives* 54:184-190
- Tang J, Peng R, Ding J (2010) The regulation of stem cell differentiation by cell-cell contact on micropatterned material surfaces. *Biomaterials* 31 (9):2470-2476
- Tsunekawa S, Asami K, Ito S, Yashima M, Sugimoto T (2005) XPS study of the phase transition in pure zirconium oxide nanocrystallites. *Applied surface science* 252 (5):1651-1656
- Wang X, Xu S, Zhou S, Xu W, Leary M, Choong P, Qian M, Brandt M, Xie YM (2016) Topological design and additive manufacturing of porous metals for bone scaffolds and orthopaedic implants: a review. *Biomaterials* 83:127-141
- Watanabe E, Yoshinari M (2016) Changes in X-ray photoelectron spectra of yttria-tetragonal zirconia polycrystal by ion sputtering. *Applied Physics A* 122 (4):339
- Weißmann V, Bader R, Hansmann H, Laufer N (2016) Influence of the structural orientation on the mechanical properties of selective laser melted Ti6Al4V open-porous scaffolds. *Materials & Design* 95:188-197
- Wu S, Liu X, Yeung KW, Liu C, Yang X (2014) Biomimetic porous scaffolds for bone tissue engineering. *Materials Science and Engineering: R: Reports* 80:1-36
- Yamane S, Iwasaki N, Kasahara Y, Harada K, Majima T, Monde K, Nishimura Si, Minami A (2007) Effect of pore size on in vitro cartilage formation using chitosan-based hyaluronic acid hybrid polymer fibers. *Journal of Biomedical Materials Research Part A* 81 (3):586-593
- Yang S, Leong K-F, Du Z, Chua C-K (2001) The design of scaffolds for use in tissue engineering. Part I. Traditional factors. *Tissue engineering* 7 (6):679-689
- Yang W, Han W, He W, Li J, Wang J, Feng H, Qian Y (2016) Surface topography of hydroxyapatite promotes osteogenic differentiation of human bone marrow mesenchymal stem cells. *Materials Science and Engineering: C* 60:45-53

- Yin L, Nakanishi Y, Alao A-R, Song X-F, Abduo J, Zhang Y (2017) A review of engineered zirconia surfaces in biomedical applications. *Procedia CIRP* 65:284-290
- Yuan Y, Lee TR (2013) Contact angle and wetting properties. In: *Surface science techniques*. Springer, pp 3-34
- Zhang P, Choy K-L (2015) The Synthesis of Single Tetragonal Phase Zirconia by Sol-Gel Route. *Int Journal of Engineering Research & Science (IJOER)*:20-21
- Zhang Q-H, Cossey A, Tong J (2016) Stress shielding in bone of a bone-cement interface. *Medical engineering & physics* 38 (4):423-426

5. FINAL REMARKS AND FUTURE WORK

During this study 3D porous scaffolds were prepared and their characterization was extensively performed. The pore size was chosen as well as wall thickness in order to ensure the 3D scaffold had proper compressive strength.

Surface topography and pore was evaluated by means of SEM images and Micro CT. Important topographical parameters that influence directly cell behavior such as roughness and the hydrophobicity was also evaluated. ZrO_2 exhibit a hydrophilic surface which is favorable for protein adhesion and thus cell adhesion and spreading.

This work reported interesting mechanical properties especially the low elastic modulus near of the bone of 3D scaffolds made of a titanium alloy, Ti_6Al_4V , ZrO_2 and PEEK. This is an interesting result as the stress shielding is one of the main reasons for implant failure in load bearing applications. The 3D cell scaffolds also revealed a high compressive stress, a special attention for the results of ZrO_2 which present high maximum compressive stress with a low elastic modulus.

The *in vitro* performance of samples was also evaluated with promising results related to cell adhesion and proliferation. The tests showed that samples were not toxic for cells and were able to host cells for the time of culture. Thus, this type of porous architecture and materials can be used for bone engineering applications since cell are one important component on this solutions.

Further research has to be done in the scope of this study. Future work should essentially focus on the following lines of investigation:

- *In vitro* assays during 28 days;
- Production of scaffolds with different pore size or interconnected pores;
- *In vivo* studies of histocompatibility by subcutaneous implantation in mice;
- *In vivo* validation in bigger animal models, implantation of bone defect in bigger animals such as goat or dogs;
- Study the effect of different surface roughness in cell behavior;
- Coat scaffolds with bioactive material such as TCP;
- Bioactivity studies to evaluate the formation of an apatite layer;
- *In vitro* evaluation with uncoated and coated scaffolds;

Three dimensional cell-scaffold constructs for application in bone tissue engineering

- Culturing cells such as stem cells to evaluate the osteogenic potential;
- Incorporation of growth factors to promote bone regeneration.